

## **BresDefender**

### **An experimental study on an emergency response measure for levee breaches**

Janssen, D.

#### **DOI**

[10.4233/uuid:0962a77b-47c6-4a0b-a090-a3381dfb8175](https://doi.org/10.4233/uuid:0962a77b-47c6-4a0b-a090-a3381dfb8175)

#### **Publication date**

2024

#### **Document Version**

Final published version

#### **Citation (APA)**

Janssen, D. (2024). *BresDefender: An experimental study on an emergency response measure for levee breaches*. [Dissertation (TU Delft), Delft University of Technology]. <https://doi.org/10.4233/uuid:0962a77b-47c6-4a0b-a090-a3381dfb8175>

#### **Important note**

To cite this publication, please use the final published version (if applicable). Please check the document version above.

#### **Copyright**

Other than for strictly personal use, it is not permitted to download, forward or distribute the text or part of it, without the consent of the author(s) and/or copyright holder(s), unless the work is under an open content license such as Creative Commons.

#### **Takedown policy**

Please contact us and provide details if you believe this document breaches copyrights. We will remove access to the work immediately and investigate your claim.

# **BRESDEFENDER**

AN EXPERIMENTAL STUDY ON AN EMERGENCY RESPONSE  
MEASURE FOR LEVEE BREACHES



# **BRESDEFENDER**

AN EXPERIMENTAL STUDY ON AN EMERGENCY RESPONSE  
MEASURE FOR LEVEE BREACHES

## **Proefschrift**

ter verkrijging van de graad van doctor  
aan de Technische Universiteit Delft,  
op gezag van de Rector Magnificus prof. dr. ir. T.H.J.J. van der Hagen,  
voorzitter van het College voor Promoties,  
in het openbaar te verdedigen op maandag 3 juni 2024 om 15:00 uur

door

**Danny JANSSEN**

civiel ingenieur, Technische Universiteit Delft, Nederland  
geboren te Delft, Nederland.

Dit proefschrift is goedgekeurd door de promotoren.

Samenstelling promotiecommissie:

Rector Magnificus,	voorzitter
Prof. dr. ir. S.N. Jonkman	Technische Universiteit Delft, promotor
Dr. ir. B. Hofland	Technische Universiteit Delft, promotor
Ir. A.J.M. Schmets	Nederlandse Defensie Academie, externe adviseur

*Onafhankelijke leden:*

Prof. dr. ir. M. Kok	Technische Universiteit Delft
Prof. dr. ir. M.H. Chaudhry	University of South Carolina, Verenigde Staten
Prof. dr. ir. R.G. van de Ketterij	Nederlandse Defensie Academie
Prof. dr. ir. C. Jommi	Technische Universiteit Delft
Prof. dr. ir. M.R.A. van Gent	Technische Universiteit Delft, reservelid

Dr. ir. E. Dado van de Nederlandse Defensie Academie heeft een aanzienlijke bijdrage geleverd aan de totstandkoming van dit proefschrift.



*Keywords:* Climate resilience, Emergency Response, Levee Breach, River flooding, BresDefender, Military engineering of Civil-military interaction, Transient groundwater flow, Expert Judgement

*Printed by:* Gildeprint

*Front & Back:* Bureau Multimedia NLDA, Peter de Vries

Copyright © 2024 by D. Janssen

ISBN 978-94-6384-593-9

An electronic version of this dissertation is available at  
<http://repository.tudelft.nl/>.

*There's no harm in hoping for the best  
as long as you're prepared for the worst.*

Stephen King



# CONTENTS

<b>Summary</b>	<b>xi</b>
<b>Samenvatting</b>	<b>xv</b>
<b>Acknowledgements</b>	<b>xix</b>
<b>1 Introduction</b>	<b>1</b>
1.1 Introduction	2
1.1.1 Background	2
1.1.2 BresDefender	4
1.1.3 Emergency response strategies	5
1.2 Knowledge gaps	6
1.3 Research objectives	7
1.4 Research questions	7
1.5 Research approach and outline	8
1.6 Research scope	10
<b>2 Experimental study of water infiltration into a partially sealed levee</b>	<b>13</b>
2.1 Introduction	14
2.2 Conceptual framework	16
2.2.1 Case of perfect connection	16
2.2.2 Case of imperfect connection, surface-seal interface layer	17
2.3 Lab scale experiments	17
2.3.1 Experimental setup lab experiments	17
2.3.2 Lab scale measurement results	20
2.4 Real-scale field experiments	22
2.4.1 Experimental setup field experiments	22
2.4.2 Real scale measurement results	23
2.4.3 Three dimensional effects in field tests	25
2.5 Numerical model and simulation	26
2.5.1 Numerical model	26
2.5.2 Numerical results: Steady state phreatic level	27
2.5.3 Time to new equilibrium phreatic level	27
2.5.4 Phreatic surface level, perfect seal	27
2.5.5 Case of imperfect seal, soil structure interface layer	29
2.6 Discussion	30
2.6.1 Determination of interface layer parameters	31
2.6.2 Three dimensional effects of the seal	31
2.7 Conclusions	32



<b>3</b>	<b>Reducing water flow through a levee breach using a pontoon</b>	<b>35</b>
3.1	Introduction . . . . .	36
3.2	Methods . . . . .	37
3.2.1	Geometrical parameters . . . . .	38
3.2.2	Intermediate scale experiments: Flood Proof Holland . . . . .	40
3.2.3	Full scale experiments: Hedwigepolder . . . . .	41
3.3	Experimental results . . . . .	43
3.3.1	Experimental results: intermediate scale. . . . .	43
3.3.2	Experimental results: full scale experiments . . . . .	45
3.4	Analysis of results: the leakage model. . . . .	46
3.4.1	levee surface analysis . . . . .	46
3.4.2	Physical parameters to characterize leakage . . . . .	49
3.4.3	Discharge reduction . . . . .	52
3.5	Discussion . . . . .	53
3.5.1	Soil erosion . . . . .	53
3.5.2	Stability of a single pontoon element docked at a levee . . . . .	55
3.5.3	Pontoon placement under dynamic conditions . . . . .	58
3.6	Conclusions. . . . .	59
<b>4</b>	<b>Operational reliability of emergency measures, a case study for the Bresdefender</b>	<b>61</b>
4.1	Introduction . . . . .	62
4.2	General model framework . . . . .	63
4.3	Damage process: available time. . . . .	65
4.3.1	General . . . . .	65
4.3.2	Overflow . . . . .	66
4.3.3	Slope instability . . . . .	67
4.3.4	Breach formation time . . . . .	68
4.4	Preparation of emergency measures: required time . . . . .	69
4.4.1	General framework . . . . .	69
4.4.2	Estimation of time required: expert judgement analysis . . . . .	70
4.4.3	Inspection . . . . .	71
4.4.4	Transport . . . . .	72
4.4.5	Placement . . . . .	73
4.5	Case studies. . . . .	73
4.5.1	Warning times . . . . .	74
4.5.2	Rhine case . . . . .	75
4.5.3	River Meuse case. . . . .	77
4.6	Discussion . . . . .	78
4.6.1	Proactive applying emergency measures. . . . .	79
4.6.2	Implicit assumptions within the model . . . . .	79
4.7	Conclusions. . . . .	80

---

<b>5</b>	<b>Conclusions and recommendations</b>	<b>83</b>
5.1	Conclusions . . . . .	83
5.2	Recommendations . . . . .	86
5.2.1	Recommendations for further research . . . . .	86
5.2.2	Recommendations for practice . . . . .	87
<b>A</b>	<b>Additional information chapter 3</b>	<b>95</b>
A.1	Determination breach time . . . . .	95
A.2	Geometrical parameters in stability model . . . . .	95
<b>B</b>	<b>Additional information chapter 4</b>	<b>103</b>
B.1	Series model . . . . .	103
B.2	Expert judgment . . . . .	103
	<b>Curriculum Vitæ</b>	<b>109</b>
	<b>List of Publications</b>	<b>111</b>



# SUMMARY

To protect low-lying areas like the Netherlands from floods, water-retaining structures, such as levees have been constructed along almost all of the rivers. These structures must comply with legal standards for water safety. These standards are derived from economic, social, and individual risk factors. Even if such structure's design meets the standards, there will always remain a probability of failure, which causes a flood, leading to both societal and material damage. Emergency measures can provide a flexible solution to reduce the remaining probability of levee failure and thus prevent the negative effects of a flood. This dissertation focuses on the application of emergency measures, specifically the BresDefender, to prevent or postpone levee failure.

In the event of an expected extreme water level, the risk of levee failure is expected to increase. In such cases, crisis protocols are triggered, initiating levee inspections to assess the levee system for potential damages. If damage is detected, the decision to implement an emergency measures may be taken. If civilian authorities lack personnel and resources, or when circumstances are very challenging, the assistance of the military can be called in.

Providing aid during national crises, such as a high-water crisis, is one of the responsibilities of the Dutch armed forces. Historically, the military's involvement has mainly focused on the placement of sandbags and assisting with evacuations. As climate change will lead to more frequent occurrence of high water levels in rivers, the military is foreseen to be omitted more often. Given the other main tasks of the military, this challenge can only be met by more efficient deployment of military personnel and resources, and sharing resources with civil partners. This concept has been coined as 'adaptive army'.

With the aim of multifunctional use of military assets, in line with adaptive use of equipment, this dissertation explores the physical operation and applications of the BresDefender. The BresDefender is a military pontoon normally employed to construct temporary floating bridges. Inspired by the heroic closure of an incipient breach at Nieuwerkerk aan den IJssel with the ship 'de twee gebroeders' during the 1953 North Sea Flood, this dissertation explores scientifically the feasibility of achieving a similar outcome with the BresDefender. When modifying the pontoon, it can be submerged against a locally weakened levee to reinforce it. The primary advantage of using a pontoon is its waterborne operation, eliminating the need for heavy equipment on the levee. The effectiveness of the BresDefender is attributed into two potential effects: its impact on water infiltrating a levee and the water flowing over a levee in the case of an emerging breach.

To investigate the spatiotemporal effect of the emergency measure on the phreatic surface through a levee, physical experiments were conducted on two different scales (see chapter 2). First, on a small scale in the hydraulic engineering laboratory of the TU Delft, followed by an intermediate scale on a 2 m high levee in Flood Proof Holland, Delft. During these experiments, the effect of (partially) sealing the outer slope with

an impermeable structure on the evolution of the phreatic surface through a levee was measured. Next, the outcome of these experiments was interpreted with the use of a numerical model. In theory, a perfect contact between the impermeable structure and the subsurface could lower the level of the phreatic surface in the covered part of the levee. However, in practice, the contact interface will not be perfect, resulting in only a minimal reduction of the phreatic surface at different outer slope sealing percentages. Nevertheless, it has been found that an impermeable seal that is in good contact with the outer slope extends the time to reach equilibrium phreatic surface conditions by approximately 50%. In the intermediate-scale experiments, the additional time to reach an equilibrium state of the phreatic surface, was found to be measurable for the case of a damaged levee surface, i.e. the local absence of a clay cover. Covering a levee to manipulate the phreatic surface is only recommended if the phreatic surface has not yet reached equilibrium conditions.

The second effect of the BresDefender on the failure behavior of a levee, as investigated in this dissertation, is its effect on the breach formation process (see chapter 3). This effect was also examined through physical experiments on an intermediate scale in Flood Proof Holland, Delft, and on full scale in the Hedwige-Prosperpolder. In the absence of flow, a multiplex plate (intermediate scale) or the BresDefender pontoon (full scale) was placed in front of a locally reduced levee crest. By creating a water level difference between the outer water level and the breach, a flow of leakage water occurred through the gaps between the pontoon and the surface of the levee. The measured seepage discharge in both experiments was less than 1% of the expected discharge that would have passed through the breach without the emergency measure. In the real scale experiments, this effect was achieved by covering the military pontoon with a flexible tarpaulin capable of adapting to the irregularities in the slope of a levee, thus creating optimal contact with the levee surface. Without the application of this tarpaulin, the measured seepage flow was 23% of the expected unrestricted flow.

Even with a reduced flow through a breach using the BresDefender, erosion of sandy material from the initial breach is still anticipated. However, the time it takes for the levee, assumed to be purely sandy, to fail at these flow rates was found to increase from 30 minutes without the measure applied, to over 24 hours with the measure placed. This extended time to failure may potentially exceed the duration of a high-water wave or provide levee managers with the opportunity to implement additional measures to stabilize the levee.

A crucial parameter in the implementation of emergency measures was demonstrated to be the quality of contact between the emergency measure and the outer slope. This emphasizes the importance of utilizing a flexible material capable of adapting to the irregularities of a levee slope. This adaptability can be achieved with both the current prototype or a structure that operates on the same principles as the BresDefender, i.e., a stiff and heavy enough object keeping a flexible sheet on place.

In addition to investigating the effectiveness of emergency measures, this dissertation also explores the reliability of the method in terms of the likelihood of preventing a levee breach (see chapter 4). For this purpose, a probabilistic model has been developed, capable of determining both the probability of arriving too late at a damaged levee and the probability of failure due to a deficiency in the water-retaining height. This model is

based on the expected time-frames established by experts through interviews, and literature review. The probability of successfully implementing emergency measures has been assessed using two different scenarios, one in the Rhine river basin and one in the Maas river basin. The probability of being too late for the Rhine scenario is 30%, assuming that the levee fails due to instability of its slope. The probability of being too late for the Maas scenario is nearly 100%, with the underlying failure mechanism being levee overflow. The time to failure of a levee body after the occurrence of overflow is short compared to the time required to apply an emergency measure. Furthermore, the model indicates that proactive action results in a proportional reduction in the likelihood of being too late.

The time-line of the logistical process can be divided into two periods: before and after the occurrence of damage to the levee. In the first period, between issuing a high-water alarm and the occurrence of damage, the emergency measure and the required personnel need to be prepared so that they are ready for deployment. If this process is initiated immediately after issuing a high-water alarm, the likelihood of not being ready when damage occurs is minimal. The second period, between the occurrence of damage and the successful placement of an emergency measure, is characterized by four processes: detecting the damage, the decision to repair the damage, transporting the emergency measure to the damage site, and finally placing the emergency measure. The model indicates that detecting the damage has the largest share in the overall logistical process, followed by placing, transporting, and decision, respectively.

Overall, the research indicates that the BresDefender can contribute to water safety, provided it is placed in time and is able to adapt to the irregularities of a levee. With further optimization of the system, the BresDefender could be deployed to provide reinforcement in the case of levee breaches. This offers possibilities to improved water safety, even in case of unforeseen circumstances.



# SAMENVATTING

Om laaggelegen gebieden, zoals Nederland, te beschermen tegen overstromingen, zijn waterkeringen aangelegd, zoals dijken. Alle waterkeringen moeten voldoen aan wettelijke normen voor waterveiligheid. Deze normen worden bepaald op basis van economische, sociale en individuele risicofactoren. Zelfs als de waterkering voldoet aan de vastgestelde normen, blijft er altijd een zekere kans op falen van de constructie, waarbij het falen van een waterkering leidt tot overstromingen. Dit zorgt voor zowel maatschappelijke als materiële schade. Noodmaatregelen kunnen uitkomst bieden om het onvoorziene risico op falen van een waterkering te verminderen en de negatieve effecten van een overstroming te voorkomen. Dit proefschrift behandelt de toepassing van noodmaatregelen, specifiek de BresDefender, die als doel hebben het faalproces van dijken te stoppen of te vertragen.

Als er een extreme waterstand in de rivier verwacht wordt, is er een kans op van het falen van een dijk aanwezig. In dit geval treden er crisisprotocollen in werking. Civiele crisisteams gaan de dijk om te controleren of er schade op een dijk ontstaat. In geval waargenomen schade, kan er worden besloten om noodmaatregelen in te zetten om een dijkdoorbraak te voorkomen. Als civiele partijen niet voldoende bekwaam personeel en middelen kan mobiliseren, wordt de hulp van defensie ingeroepen.

Het is een van de hoofdtaken van de Nederlandse krijgsmacht om hulp te bieden bij nationale crises zoals een hoogwatercrisis. Historisch gezien was het verzoek aan defensie voornamelijk gericht op assistentie bij het plaatsen van zandzakken en het verlenen van ondersteuning bij evacuaties. Klimaatverandering zal in de toekomst tot meer frequent hoogwater in de rivier leiden, waardoor de hulpvraag voor defensie naar waarschijnlijkheid groter wordt. De Nederlandse krijgsmacht dient ook zijn andere hoofdtaken uit te voeren. Dit vraagt om een efficiëntere toepassing van militair personeel en middelen, die gedeeld kunnen worden met civiele partners. Dit concept wordt 'adaptive krijgsmacht' genoemd.

Met het oog op het multifunctioneel inzetten van defensiemiddelen, zijn in dit proefschrift de fysieke werking en toepassingsmogelijkheden van de BresDefender onderzocht. De BresDefender is een militair ponton, dat onder normale omstandigheden wordt gebruikt om tijdelijke, drijvende bruggen te bouwen. Geïnspireerd op de heroïsche afsluiting van een beginnende bres bij Nieuwerkerk aan den IJssel, met het schip 'de twee gebroeders' tijdens de Watersnoodramp in 1953, wordt in dit proefschrift onderzocht of een soortgelijk resultaat ook op een wetenschappelijk onderbouwde manier kan worden behaald met de BresDefender. Door het ponton aan te passen, kan het tegen een lokaal verzwakte dijk worden afgezonken om deze dijk lokaal te versterken. Het grootste voordeel van het gebruik van een ponton is plaatsing vanaf het water, waardoor het gebruik van zwaar materieel op een dijk onnodig is. De effectiviteit van de BresDefender is opgedeeld in twee mogelijke effecten. Ten eerste, het effect op het water dat door een dijk infiltreert. En ten tweede, het water dat over een dijk heen stroomt in het



geval van een beginnende bres.

Om het effect van een noodmaatregel op het freatisch vlak in een dijk, te onderzoeken in zowel tijd als ruimte, zijn er fysische experimenten op twee verschillende lengteschalen uitgevoerd (zie hoofdstuk 2). Eerst op kleine schaal in het waterbouwkundig lab van de TU Delft, gevolgd door veldexperimenten op een 2 m hoge dijk in Flood Proof Holland, Delft. Tijdens deze experimenten is het effect van het (deels) afdichten van het buitentalud met een ondoorlatende constructie op het verloop van het freatisch vlak door een dijk in tijd en ruimte gemeten. De uitkomst van deze experimenten is geïnterpreteerd met behulp van een numeriek model. In theorie zou een perfecte aansluiting tussen constructie en ondergrond het niveau van het freatisch vlak door een dijk kunnen verlagen. Echter, in de praktijk blijkt deze aansluiting niet perfect te zijn, wat leidt tot een minimale verlaging van het freatisch vlak bij verschillende afdichtingspercentages van het buitentalud. Een goed afsluitende afdekking van het buitentalud zorgt er wel voor dat de tijd tot het bereiken van een evenwichtstoestand van het freatisch vlak, de tijd om een dijk te vullen met water, met ongeveer 50% kan worden verlengd. Bij de experimenten in het veld was de extra tijd tot het bereiken van een evenwichtstoestand van het freatisch vlak vooral meetbaar in het geval van een beschadiging aan een kleilaag die een doorlatende zandkern van de dijk afdicht. Het afdekken van een dijk om het freatisch vlak te beïnvloeden heeft alleen effect als het freatisch vlak nog niet de evenwichtstoestand heeft bereikt.

Het tweede effect op het faalgedrag van een dijk dat onderzocht is in dit proefschrift, is het effect van de plaatsing van een stijve constructie op het bresvormingsproces (zie hoofdstuk 3). Dit effect is onderzocht met behulp van fysische veldexperimenten in Flood Proof Holland, Delft en in de Hedwige-Prosperpolder. Een multiplex plaat (Flood Proof Holland) of het BresDefender ponton (Hedwige-Prosperpolder) is zonder de invloed van stromend water voor een lokale verlaging van een dijkkrui geplaatst. Door een waterstandsverschil tussen het water in het basin en de bres te creëren, ontstond er een stroming van lekwater door de openingen tussen het ponton en de ondergrond van de dijk. Het gemeten lekdebiet tijdens beide experimenten is minder dan 1% van het verwachte debiet dat door de bres had gestroomd zonder noodmaatregel. Tijdens de experimenten op ware schaal is dit effect gehaald door het militaire ponton te bekleden met een flexibel zeil, dat zich aan kan passen aan de oneffenheden in het talud van een dijk. Zonder gebruik te maken van dit zeil was het gemeten lekdebiet 23% van het te verwachten ongehinderde debiet.

Ook bij een gereduceerd debiet door een bres, met een geplaatste BresDefender kan er nog steeds erosie van het zandlichaam verwacht worden. De tijd die het duurt voordat de dijk, in deze studie beschouwd als een homogene zanddijk, tot falen komt bij met deze debieten is echter toegenomen van 30 minuten zonder maatregel naar meer dan 24 uur met een tijdig geplaatste noodmaatregel. Deze toename in de tijd tot falen kan mogelijk langer zijn dan de duur van een hoogwatergolf of biedt dijkbeheerders de mogelijkheid om, extra maatregelen te nemen om de dijk te stabiliseren.

Een belangrijke parameter bij het gebruik van noodmaatregelen blijkt de aansluiting tussen de noodmaatregel en het buitentalud van de dijk te zijn. Dit illustreert de noodzaak van het gebruik van een flexibel materiaal dat in staat is om zichzelf aan te passen aan de oneffenheden van een dijktalud. Dit kan worden gerealiseerd met zo-

wel het huidige prototype als een constructie dat werkt volgens dezelfde principes als de BresDefender. Het gedeomnstreerde effect geeft dus ook handvatten voor succesvol geïmproviseerde interventies tijdens hoogwatercrises.

Naast de effectiviteit van de noodmaatregel is ook de efficiëntie ervan onderzocht. In dit proefschrift is deze efficiëntie geformuleerd als de kans op het voorkomen van een dijkdoorbraak (zie hoofdstuk 4). Hiertoe is een probabilistisch model ontwikkeld dat zowel in staat is om de kans te bepalen op te late interventie in geval van een beschadigde dijk, als de kans op falen door een tekort aan waterkerende hoogte. Dit model is gebaseerd op de verwachte tijdschalen zoals vastgesteld met behulp van experts en literatuuronderzoek. De kans om noodmaatregelen succesvol te plaatsen is bepaald aan de hand van twee verschillende casussen, één in het stromingsgebied van de Rijn en één in dat van de Maas. De kans om te laat te zijn voor de casus Rijn is 30%, gegeven dat de dijk faalt door instabiliteit van het dijktalud. De kans om te laat te zijn voor de casus Maas is nagenoeg 100%, waarbij het onderliggende faalmechanisme dijkoverloop is. De tijd tot het falen van een dijklichaam na het optreden van overloop is kort vergeleken met de benodigde tijd voor het plaatsen van een noodmaatregel. Het model geeft bovendien aan dat proactief handelen leidt tot een evenredige verlaging van de kans op te laat zijn. De efficiëntie van een interventie neemt dan toe.

De tijdschalen in het logistieke proces kunnen worden onderverdeeld in twee periodes, voor en na het tijdstip waarop schade aan de dijk optreedt. In de eerste periode, tussen het afgeven van een hoogwateralarm en het ontstaan van schade, dient de noodmaatregel en het benodigde personeel gereed gemaakt te worden, zodat ze gereed zijn voor onmiddellijke inzet. Indien dit proces direct wordt gestart na het afgeven van een hoogwateralarm, is de kans om niet gereed te zijn bij het optreden van schade minimaal. De tweede periode in het logistieke proces, tussen het ontstaan van schade en het succesvol plaatsen van een noodmaatregel, wordt gekenmerkt door 4 deelprocessen: het detecteren van de schade, het besluit om de schade te repareren, het transporteren van de noodmaatregel naar de schade en tenslotte het plaatsen van de noodmaatregel. Het model voorspelt dat het detecteren van de schade de tijd kritische schakel is in het totale logistieke proces, gevolgd door respectievelijk het plaatsten, het transport en de beslis-sing.

Dit onderzoek toont aan dat een noodmaatregel, zoals de BresDefender een bijdrage kan leveren aan de waterveiligheid, op voorwaarde dat deze op tijd is geplaatst en flexibel genoeg is om goed te kunnen aan de oneffenheden van een dijk. Na verdere optimalisatie van het systeem zou de BresDefender kunnen worden ingezet om versterking te bieden bij doorbrekende dijken. Dit biedt mogelijkheden om, zelfs onder onvoorziene omstandigheden, de waterveiligheid te waarborgen.



# ACKNOWLEDGEMENTS

Reflecting on the last 5 years of work, all encapsulated in this booklet, brings immense joy as I reminisce about this incredible journey and the individuals who supported me in various ways throughout the process. First and foremost, my sincere gratitude goes to my supervisory team, consisting of Alexander, Bas, Edwin and Bas. Alexander, thank you for all of the invaluable discussions we had, especially those in Den Helder. The *Wouter*, the dame Blanche contest, which was undoubtedly won by *Witte raaf*, and the Piet Paaltjens tour made the journey memorable.

Bas Hofland, your boundless enthusiasm for every topic we discussed made everything seem effortless. Bas Jonkman, thank you for sharing your expert views on the world of flood risk and providing lightning-fast review responses. Edwin, thank you for the valuable discussions and for safeguarding the process.

A special acknowledgement to the Dutch Defense academy for their financial support of the research. A shoutout to the Defense colleagues Dennis, Sebastiaan and Chris. Dennis, thanks for coming up with practical and realistic solutions for the construction of several measurement setups. Sebastiaan, thank you for exemplifying the real military "do" approach. Chris, thank you for the valuable input in the research, shedding light on the thesis from another angle.

I extend my appreciation to the Water Risk Training and Expertise Centre for fostering civil-military collaboration, enabling the testing of the BresDefender prototype in the Hedwige-Prosperpolder. Thanks to everyone involved in the Polder2c's research project, for their advice and assistance in the in the full-scale experiments. A heartfelt thanks to the team from *105 Genie Compagnie Waterbouw* for their significant contribution to the BresDefender experiments during the large scale tests. The *Crisis Expert Team Waterkeringen* are also thanked for supporting the research in both advise and filling in the questionnaire, which served as the basis for one of the chapters in the thesis.

The lab technicians of the TU Delft hydraulic engineering laboratory deserve special mention for their support and advise in all of the conducted experiments. Thereby, the people of VPdelta+ are thanked for opening up their test facility Flood Proof Holland and providing logistical support.

Furthermore, I express my gratitude to Bart, Lucas, Merijn, Luuk, Ruud, and Dewa for their valuable contributions to the thesis. Whether as part of their own thesis or during their internship, the ideas and discussions we had truly sparked my imagination and elevated this thesis to a higher level. Additionally, I would like to thank all of the TU Delft colleagues who provided valuable content-wise input or offered some distraction from thesis writing. Special thanks, but not limited to: Miguel, Gina, Pengxu, Dirk, Mario, Su, Anne, Erik, and Jill.

Lastly, I would like to extend special thanks to all my family and friends who supported me in one way or another during this journey. First and foremost, my gratitude goes to my parents, stepparents, and siblings for their unwavering support throughout the process. To my dear friends, Tom, and the people from *het hok*, thank you for providing some distraction and offering innovative ideas that could be applied in the thesis.

# 1

## INTRODUCTION

*Wie nooit aan zee gewoond heeft,  
weet eigenlijk niet wat of waaien is*

Piet Paaltjens

## 1.1. INTRODUCTION

### 1.1.1. BACKGROUND

Low-lying delta areas, such as the Netherlands, are susceptible to flooding from both marine and riverine sources. This requires an extensive hydraulic infrastructure for flood prevention, such as water-retaining structures, like levees. In the Netherlands, the design requirements of levees are currently based on the assessment of individual, societal and economic risks (Slootjes and Most, 2016). This assessment leads to a residual level of risk, even if the defenses meet the required standards (Waal, 2018). Nevertheless, the potential consequences of an actual flood are severe, such as loss of life and large damage to properties (Jonkman, 2007). These flood risks may even become larger in the future, given the expected increase in storm intensity resulting from climate change (Kundzewicz et al., 2013). Incorporating measures into the water safety protocol to mitigate both accepted and unforeseen risks could prevent future floods, or at least reduce their consequences.

The protection against water in the Netherlands is based on three levels of a multi-layered safety approach (MinIenM, 2009). The first layer in this approach is protection, to avoid flooding through the use of water-retaining structures such as levees. The second layer is spatial design, that aims to reduce the effects of flooding by spatial interventions. And, the third and last layer is disaster control and emergency measures, e.g. evacuation, to avoid societal disruption. Mitigation of damages as a consequence of the accepted and unforeseen risk can be achieved in the third layer, for instance by the application of emergency response measures. An integral approach with respect to the various layers of total flood safety could lead to improved disaster preparedness (Bosoni et al., 2021).

Effective emergency response requires the presence of emergency protocols, since the time available to respond during a high-water crisis will be limited (CIRIA, 2013). Effective disaster control demands a thorough understanding of available emergency measures and their capability to arrest or reverse an (initial) failure mechanism (Schierreck, 1998). Currently, emergency response guidelines recommend the utilization of sandbags, big-bags and geo-textiles for the mitigation of various failure mechanisms (Hofmann et al., 2006).

Any levee failure process starts with the initiation of one or more failure mechanisms, as outlined by Schierreck, 1998. The extent of failure will progress, eventually causing water to flow over the crest of the levee, in the end reaching the final stage of the failure process, which is full levee breaching (Van et al., 2022). During this final stage, water flowing over the levee's crest leads to soil erosion. Ultimately, the levee is no longer able to fulfill its water retaining function, a condition referred to as failure. The levee breaching process has been found to consist of several stages, of which the early stages are characterized by a continuous discharge through a relatively small area, while the later stages are characterized by large discharges through larger areas (D'Eliso, 2007; Visser, 1998; Zhu, 2006).

Historical attempts to intervene in the breaching process did involve the application of vessels, as illustrated in figure 1.1 (Henning and Jüpner, 2015; Rijkswaterstaat, 1961), soil filled bags placed by helicopter (Norfolk, 2020; Seed et al., 2006) or the application of other large items available near the breach location. Many of these attempts to intervene

in the breach process proved unsuccessful. They only managed to contain the breach after the levee had reached the state of failure.



Figure 1.1: (left) Successful breach closure with vessel Nieuwerkerk aan de IJssel, Netherlands 1953 and (right) unsuccessful breach closure with vessels Fischbeck, at the Elbe river, 2013 (Mauritius Images / Alamy Stock Photo)

Past, experiments have been conducted to test the effectiveness of emergency measures. These tests either involved the application of intervention measures to temporarily increase the crest height of the levee with e.g. sandbags (Massolle et al., 2018; Pinkard et al., 2007) or repair measures applied in the late states of the breach formation process (Resio et al., 2011). In the past, physical experiments to mimic real-world levee breaches have been conducted. An example is the levee breach of the New Orleans 17th Street Canal during Hurricane Katrina. Within this experiment the maximum flow velocities and the best closure method for the specific levee breach were investigated (Sattar et al., 2008; Van Emelen et al., 2012). This experiment also considered the minimal required weight of a sandbag to be applied successfully given the actual flow velocities (Chaudhry et al., 2010).

Implementation of emergency measures is a labour-intensive effort, necessitating the presence of a dedicated workforce (Nat, 2012). Availability of well-trained people is an important aspect in successful application of emergency measures (Schmidt, 2014). Here, successful application of the emergency measure means that the failure process is interrupted and the water retaining function of the levee is maintained. In cases where civil authorities lack the necessary resources, military capabilities may be mobilized to provide the required personnel and support. Within the Dutch context, this complies with the third main task of the Dutch army as formulated in the *Nederlandse Defensie Doctrine* (Sellmeijer, 2019): to offer support during national crises situations such as floods. In these cases the Dutch military is able to support with personnel and equipment (Reijnen et al., 2018). Three (recent) instances of high water crises in the Netherlands where the military provided emergency assistance were the Watersnoodramp in 1953 (Rijkswaterstaat, 1961), the extensive evacuation of Rivierenland in 1995 (TAW, 1995), and the 2021 summer flood in Limburg (Rongen et al., 2021). During these floods, the military was mainly involved in supporting the evacuation of people and in placing sand- and bigbags serving as emergency measures.



### 1.1.2. BRESDEFENDER

In this research, the BresDefender, which literally translates to *BreachDefender*, is the waterborne emergency measure that is scrutinized. The BresDefender is an emergency response measure which intends to mitigate damage in the early stages of the levee breaching process. The current BresDefender prototype is a floating pontoon, normally used by the military to construct floating, temporary bridges (figure 1.2). By adjusting these pontoons in an appropriate manner, they can be filled with water, after being shipped and strategically positioned on a weakened levee section. The BresDefender can be installed through a waterborne operation, reducing the need for heavy machinery on the levee section that may already be locally weakened. Furthermore, several pontoons can be coupled to increase the effective length on which the measure can operate. Typical dimensions of the pontoon, as used in this thesis, are summarized in table 1.1.

Table 1.1: Dimensions BresDefender prototype

	Value	Unit
Length pontoon top	8.1	m
Length pontoon bottom	6.1	m
Width pontoon	6.7	m
Height pontoon	1.1	m
Mass empty pontoon	5450	kg
Volume pontoon	52.4	m <sup>3</sup>

Initially, the BresDefender prototype was successfully tested during the 2014 civil-military crisis training exercise *Alert*. However, little to no details of this exercise have been reported. All available background knowledge regarding functioning of the BresDefender prototype is based on photographs and interviews with people who were present during the exercise. Preliminary laboratory experiments have been conducted to test the effect of a scaled BresDefender on a failing levee (Elsing, 2018). The results of these experiments were promising, but more research was needed to scientifically underpin the effect of the BresDefender on the levee failure process. This has led to start of the research presented in this thesis.



Figure 1.2: BresDefender pontoon connected to a boat for transportation

### 1.1.3. EMERGENCY RESPONSE STRATEGIES

Successful application of emergency measures does rely on several critical aspects: detection of the weak spot that has to be reinforced, timely deployment of the measure at the required location, safe operation conditions for the personnel involved in properly placing the emergency measure, and sufficient structural resistance of the installed measure (Lendering, 2018). Furthermore, early flood warning systems and adequate crisis decision procedures are important aspects in the emergency response process (Pappenberger et al., 2015; Sene, 2008). All of the above mentioned aspects of a high water crisis are summarized in figure 1.3, which sketches the progress of damage on a levee (system) over time and the possible effect of an emergency intervention on the damage growth process. Here, damage may refer to either deformation or erosion of the levee.

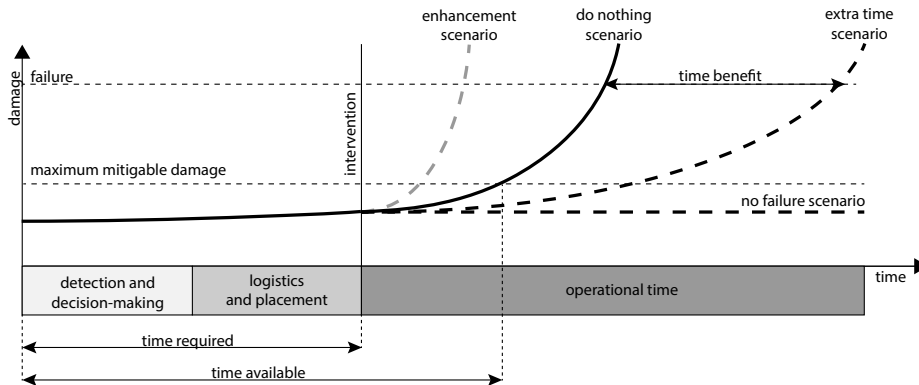


Figure 1.3: Application of emergency measures: the development of damage to a levee over time (upper part) and logistical aspects for emergency response (lower part) as presented in Janssen et al., 2021

The concept, as presented in figure 1.3 shows two different time scales. First the time required ( $t_{req}$ ), which depends on details of damage detection, decision making and logistics involved in emergency measure placement. Secondly, the time available ( $t_{avail}$ ), which depends on levee characteristics. An emergency measure is assumed to be in time if the required time to properly position an emergency measure on a damaged levee section is smaller than the time for the damage to exceed the mitigable damage level. When the breach dimensions or flow velocity through the breach have become too high, the damage is considered to be beyond repair. The time required before intervening in the damage process consists of four steps: detection, decision making, logistics and placement. Detection involves identification of the presence of damage at a certain location on the levee. Decision making relates to the chain of consultations leading to the decision of launching emergency measures. Logistics involves the transportation of necessary resources from storage to the required levee section. Placement involves the placement of the emergency measure to ensure optimal performance.

Intervening in the damage process can lead to several outcomes (figure 1.3). When the extend of damage exceeds the failure threshold level, the levee can no longer fulfill its primary purpose, which is to maintain a pressure head difference between the river and

the low-lying area. Then, the failure has led to the inundation of the hinterland due to flooding. The effect of intervention through an emergency measure is relative to the 'do nothing' scenario, the scenario which would occur when no emergency measure is being placed at all. A first possible outcome after intervention in the damage process is the 'no failure' scenario. In this case the emergency measure completely stops the development of damage over time, stabilizing the damaged levee. A second possible scenario is the 'extra time' scenario, in which the time till reaching the failure threshold is extended compared with the 'do nothing' scenario. A third scenario is the 'enhancement' scenario, in which case an intervention does reduce the time to failure. This scenario should be avoided at all times. All of the aspects mentioned should be considered in assessing the effectiveness of an emergency measure.

## 1.2. KNOWLEDGE GAPS

The knowledge gaps that drive this research effort are identified in line with figure 1.3, distinguishing the time required before intervention, and physical processes related to levee integrity after intervention in the levee failure process. Time is a crucial factor in assessing the success of emergency measures. Time reigns the duration of the flood wave, the logistical effectiveness and the spatio-temporal resilience of levees after intervention (Van et al., 2022). The inherent heterogeneity of levees complicates the prediction of time-to-failure, requiring the implementation of fragility curves (Kolen et al., 2021; Marijnissen et al., 2019) or advanced probabilistic approaches (Pol et al., 2023). Additionally, the location of a potential levee breach will be uncertain, necessitating assumptions to accurately estimate the appropriate time frames within a high-water crisis, along with their corresponding uncertainties. This requires a probabilistic model, coupling the physical failure behavior of a levee with the logistical considerations involved in applying an emergency measure, to estimate the likelihood of successful intervention. Moreover, it will allow to identify possible improvements in emergency response.

The underlying levee breaching physics is relatively well understood, in particular for the case of homogeneous levees constructed of sand (Visser, 1998) and clay (Zhu, 2006). However, the physics of levee breaching processes when emergency measures are applied, are much less researched. Historical interventions in the breaching process often occurred in the later stages, where breach dimensions, and flow velocities together, were relatively high. In these cases, attempts have been reported to close the breach with trucks, vessels, big-bags and other sizable items available (Foster, 2011; Sattar et al., 2008). However, in many cases the hydraulic loads on these objects were too large, causing them to flow away. A notable success story is the placement of the vessel *de twee gebroeders*, effectively positioned in front of an early stage breach, to prevent the flooding of a large polder area near Nieuwerkerk aan den IJssel, during the Dutch *Watersnoodramp* in 1953 (figure 1.1). Witness reports emphasized the crucial role of improvised actions of the local authorities (Rijkswaterstaat, 1961). Several pioneering studies have investigated the use of emergency measures to stop levee breaching (Albers, 2014; Joore, 2004), however, validated emergency measures to stop levee breaching in its early stages is hardly available (Foster, 2011).

A physical condition that can accelerate failure processes of levees is the phreatic surface level, which may result in slope instabilities caused by saturation of the soil (Van

et al., 2022). Guidelines (Darmstadt, 2006) and historic events (TAW, 1995) have demonstrated the use of seals to influence the phreatic surface level, regardless of damage to the outer slope of the levee. However, the spatio-temporal effects of such emergency measures on the phreatic surface level remain unknown.

In response to new global threats, the Dutch Defence sought for multifunctional application of equipment (MinDef, 2020), in alignment with legally defined third task of the Dutch military, which is to provide support during national crises (Sellmeijer, 2019). The Netherlands Engineer Regiment is equipped with tools available for hydraulic engineering applications, e.g., constructing floating temporary bridges. To support during national high-water crises, the Regiment may consider application of their equipment in a way that is was not intended for. This aligns with the concept of an *adaptive army*. Based on the promising primarily results of tests with the BresDefender prototype, the Regiment sought to acquire more scientifically underpinned data for the application of the BresDefender during a high-water crisis.

### 1.3. RESEARCH OBJECTIVES

The goal of this thesis is to provide a scientific underpinning for the knowledge gaps outlined in section 1.2 and to address the demands posed by the project stakeholders. This thesis contributes to these objectives by contributing to the scientific understanding of both the physical and logistical processes involved in implementing a waterborne emergency measure to prevent or postpone the levee breaching process in its early stages. A comprehensive and scientific description of these processes will aid the water safety community in adopting a more structured emergency response approach for these water crises. Moreover, the research outcomes can also help to define boundary conditions for other successful improvised, waterborne emergency interventions. The case of BresDefender shall thus be considered as a special case of a wider range of emergency measures, whose more fundamental workings principles will not be too different from the BresDefender case.

### 1.4. RESEARCH QUESTIONS

As stated, the objective of this thesis is to identify and quantify the most important parameters essential for the successful application of emergency measures in the early stages of a levee breach. This leads to the formulation of the main research question, which derives from identified knowledge gaps:

*What are the key factors and critical parameters that allow for the effective application of early-stage emergency measures, specifically the BresDefender, preventing or postponing the development of levee breaches?*

In this context, the effectiveness of an emergency response intervention is defined as further development of levee breaches, such that the levee will survive the flood, and potential flooding of the hinterland is drastically reduced. To address the main question, three research questions have been formulated, focusing on the effectiveness and efficiency of emergency measures.

- RQ1.** What is the spatio-temporal effect of an impermeable cover on the phreatic surface within a levee?
- RQ2.** What are the key parameters that influence the flow through an initial breach when applying emergency measures, which act as a seal and arrest the water flow in a breach, such as the BresDefender system?
- RQ3.** What are the critical steps in the logistical process in the (pre-)implementation phase of an emergency measure and how do they affect the likelihood of success?

## 1.5. RESEARCH APPROACH AND OUTLINE

This thesis focuses on two important aspects of applying emergency response measures as presented in figure 1.3. These are the logistical operation before, and the physical response after implementation of an emergency measure. The first two chapters of this thesis focus on the effectiveness of an emergency measure in the form of a stiff seal, assuming successful implementation. Physical aspects of the effect of interventions are separated into the effect of an emergency measure on the water flowing over and the water flowing through a levee, respectively.

The validation of the effectiveness of an emergency measure is achieved through physical experiments on three different length scales, as summarized in table 1.2. Here, the length scale refer to the water-retaining height of the levee in the various experiments. The smallest length scale involves laboratory experiments conducted at the TU Delft Hydraulic Engineering Laboratory. The second scale involved intermediate scale tests conducted at Flood Proof Holland (FPH) in Delft, an experimental area where emergency response measures can be tested. These experiments were performed on a 1.8 m high levee situated in a water basin. The third test site involved real scale experiments within the Hedwige-Prosperpolder (abbreviated as Hedwigepolder), where a living lab environment was created. A large water basin was constructed with an area of 150 m to 50 m surrounded by a 5 m high levee in the former Hedwigepolder, the Netherlands. This allowed experiments with a real-scale BresDefender at water heights that resemble emergency conditions. Figure 1.4 shows the experimental environments which were used within this research to access the length scales of interest.

Table 1.2: Physical model tests conducted on various scales within research

	Experiment	Scale [m]	Focus	Chapter
A	Hydraulic engineering laboratory	Small	Phreatic line	2
B	Flood Proof Holland	Intermediate	Phreatic line Inflow	2 and 3
C	Hedwigepolder	Full	Inflow Operation	3

Chapter 2 studies the the spatio-temporal behavior of the phreatic surface through a levee, with a focus on how damage to the outer slope influences this phenomenon. A



Figure 1.4: (left) TU Delft hydraulic laboratory test site (middle) Flood Proof Holland test site (right) Hedwige-Prosperpolder test site

schematisation of this scenario is shown in figure 1.5. The effectiveness of emergency measures on the phreatic surface through a levee is demonstrated using physical experiments at laboratory and intermediate scales. A limit equilibrium analysis was employed to predict the outcomes of the tests and subsequently validated with the experimental data. Then experimental data were used to validate a theoretical model which describes the spatio-temporal behavior of the phreatic surface through a levee.

The response to water flowing over a levee, by implementation of an emergency measure, is examined in chapter 3. The focus in this chapter is to investigate the impact of an intervention on the breaching process, specifically for scenarios in which a levee has experienced a local reduction in crest height. This scenario is also schematized in figure 1.5. The effectiveness of emergency measures on the mitigation of levee breach formation is demonstrated using physical experiments on intermediate and full length scales. The full scale experiments involved application of the real scale BresDefender prototype (figure 1.2). The data thus collected then analyzed and incorporated into a physical based model.

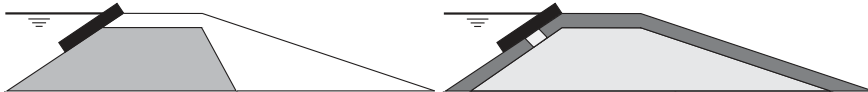


Figure 1.5: (Left) Application of an emergency measure to intervene in the levee breaching process caused by a local crest height reduction (chapter 2) and (right) applying an emergency measure to intervene in the phreatic surface level to reduce water inflow (chapter 3)

Next, the results and lessons learned from the chapters describing the physical effects of an intervention on levee failure, serve as input for chapter 4. In this chapter the research concentrates on the efficiency of applying emergency measures, defined as minimizing the probability of failure caused by the logistical process and insufficient structural resistance. This chapter concentrates on minimizing the time between a flood warning and implementation of an emergency measure. Minimizing this time would allow for enhancing the success rate of emergency measures. A probabilistic (monte carlo) model has been developed to estimate the critical duration of time steps in the process from the initial high-water warning to full placement of the seal. The model takes into account both expert judgment analysis and an extensive literature review as input sources. The model is applied to two case studies relevant to the Netherlands,

specifically the Meuse and Rhine river basins.

Finally, the key lessons learned from each individual chapter, as well from a more integrated point of view, are summarized in chapter 5, along with recommendations for future research. The research framework is depicted in figure 1.6, illustrating the inter-connection of the various chapters within this thesis.

All raw data acquired from the various experiments is made available through the 4TU repository (Janssen, 2023).

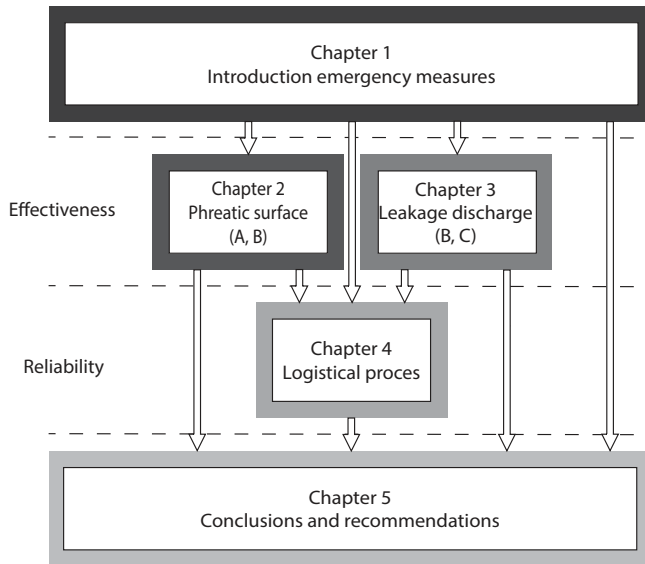


Figure 1.6: Flow chart of this thesis, the letters refer to the scale of experiments, introduced in table 1.2

## 1.6. RESEARCH SCOPE

The primary focus of this research is to validate the effectiveness of a waterborne emergency measure to stop the levee breaching process in its early phases. This paragraph describes the aspects that are not taken into account during the study, but should be incorporated to increase the technical readiness level of emergency response measures, and the BresDefender in particular. At first, the dynamics of the placement process of an emergency measure is not taken into account. Within this thesis, it is assumed that the placement of the emergency measure was successful, neglecting the dynamic process which occur when sealing a breach. Furthermore, external physical conditions which will set the application limits for placement, such as wind, waves and levee accessibility are not considered either. For real life cases, the conditions mentioned should be taken into account, most importantly to ensure the safety of the personnel operating the emergency measure. Secondly, the internal strength of the emergency measure, to withstand the loads of the pressure head difference was assumed to be sufficient within the research. A third choice within this research is to consider the application of only

a single BresDefender unit. In real life conditions, the length of the pontoon should be increased to be able to repair larger failures. This could be achieved by mechanically coupling several pontoons.

### PROJECT CONTEXT

The majority of the research was funded by the Dutch Ministry of Defence, except for the large scale experiments in the Hedwige-Prosperpolder, which were part of the Interreg Polder2C's project (polder2cs.eu). The experiments involving the BresDefender were part of the emergency response work package and primarily focused on civil-military collaboration during a flood crisis and the role of the military within the crisis response. The primary objective of this research, and the cooperation of defense within the Polder2C's project, was to provide experimental and theoretical foundations for high-water emergency measures within the military toolbox that can be employed to assist civil authorities during a high-water crisis. These findings may be generalized to optimize the successful employment of the BresDefender in specific, and provide guidelines for optimal improvised approaches to emergency response.





# 2

## EXPERIMENTAL STUDY OF WATER INFILTRATION INTO A PARTIALLY SEALED LEVEE

*Unfortunately, soils are made by nature and not by man,  
and the products of nature are always complex...*

Karl von Terzaghi

---

This chapter has been submitted as: D. Janssen, D.P. Hommes, A.J.M. Schmets, B. Hofland, C. Zwanenburg, E. Dado and S.N. Jonkman. Experimental study of water infiltration into a partially sealed levee.

## 2.1. INTRODUCTION

During extreme high-water events, a levee system will be subjected to increased hydraulic loads, which may trigger various failure paths (Van et al., 2022). These failure paths include both internal and external processes. Internal processes are caused by a rising phreatic surface level in the levee, while external processes are caused by e.g., wave loads and lateral flow. The various failure processes can enhance each other, leading to failure of the levee, followed by an uninterrupted water flow through the levee breach into a low-lying area. Implementing an emergency measure means externally intervening in the damage process to locally improve the strength of a levee. Here we focus on the effect of an emergency response intervention that intends to affect the development of the phreatic levels in a levee due to riverside infiltration, which may promote damage processes.

Historical attempts to decrease the water infiltration into a levee often included the application of geotextiles. In 1995, a levee along the river Rhine, near Ochten, the Netherlands, which showed visual deformations of the levee body, was covered with geotextile to prevent levee failure (TAW, 1995). The levee survived, however, the contribution of this emergency measure on the local resistance of the levee was not determined then. In case of damage of the outer levee slope, guidelines for emergency response to block the inflow of seepage water basically recommend the use of geotextiles surrounded by sandbags (Hofmann et al., 2006). These guidelines are based on best practice, but little is known about the increment in local resistance to water inflow that can be achieved by applying these measures.

Circumstances might be such that placement of a seal is preferred from the water side. This can be achieved by transporting a floating, stiff structure over the water to the required location. The floating structure's bottom then holds a flexible sheet, which can adjust to the levee surface. Through partially submerging the structure at the site of interest, a seal at the levee's outer surface is established, kept in place by the anchored structure. This waterborne emergency method can be realized by using a military pontoon as the floating structure (Janssen et al., 2021). In this way, one can simultaneously locally raise a levee's crest and partly seal its outer surface. The phreatic level response of such seal is the subject under investigation in this study. Furthermore, the influence of the pressure that holds the seal in place will be neglected here.

Here, we consider a levee as a soil structure that allows infiltration of external water given an external water source at elevated hydraulic head levels. For the case of a high-water wave in a river, this pore water flow through the structure is caused by the hydraulic pressure difference between the river and the landside of the levee. The same effect may also be caused by precipitation and evaporation (CIRIA, 2013). Related to water flow within a levee during extreme water events, two fundamental timescales can be identified: the duration of the flood wave, and the time required for the phreatic surface to adjust to a new steady state situation (Beber et al., 2023; Vahedifard et al., 2020). In the case considered here, schematized in figure 2.1, the water in the river rises from average to elevated or high levels. Subsequently, the phreatic surface level in the levee will adjust, until a stationary state has been reached. This new steady state pressure head  $h$  on a specific location in the levee is reached at time  $t$ .

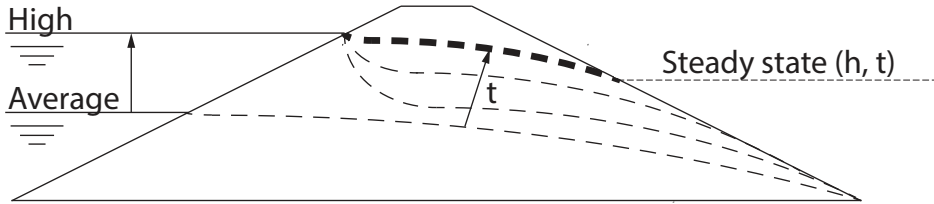


Figure 2.1: Development of the phreatic surface level in space ( $h$ ) and time ( $t$ ) through a levee after a sudden increase of the outer water level from average to extreme (high) conditions.

Levee failure mechanisms that are typically triggered by increased phreatic surface levels, are slope instability and internal erosion (Schierck, 1998). Firstly, an increased phreatic surface leads to increased local water pressures and decreases the effective stress of the soil. Hence, the shear strength reduces, which ultimately leads to mobilizing of one, or several consecutive slip planes, causing structural failure of the levee by slope instability (Van et al., 2022). Secondly, an increase of the phreatic level will also be accompanied by higher flow gradients in the levee, increasing the probability of internal erosion processes (Rijkswaterstaat, 2019).

In this study, a heterogeneous levee is assumed to consist of a permeable core, covered with a clay layer; this is assumed to be a Dutch standard levee, immediately after construction (Rijkswaterstaat, 2019). Local damage to the cover layer will reduce the resistance of the soil mass to water infiltration. The inflowing water will distribute itself in the three dimensions that make up the levee. The surface damage can have many physical causes, such as bad maintenance of the grass cover or impact damage by fallen trees. In recent years the issue of burrowing animals in levees has become an important issue in The Netherlands (Berg and Koelewijn, 2023), for example beaver dens that penetrate deep into the core of a levee (Žilys et al., 2009).

Here we start from the earlier observation that geotextiles have been applied to seal the outer slope of levees during high water crises. This practice is experience-based; a more fundamental understanding of the underlying mechanism of the positive effect of a seal on the 'survival rate' of levees during high water crises is still needed. Obviously, placement of a seal will locally decrease the inflow rate of water, which consequently would measurably influence the spatiotemporal behavior of the phreatic level, at least when the system is considered purely 2-dimensional. The change of phreatic level can then be related to the observed increase in failure resistance of a levee. Therefore, this study aims to research the phreatic surface's response to the placement of a seal at the outer slope of a levee.

A series of experiments has been designed to find out whether placement of a seal has a measurable and predictable influence on the phreatic surface. First, laboratory scale experiments are conducted. These laboratory experiments can be considered to represent an almost 2-dimensional case, i.e., the condition of an infinitely wide seal. Experiments intend to capture the phreatic response, by measuring the pressure head throughout the levee as a function of location and time. These experiments are then repeated for field conditions at the real-scale, which obviously captures the 3-dimensional effect of the seal if it were present. A final step towards actual but unfavorable emergency

conditions was achieved by artificially introduction of damage to the seal-covered outer slope and establishing the phreatic surface also for this scenario.

The laboratory experiments have been conducted on a homogeneous levee in the TU Delft Hydraulic Engineering Laboratory, while three-dimensional field experiments took place on a heterogeneous levee in the TU Delft test facility Flood Proof Holland. The experimental scenarios can also be studied by numerical simulations. Comparison of experiment and simulation should allow to show whether a 2D model already captures the essential features of the full-scale experiment. In a similar way, the quality of the seal could be obtained by comparing the temporal development of the phreatic line.

In conclusion, this research studies the effect of an impermeable seal placed at the outer slope of a levee. The anticipated effect of interest here is the change of the phreatic surface in space and time. This paper is further organized as follows. First, the conceptual framework of the spatiotemporal behavior of the phreatic surface in a levee, and how this framework changes when the outer slope is sealed in both ideal and non-ideal circumstances, is presented. Then the design and results of laboratory-scale experiments and the three-dimensional, real-scale experiments are presented. Finally, comparison of the experimental results and numerical simulation contributes to better understanding of the mechanisms that lead to delayed response of sealed levees.

## 2.2. CONCEPTUAL FRAMEWORK

Here, we introduce two aspects that together provide a conceptual framework for understanding the effect of a seal on the spatiotemporal development of the phreatic surface level in a levee. The first aspect considers idealized conditions, assuming a perfect connection between the levee surface and the seal. The second aspect includes an interface layer, which allows to address also non-ideal conditions (such as damages grass layers or a non-perfect soil-seal interface), aiming to be able to model realistic practical applications. Both cases assume idealized two-dimensional conditions.

### 2.2.1. CASE OF PERFECT CONNECTION

In idealized conditions, the connection between the seal and the soil is assumed to be perfect, without any voids. The length of the impermeable seal is considered a variable, which is expressed as a coverage ratio  $C$  (equation 2.1). The length of the seal,  $L_p$ , is the length of the seal from the outer water level to the lowest part of the seal. The length of the uncovered slope below water surface,  $L_w$ , is the length from the lowest part of the seal to the toe of the outer slope of the levee (figure 2.2).

$$C = \frac{L_p}{L_w + L_p} \cdot 100\% \quad (2.1)$$

If the outer levee slope is sealed to limit the inflow of water, the development of the phreatic surface level through a levee in space and time will adjust according to the new boundary conditions (figure 2.2). The length of the flow path will increase, caused by the presence of the seal. However, the total pressure head difference between the boundary conditions remains the same. This leads to a reduced gradient of the flow and herewith a lower Darcy velocity ( $q$ ). Thus the time to reach steady state ( $\Delta t$ ) will increase compared

with the case without a seal. Next to that, a reduction in steady state phreatic water level ( $\Delta h$ ), compared with the undisturbed case is expected.

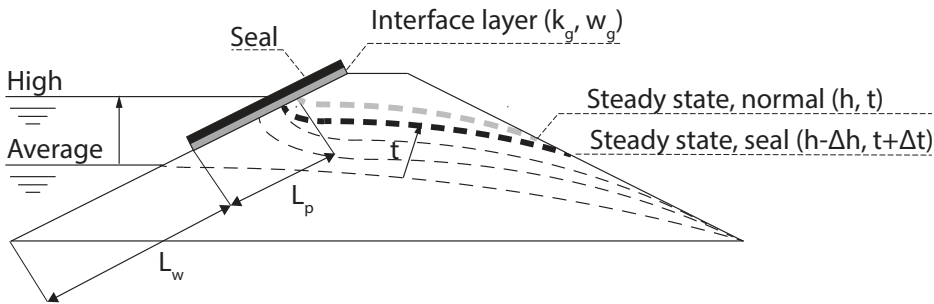


Figure 2.2: Development of the phreatic surface level in space and time through a levee after an increase of the water level from average to extreme (high) conditions, while applying an impermeable seal on the outer levee slope.  $\Delta h$  is the difference in phreatic surface level, and  $\Delta t$  the difference in time to reach these conditions, as compared to the situation without a seal.  $k_g$  is the resistance of the interface layer and  $w_g$  the width of an interface layer, these values represent a non-idealized surface-seal connection

### 2.2.2. CASE OF IMPERFECT CONNECTION, SURFACE-SEAL INTERFACE LAYER

The boundary conditions in the real world will not be perfect. The levee surface will, in practice never be entirely smooth, and the seal will not be able to completely adjust itself to these irregularities. The occurring surface-seal distances will allow water to flow underneath the seal. This water will be able to seep into the levee, reducing the effectiveness of the seal. This practical limitation requires the need for an extra interface layer in the conceptual model (figure 2.2). Two parameters are introduced to take account for these irregularities, the thickness ( $w_g$ ) and the hydraulic conductivity of the new interface layer ( $k_g$ ). The thickness,  $w_g$  does essentially originate from irregularities of the outer slope of the levee. The hydraulic conductivity of the interface layer,  $k_g$ , represents the resistance of the infiltrating water flow in the interface layer, caused by the fraction of seal in contact with the levee its surface.

## 2.3. LAB SCALE EXPERIMENTS

### 2.3.1. EXPERIMENTAL SETUP LAB EXPERIMENTS

Experiments were conducted in a flume in the TU Delft Hydraulic Engineering Laboratory. These experiments aimed to determine the effect of a seal on the phreatic surface level through a model levee in space and time. A homogeneous sand levee with a width along the levee axis of 0.77 m and a height of 0.8 m was constructed in the sedimentation flume of the laboratory. The crest width of levee was set to 0.2 m, the gradient of the outer slope to 1:2 and the gradient of the inner slope to 1:3. A sketch of this test setup is shown in figure 2.3. The inner slope of the levee was covered by a water permeable geotextile, covered by a gravel layer, to avoid internal erosion, the movement of the grains on the inner slope, caused by the exit gradient of the flow (figure 2.4). The levee was

constructed by applying subsequently multiple layers of sand, each of approximately 5 cm thickness. After a layer was placed, it was compacted using the weight of a human operated masonry trowel.

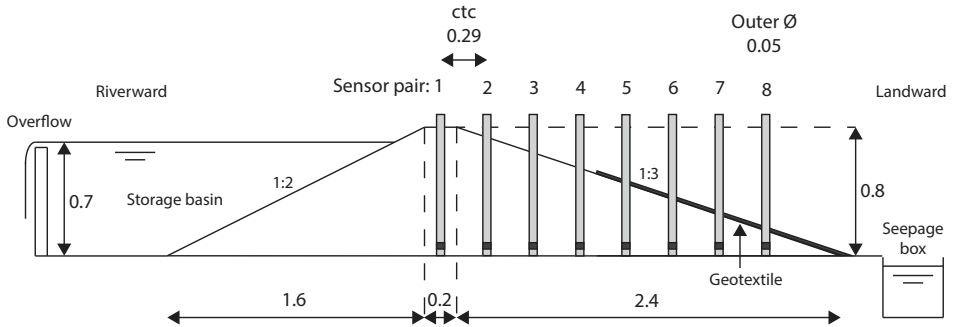


Figure 2.3: Dimensions test levee, sensor rows and various important parameters (dimensions in m), c.t.c. is center to center distance.

The levee was built out of standard silver sand. Several soil parameters were determined in the laboratory and are shown in table 2.1. The saturated permeability,  $k_{sat}$ , of the sand was determined with a falling head test. A HYPROP experiment (Schindler, 1980) was conducted to determine the soil water characteristic curves (SWCC) and the saturated volumetric water content,  $VWC_{sat}$ . It should be noted that the experiments to determine soil parameters were conducted with the same sand, but did not represent in-situ soil samples, thus the sand may possess a different density in the experiment.

Table 2.1: Soil parameters silver sand from which the model levee has been constructed

Parameter	Value	Unit
$d_{50}$	0.4	mm
$k_{sat}$	$5.12 \times 10^{-3}$	m/min
$VWC_{sat}$	0.347	-

The local pressure head near the bottom was measured using electronic pressure sensors (*Honeywell*, 24PC) that were installed in standpipes in the cross section of the levee. Two rows of eight PVC standpipes were glued to the bottom of the flume. The center to center (c.t.c.) distance of the standpipes in the direction parallel to the levee's crest was 0.35 m, the c.t.c. distance in longitudinal direction was 0.29 m. The outer diameter of the PVC standpipes was 0.05 m. Water was able to flow into the standpipe through a water inlet, which was located between 0.04 and 0.08 m from the flume bottom. The pressure sensor automatically corrected for the atmospheric pressure by using a Wheatstone bridge. The output of the sensor was a voltage, which could be transformed into a water pressure using a calibration factor. The sampling interval of the sensors was set to 60 seconds.

Seepage water that flowed through the levee was collected in a seepage box at the landward toe of the levee. The water level in the box was measured using a *Temptonic*



Figure 2.4: (left) Landward and (right) riverside view of the experimental setup for LT-4.

*G-Series GH* rod location sensor. The measurement interval of the rod was set to 60 seconds. The leakage discharge through the model levee was determined by determination of the fill rate of the box, correcting for its irregular shape.

The main goal of the experiments was to determine the effect of an impermeable seal on the phreatic surface level through a levee in space and time after a sudden increase of the outer water level. The seal consisted of an impermeable steel stiff plate (1.44 m length, 0.77 m width and a 8 mm thickness), covering the wetted outer slope of the levee (figure 2.4). To prevent water to enter the levee through the area between the plate and the glass sidewalls of the flume, this slit was closed with an impermeable tape.

In total, four experiments were conducted, of which two experiments served as a repeated for the reference case without the application of a seal. The other two experiments were conducted with a near total coverage of the outer slope. The latter two experiments differ in the presence of a toe, sealing the inlet at the bottom of the outer slope. This toe structure consisted of an extra layer of sand up to the lower edge of the seal plate. It is shown in the right image of figure 2.4. The reason for applying this toe were the openings were observed between the plate and the sand body. These were caused by the stiffness of the plate and the irregularities of the outer slope, allowing water to flow underneath the plate. The maximum observed opening was approximately equal to the thickness of the plate (8 mm). The toe had a width of 10 cm and a height of 5 cm. The lab scale experiments performed for model levee with and without a steel seal cover at the outer slope of the model level are summarized in table 2.2.

Table 2.2: Scaled lab experiments on phreatic response to sudden rise of water level

Test number	Coverage [%]	Note	Fill time [min]	$Q_{steady}$ [l/s]	
				Sensor	Per $m^1$
LT-1	0	Reference	44	0.026	0.034
LT-2	0	Reference	50	0.026	0.034
LT-3	99	-	42	0.026	0.034
LT-4	99	Riverward toe	41	0.022	0.026



Before the start of the experiment, the pressure sensors were turned on for at least one hour, to determine the initial conditions of the sensors. After this, water was allowed to enter the storage basin (figure 2.3) through a hose. The maximum water level was 0.7 m, which was enforced using an overflow structure at the end of the storage basin. During the experiments, a continuous inflow of water in the basin was maintained, to keep a constant water level in the storage basin. The time needed to fill the storage basin, the fill time, is given in table 2.2. The output voltages of the pressure sensors were monitored during the experiment. When these voltages exhibited no increase in value, at the  $10^{-3}$  digit, for least one hour, one could assume that the phreatic surface level in the levee had reached steady state conditions. When these conditions were achieved, water was removed from the basin, and the pore water release process from the levee was measured in a similar way as during filling. A new experiment starts if the water level, as measured by the pressure sensor, had equilibrated at the initial measured value. One experiment was performed per day.

### 2.3.2. LAB SCALE MEASUREMENT RESULTS

The main results of the experiments are summarized in Table 2.3. It shows the time required to reach steady state,  $t_{steady}$ , for each experiment together with the corresponding steady state water level  $h_{steady}$ , for each location, in each pressure sensor. At  $t = 0$ , water starts to enter the basin. The time to steady state is the time required from opening the hose at the start of an experiment until the measured gradient ( $\frac{\delta h}{\delta t}$ ) has become smaller than  $1 \times 10^{-3}$  m/min. The steady state time has been determined after the experiments, incorporating the sensor specific voltage to height calibration factor. This gradient is assumed to provide a good estimation of the steady state time, since this gradient represents more than 90 percent of the maximum steady state level, for the worst-case scenario (LT-4). Allowing a smaller gradient would increase the time to steady state, whereas the increment in water level would be small. The parameter  $h_{steady}$  is the maximum measured value of the individual sensor.

Table 2.3: Main results laboratory experiments (Figure 2.3 for sensor locations)

Sensor pair	$t_{steady}$ [min]				$h_{steady}$ [min]			
	Test: LT-1	LT-2	LT-3	LT-4	LT-1	LT-2	LT-3	LT-4
1	83	87	119	147	0.48	0.48	0.49	0.50
2	84	89	93	134	0.44	0.44	0.47	0.41
3	90	101	126	165	0.41	0.40	0.37	0.36
4	84	88	91	135	0.37	0.38	0.32	0.34
5	80	85	82	119	0.32	0.32	0.31	0.31
6	77	80	78	113	0.26	0.26	0.26	0.25
7	72	77	75	105	0.17	0.17	0.18	0.17
8	67	72	88	-	0.10	0.10	0.10	0.10
Mean	80	85	94	112				

The steady state leakage discharge data through the model levee,  $Q_{steady}$ , is provided in table 2.2. The sensor steady state discharge is the discharge as measured by the sensor. While the  $\text{per m}^1$  is the steady state discharge corrected for the flume width. The steady

state leakage discharge was determined by measuring the water level in the discharge box over time.

Figure 2.5 shows the measured phreatic water level for sensor pair 1, 3, 5 and 7 over time, for the different tests (Table 2.2). The presented data is the data measured by the right sensor in the sensor row, as seen from the crest. For sensor pair 3 and 4, the measurements of the left sensor are used, caused a defect in the right sensor. Figure 2.6 shows the spatial pattern of the phreatic surface level through the levee at different times at each sensor pair position, figure 2.6 is constructed from the data as presented in figure 2.5. The reported water levels are related to the initial conditions of the sensors. The mean time required for the LT-1 and LT-2, the reference case, to reach steady state conditions ( $t_{steady}$ ) is the same order of magnitude of 80 to 85 minutes. The time to reach steady state conditions for the LT-3 is about 40 minutes longer for the first three riverward sensor rows. However, this increase in time to steady state disappears for the sensor rows closer to the landward toe of the levee, in line with expectations. In LT-4 (with seal and berm), the time required to reach steady state conditions increases over the entire cross-sectional profile of the levee. Steady state phreatic surface levels are found to be nearly equal for all the experiments. Only a slight lowering of the phreatic surface at sensor pairs 3 and 4 may be present, although this difference is close to the measurement accuracy. This accuracy includes the accuracy of the sensors (+/- 1 cm) and the measurement accuracy of the elevation of the sensors (+/- 1 cm).

The presence of the toe at the bottom of the levee in LT-4, clearly shows a large influence on the development hydraulic head in the levee. It should be noted that roughly up to 100 minutes the phreatic level is significantly lower than the case without toe and the reference case. This corresponds to an increase in time of 25% to 50% relative to the scenario without toe and the reference scenario respectively to reach the steady state phreatic level.

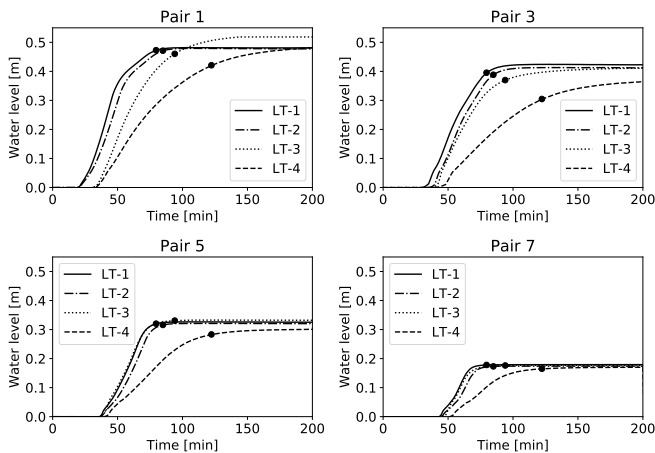


Figure 2.5: Water level over time for sensor pair 1, 3, 5 and 7 in the model-levee of the lab experiment, black dots represent steady state time

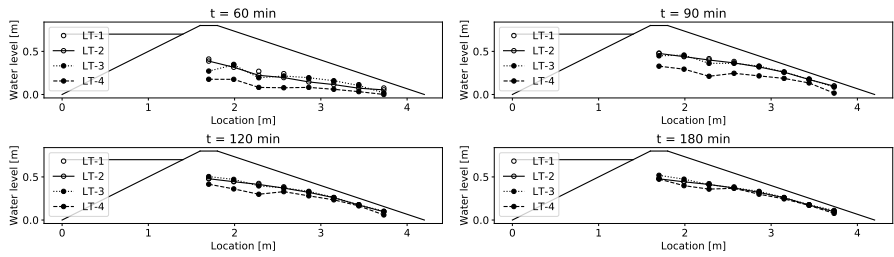


Figure 2.6: Measured phreatic levels in the model-levee at several times after riverside water level rise

## 2.4. REAL-SCALE FIELD EXPERIMENTS

### 2.4.1. EXPERIMENTAL SETUP FIELD EXPERIMENTS

To gain insight in the effects of an impermeable seal on the development of the phreatic surface level through a levee with a clay cover in space and time, experiments were prepared at the TU Delft test facility Flood Proof Holland. These experiments aimed to measure the development of the phreatic surface over time in a real heterogeneous levee. The levee consisted of a sand core ( $k = 1.2 \times 10^{-4}$  m/min) overgrown by grass. The clay had a thickness of 0.3 m on the outer slope and 0.5 m on the inner slope of the levee. The levee had a height of 1.6 m and a crest width of 1.0 m. The 1:2.9 outer slope had a length of 4.6 m in horizontal direction and the 1:4.1 inner slope a length of 6.6 m. The experimental setup is shown in figure 2.7.

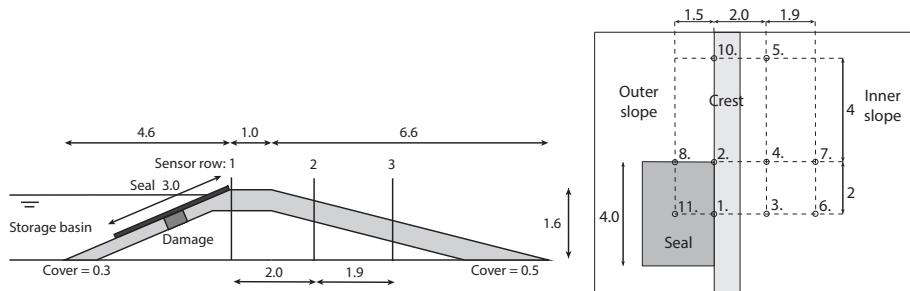


Figure 2.7: (Left) Cross section of the experimental setup at Flood Proof Holland. Damage is  $0.5 \times 0.5 \times 0.3$  m, seal is  $3.0 \times 4.0$  m. (dimensions in meters) and (right) top view of experimental setup Flood Proof Holland, indicating the numbers and corresponding location of the applied sensors.

The goal of the experiments was to measure the response of the phreatic level for various conditions of the outer slope of the levee. Therefore, conditions have been prepared with and without damage to the clay layer, to test the difference in response of the phreatic level. Laboratory measurements have indicated that the most important parameter to reduce the inflow of groundwater were the soil-structure contact details. The damage is achieved by digging a square hole on the outer slope of the levee, with dimensions of 0.5 times 0.5 m and a depth of 0.3 m, this depth is equal to the thickness of the cohesive clay cover material of the levee (figure 2.8). Reaching the core material

was confirmed through a visually observed change of soil color. The damage was located in the center of the cover seal, at the location of sensor 11 in figure 2.7.

Six different experiments were conducted, with different cover materials for the levee and two different damage cases (table 2.4). The development of the phreatic surface level over space and time without a cover was compared to the scenarios with the damage covered by a semi stiff plate and a flexible sheet. The plate cover consisted of a structure which was slightly able to adjust itself to the irregularities of the outer slope, the plate was made of plywood and weighted by sandbags. The sheet cover consisted of a flexible plastic sheet, weighted by sandbags, which was able to adjust its shape to the irregularities of the levee surface. Both the plate and the sheet were 4 m wide, in the direction of the crest and 3 m long, perpendicular to the crest.

Table 2.4: Real-scale experiments performed to measure the influence of a seal on the phreatic surface level in space and time,  $t_{s,n}$  represents the steady state time of a sensor (figure 2.7), while  $t_{s,mean}$  is the mean value of the three sensors shown.

Test number	Seal	Damage	$t_{s,1}$ [hr]	$t_{s,3}$ [hr]	$t_{s,6}$ [hr]	$t_{s,mean}$ [hr]
FT-1	No	No	3.25	6.25	5.75	5.08
FT-2	No	Yes	3.25	6.00	5.75	5.00
FT-3	Plate	No	3.25	6.00	6.75	5.33
FT-4	Plate	Yes	3.25	6.50	6.00	5.25
FT-5	Sheet	No	3.25	6.75	7.00	5.67
FT-6	Sheet	Yes	5.25	6.75	6.00	6.00

Within the levee, three rows of standpipes were placed (figure 2.7), which contained small holes to measure the phreatic surface level in the levee. The first row of 3 sensors was located at the center of the impermeable structure. The second row of 3 sensors was placed at the end of the structure, while the third row of 2 sensors was placed a few meters from the structure. In each standpipe, a Tasseron pressure sensor (6 m range) was placed, the measurement interval of the sensors was set to 15 minutes. The location of the sensors are represented by the red dots in. Filling of the approximately 150 m<sup>3</sup> basin took 45 minutes. A more detailed description of the test setup can be found in Hommes, 2022.



Figure 2.8: (left) Reference case with damage, (middle) plate and (right) sheet Flood Proof Holland

### 2.4.2. REAL SCALE MEASUREMENT RESULTS

The time to steady state is as before, defined as the time to the state when the hydraulic gradient at the locations of the individual sensors, for the various test cases becomes smaller than  $1 \times 10^{-3}$  m/min. The steady state values,  $t_s$ , for the sensors 1, 3 and 6,

located along the centerline axis of the seal, in the direction perpendicular to the levee crest (figure 2.7), together with the average time to steady state for the three sensors can be found in table 2.4. The time to reach steady state conditions is found to increase for the undamaged tests FT-3 and FT-5 compared to FT-1. The same trend is observed when comparing the tests with damage FT-4 and FT-6 with FT-2. The observed increase in time to steady state is larger for the tests including a sheet, compared to the tests with the plate.

In figure 2.9, the water level in the standpipes located at the center of the seal, over time is plotted for the reference case (FT-1), the plate case (FT-3) and the sheet case (FT-5) all without damage to the outer slope of the levee. Comparing the reference case with the plate case (FT-1 and FT-3) it can be observed that the fill curves of both tests do not show any spatiotemporal differences in the filling behavior. When comparing the reference case with the sheet case (FT-1 and FT-5) a difference in the fill curve can be observed, the curve for the undamaged sheet case shows an increment in time to reach steady state conditions. This observed effect of the seal is larger near the crest (sensor 1) while the effect of the seal closer to the inner toe of the levee is almost negligible (sensor 6).

The development water level in the standpipes located in the center of the seal over time for the cases with damage to the outer slope of the levee, for the reference case (FT-2), the plate case (FT-4) and the sheet case (FT-6) are shown in figure 2.10. The same trends are observed as the cases without damage to the outer slope. The effect of a plate (FT-4), on the development of the phreatic surface is still minimal compared with the reference case (FT-2), however the effect is more present compared with the cases without damage to the outer slope. The effect of a sheet on the fill curve with damage to the outer slope appears to be more present when comparing it to the undamaged case, especially for sensor 3 and 6.

These larger scale experiments on a heterogeneous levee confirm the effect of the soil-structure interface on the spatiotemporal behavior of the phreatic surface. The effect of the stiff plate was found to be negligible, while the flexible sheet clearly changed the behavior of the phreatic surface underneath it. The experimental data shows that the reduction in phreatic surface level over time is only temporal. The effect of the seal is found to be larger for the case with damage to the clay layer on the outer slope of the levee.

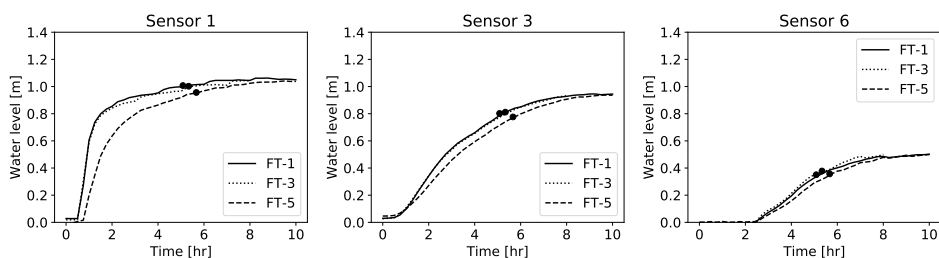


Figure 2.9: Full scale field trial results showing the results of FT-1, no damage no seal, FT-3, no damage with plate and FT-5, no damage with sheet

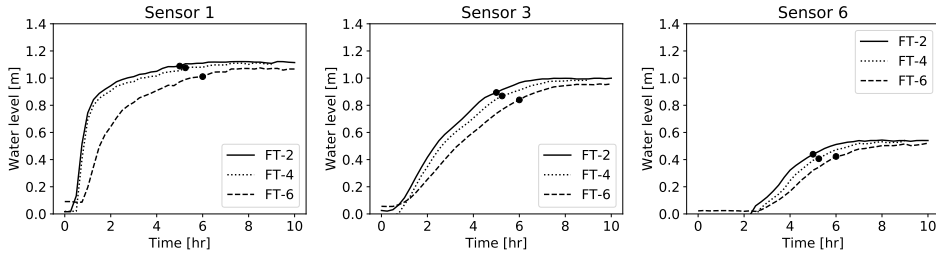


Figure 2.10: Full scale field trial results showing the results of FT-2, damage no seal, FT-4, damage with plate and FT-6, damage with sheet

**2.4.3. THREE DIMENSIONAL EFFECTS IN FIELD TESTS**

Until now, the problem has been treated as purely two dimensional, while in reality, the problem is completely three dimensional. Figure 2.11, shows a top view of the field tests performed in Flood Proof Holland, two hours after the start of the experiments. The red dots in the figure represent the location of the standpipes. The left graph shows the difference in measured water level between FT-1 and FT-5, the reference and the sheet tests for the undamaged outer slope. The right graph shows the difference in measured water level between FT-2 and FT-6, the reference and the sheet test for the damaged outer slope. Both figures are obtained by multi quadratic interpolation of the measured values of the standpipes in the inner slope of the levee. After which the interpolated values were mirrored along the center of the setup (lateral symmetry of the phreatic pattern was assumed).

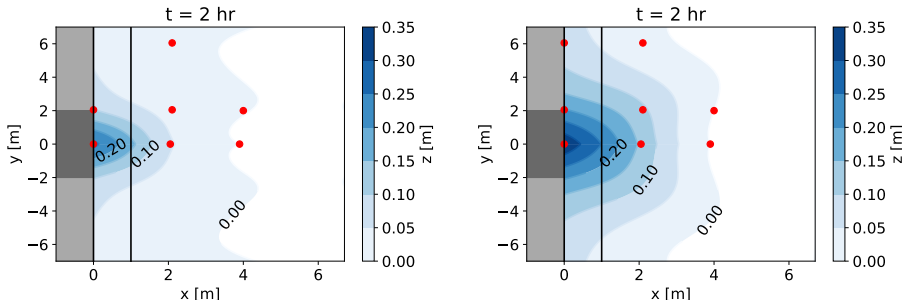


Figure 2.11: Top view of the test setup, difference in phreatic surface over time between experiments (left) FT-1 minus FT-5, and (right) FT-2 minus FT-6 . The red dots indicate the location of the standpipes. The region  $-1 < x < 0$  represents the outer slope,  $0 < x < 1$  represents the crest and  $x > 1$  represents the inner slope. The emergency measure (seal) is located on the outer slope between  $-2 < y < 2$  and  $-2.8 < x < 0$ .

Figure 2.11 shows that the difference is phreatic surface level after 2 hours with and without a seal is larger close to the crest than closer to the toe, which is in line with the two dimensional representation of the results in figure 2.9 and figure 2.9 Furthermore, it can be observed that the influence of the seal in the y-dimension is larger with outer

slope damage compared to the situation without damage. The effect of the dimensions of the seal in the  $y$ -direction, in relation to the influence area of the seal is unknown.

## 2.5. NUMERICAL MODEL AND SIMULATION

In this paragraph we introduce a simplified numerical model to capture the possibilities of using an interface layer to estimate the spatiotemporal development of the phreatic surface through a levee, covered by a seal. This exhibition has only be performed on the homogeneous sand levee, which was tested in the laboratory. NS-1 models the LT-1 case, NS-3 the LT-3 case and NS-4 the LT-4 case. First the case with a perfect soil-structure interface layer is modeled, where after the interface layer is added. The application of numerical simulations for the field tests are part of the discussion.

### 2.5.1. NUMERICAL MODEL

The model was built, using the transient groundwater flow module of Plaxis limit equilibrium (V21), which solves Darcy's equations for both saturated and unsaturated groundwater flow problems (Bently, 2021). The laboratory geometry, as presented in figure 2.3, was implemented in the model. The boundary conditions used for the model comprised of a specific head boundary condition, where the head increased linearly to its maximum value of 0.7 m, over a period of 50 minutes (table 2.2). The impermeable bottom in the laboratory was modelled as a no flux boundary. Since details of the outlet of the phreatic surface was not known, the inner slope was defined as a review or drain boundary condition. The review boundary determines the location where the pressure head is zero at the inner slope. Finally, the seal on the outer slope was defined as a no flux boundary, where the ratio  $L_w$  and  $L_p$  was defined by the closure percentage (figure 2.12). The output value for the pressure sensors in the model correspond to the location of the water inlets of the standpipes as applied in the laboratory experiment.

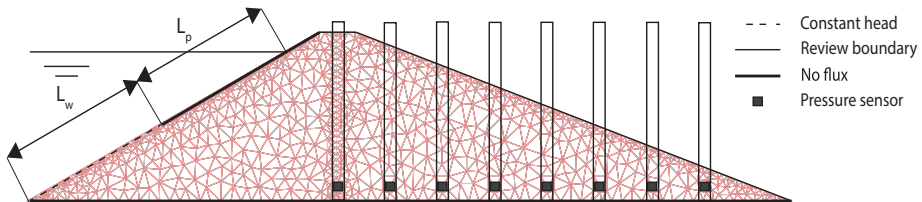


Figure 2.12: Boundary conditions with closure and location pressure sensors in standpipes, including mesh for the numerical simulation of the laboratory experiments, the dimensions of the levee are to be found in figure 2.3.

The soil material is defined by the saturated permeability and the volumetric water content as defined in the laboratory (table 2.1). The applied soil water characteristic curve was fitted using the Fredlund and Xing, 1994 fit, which was found to be a good representation of the SWCC (Rahimi et al., 2015). A triangular mesh is applied within the entire geometry, applying a minimum interior angle of 30 degrees, a maximum length on region boundaries of 0.112 m and a tolerance of 0.001 m, resulting in a mesh with 1769

elements (figure 2.12). Increasing and decreasing the mesh density with a factor two, did not change the output results for the reference case.

### 2.5.2. NUMERICAL RESULTS: STEADY STATE PHREATIC LEVEL

Figure 2.13 shows the steady state measured pressure heads in the laboratory for both LT-1 and LT-2 and the computed pressure height with the corresponding phreatic surface, NS-1, as obtained for the numerical model. The difference between simulated and measured pressure heads shows a decreasing trend towards the landward toe of the levee profile (ranging from 8 cm at sensor pair 1 to 0 cm at sensor pair 8). This difference in output value will not impact the results of the study, since the main findings of the laboratory measurements are time differences and not pressure head differences in the steady state. These differences could either be caused by the effects in Z dimensions in the laboratory experiments or the measurement accuracy of the laboratory measurements. A method to deal with this difference could be the inclusion of a correction factor, which would only depend on the x coordinate of the pressure sensor.

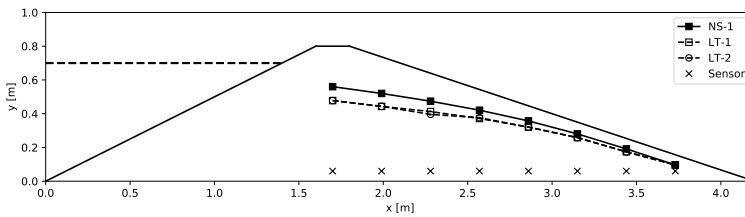


Figure 2.13: Reference case numerical and experimental data

### 2.5.3. TIME TO NEW EQUILIBRIUM PHREATIC LEVEL

An important finding of the laboratory experiments was the additional time to reach steady state conditions for a certain closure percentage after transient increase of river-side water levels. As the soil is considered homogeneous, the shape of the phreatic surface and pressure head distribution for the steady state are not expected to vary with  $k$ . However, the time to reach steady state conditions,  $t_{steady}$ , is expected to vary with  $k$ . The permeability of the soil was fitted to the time to steady state as measured in the laboratory experiments. Table 2.5 shows the results of the calibrated numerical model. Figure 2.14 compares the measured and estimated fill rate in the pressure sensor over time, for sensor pair 1, 3, 5 and 7. The lowest mean average error (MAE) is found for the model with a permeability factor  $k = 7.62 \times 10^{-3}$  m/min.

### 2.5.4. PHREATIC SURFACE LEVEL, PERFECT SEAL

To gain insight in the numerical prediction of steady state level and the time required to reach this level, numerical runs, were conducted for various closure percentages (table 2.6), including the geometry (figure 2.3) and calibrated soil parameters from the heterogeneous laboratory tests ( $k = 7.62 \times 10^{-3}$  m/min). The coverage percentage, as mentioned in the table indicates the percentage of wetted outer slope covered by the impermeable seal (equation 2.1). There are two cases with a 50 percent coverage percentage.



Table 2.5: Calibration  $k$ -factor for NS-1, to fit the results for the reference case, LT-1.  $\Delta t$  is the difference between LT-1 and NS-1

	Sensor row									
	1		3		5		7		MAE	[min]
$k$ [m/min]	$t_{steady}$ [min]	$\Delta t$ [min]	$t_{steady}$ [min]	$\Delta t$ [min]	$t_{steady}$ [min]	$\Delta t$ [min]	$t_{steady}$ [min]	$\Delta t$ [min]		
$5.12 \cdot 10^{-3}$	113	+28	113	+18	112	+30	107	+32	28.13	
$6.12 \cdot 10^{-3}$	99	+14	99	+4	98	+16	94	+19	14.75	
$7.12 \cdot 10^{-3}$	89	+4	89	-6	89	+7	85	+10	6.63	
$7.62 \cdot 10^{-3}$	85	0	85	-10	85	+3	81	+6	4.25	
$8.12 \cdot 10^{-3}$	82	-3	82	-13	81	-1	78	+3	4.50	
Lab	85		95		82		75			

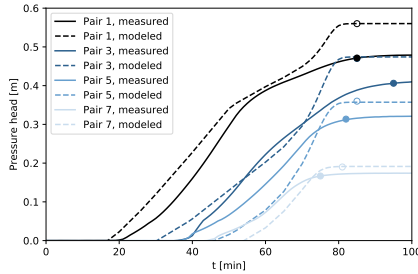


Figure 2.14: Pressure head in sensor pair 1, 3, 5 and 7 over time for  $k = 7.62 \times 10^{-3}$  m/min, LT-1 are the solid lines and NS-1 the dashed lines, dots indicate steady state phreatic level

In the normal 50 percent case, the seal is covering the top half of the levee as in all other configurations, while in the minus 50 percent case, the plate covers the lower part. These results indicate that applying a seal on the lower half of the outer slope does not change the pressure at the sensor location, when comparing it with the zero percent closure case. However, the time to steady state is much longer for the 50 percent coverage of the upper half of the levee. For the other cases, both the steady state level reduce and the time required to reach these conditions increases.

In figure 2.15, the calculated time to steady state ( $t_{steady}$ ) is presented for the seal-coverage percentages as presented in table 2.6. It is observed that these numerical points closely follow an exponential trend as given by (equation 2.2), here  $C$  is the numerical value of the seal-coverage percentage. The parameter  $a$  is found to be 82 min and  $b$  to 0.02, based on the test data as presented before. The RMSE for the given values is 43.4 min, the prediction of the 99% cover value has the largest influence on this error.

$$t_{steady} = a \times e^{b \times C} \tag{2.2}$$

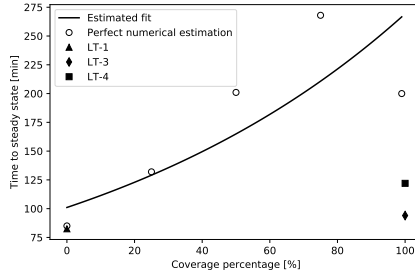


Figure 2.15: Graph time to steady state versus seal-coverage percentages, with exponential fit and measured values.

Table 2.6: Time to steady state, pressure head in pressure sensor for the various sensor pairs and steady state discharge for several outer slope coverage percentages as modeled for ideal seal-surface conditions.

Coverage [%]	$t_{steady}$ [min]	$h_{steady}$ [m]				$Q_{steady}$ [ $\times 10^{-3}$ l/s]
		Row 1	Row 3	Row 5	Row 7	
0	85	0.56	0.47	0.36	0.19	13.3
25	132	0.52	0.44	0.34	0.19	11.5
50	201	0.47	0.41	0.32	0.19	9.8
- 50	85	0.56	0.47	0.36	0.19	13.3
75	378	0.41	0.36	0.29	0.18	8.1
99	797	0.25	0.22	0.18	0.13	4.8

### 2.5.5. CASE OF IMPERFECT SEAL, SOIL STRUCTURE INTERFACE LAYER

To improve the ability of the numerical model to match experimental results, an interface layer was added to the levee surface to take into account the time-delay in reaching steady-state, as observed in the data and described in conceptual framework and the previous section(s). This allows for a more accurate estimation of the time to steady state, when applying a non-perfectly attached seal.

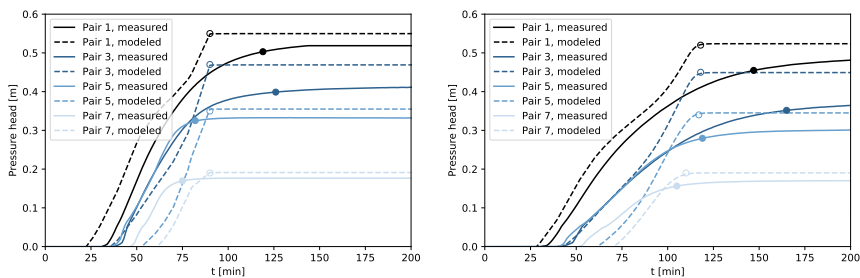
Within the interface layer, two different model parameters are included, the thickness of the interface layer  $w_g$  and the permeability of the interface layer  $k_g$  (figure 2.2). In the laboratory tests, a distance in the order of 1 cm was observed between the soil and the structure, for that reason, the  $w_g$  layer thickness is set to 1 cm. The  $k_g$  value will be used as a calibration factor, the calibrated values for the two numerical cases, NS-3 for 99% coverage of plate without toe and NS-4 for 99% coverage of plate with toe, are presented in table 2.7. It was found that the interface layer,  $k_g$ , leads to the best estimation of time to steady state of 2.5 m/min for NS-3 and 1.25 m/min for NS-4.

In figure 2.16 the output of the updated model is compared with the measured values in LT-3 and LT-4, for sensor pair 1, 3, 5 and 7. That is now the updated model of the imperfect seal, as described above, is used. The simulated and obtained time history of the pressure head show reasonable agreement now. The numerically determined time to steady state for NS-3 has become 94 minutes and 118 minutes for NS-4. This com-

Table 2.7: Calibration of  $k_g$  for numerical simulations, LT are the results from the laboratory and NS the results from the numerical simulation.

Simulation	$k_g$ [m/min]	$t_{s,LT,mean}$ [min]	$t_{s,NS}$ [min]
NS-3	2.0	94	100
NS-3	2.5	94	94
NS-3	3.0	94	90
NS-4	1.0	122	130
NS-4	1.25	122	118
NS-4	1.5	122	111

pairs to the experimentally obtained times to steady state of 94 minutes for LT-3, and 122 minutes for LT-4. In NS-3, the steady state conditions are reached quite abruptly, also when comparing it with NS-1 (figure 2.14) and NS-4 (figure 2.16). This could be explained by the high permeability of the interface layer, which reaches steady state conditions faster than interface layers with a lower permeability. This effect is numerically modelled through the entire levee, and deviates from the observed fill curves. The model update finds values that are indeed close to the observed ratios, thus the interface layer could be a good representation of imperfect seal-soil conditions.

Figure 2.16: Measured and simulated data for updated –imperfect seal- model, both at 99% coverage. Both for test 3,  $k_g = 0.76$  m/min

A summary of the estimated numerical values is shown in table 2.8. The reduction in outflow discharge for the numerical cases 1 and 4 is 16.7%, while the measured reduction is 23.5%, which is in the same order of magnitude. The physical measurement does not show a reduction in steady state pressure height for the first sensor pair (LT-1 and 4), while the numerical estimates show a reduction of 8.9%.

## 2.6. DISCUSSION

The results of this research show that a seal influences the spatiotemporal characteristics of the phreatic surface through a levee. Increasing the time to reach steady state phreatic conditions, will most likely increase the time available until certain failure mechanisms are triggered. These related mechanisms include failure through seepage and slope stability (Schierck, 1998). This extra time allows levee managers extra time to install addi-

Table 2.8: Time to steady state pressure head for sensor pairs, and associated steady state discharge for the three numerical cases of interest

Test	$t_{steady}$ [min]	$h_{steady}$ [m]				$Q_{steady}$ [ $\times 10^{-3}$ l/s]
Number		Row 1	Row 3	Row 5	Row 7	
NS-1	85	0.56	0.47	0.36	0.19	13.3
NS-3	94	0.55	0.47	0.35	0.19	12.8
NS-4	118	0.52	0.45	0.34	0.19	11.9

tional emergency measures or extra time to evacuate people or livestock (Janssen et al., 2021). Furthermore, the extra time acquired to reach steady state phreatic conditions should be compared with the duration of a flood wave. This paragraph introduces possibilities to improve the quality of the estimated of the spatiotemporal effects of a seal, using numerical models that integrate the interface layer. Furthermore, further research aimed at achieving the optimal effect of a seal is discussed in this paragraph.

### 2.6.1. DETERMINATION OF INTERFACE LAYER PARAMETERS

The interface layer added to the numerical simulation has been demonstrated to capture the reduction of seepage entering the levee considering leakage and water flow around a non-perfect seal. In the current analysis on the effect of the interface layer on the spatiotemporal behavior of the phreatic surface level, the  $k_g$  and  $w_g$  factors were only calibrated for the laboratory case, which consisted of a steel plate. The parameters have not been determined for the field tests within this manuscript. The seal parameters should be determined using a three-dimensional model numerical model, to also include the three-dimensional effects of the seal. A two-dimensional model will not be sufficient for the current dataset, since the seal only had a limited length in the field tests. The  $w_g$  factor of different types of seals should be determined taking the flexibility of the seal into account, together with the irregularities in the outer slope of the levee. The  $k_g$  factor has to be calibrated within a numerical model, using the data from the field tests. Calibrating the interface layer parameters for different types of seals and varying degrees of levee cover and inhomogeneities, allows levee managers to estimate the effect of this seal on a levee consisting of local soil materials having a certain geometry. This allows the levee manager to act based on site specific conditions and provide a corresponding estimate of rise of the phreatic line.

### 2.6.2. THREE DIMENSIONAL EFFECTS OF THE SEAL

The presence a seal seems to have a distinct effect direction alongside the slope (Y-direction), illustrated in figure 2.11. This influence area has a certain curvature, which could be identified as bowl-shaped. During the experiments, the width of the seal in Y-direction was kept constant. Increasing the width of the seal, is expected to increase the influence area of the seal, i.e. the area in which the phreatic surface will change. Further research should be conducted to determine the minimal required seal dimensions to acquire a local increment in levee stability over a certain amount of distance. This knowledge helps emergency response managers to determine the minimal required length of

seal to optimize its effect on flood risk safety.

## 2.7. CONCLUSIONS

Here we studied the effect of a seal on the development of the phreatic level in space and time in a levee during a high-water event. Increasing phreatic water levels will negatively affect the safety and integrity of the levee, particularly for internal erosion and instability. We presented a conceptual framework, laboratory experiments, field experiments and numerical simulations for configurations of increasing complexity. This provided insight into the response of the phreatic level following a sudden rise of riverside water levels, for a case in which a seal has been placed on the outer slope of the levee.

Three different laboratory experiments have been conducted within the research on a heterogeneous sand levee, a reference case, a case where the outer slope was covered by an impermeable seal plate and a case with a steel plate where the inflow of sand was obstructed by a sandy toe. For all of the experiments, the steady state phreatic level was approximately the same. However an increase in time to reach steady state was observed of 25% of the sealed case and 50% for the sealed case with a toe. The largest effect of the seal was mainly in the early phase of the experiments.

In the field tests, the three-dimensional effects of a seal on a heterogeneous levee have been explored. The tests consisted of a reference case, a case covered with a plywood plate and a case with a flexible seal. All of the mentioned tests were conducted with and without damage to the outer slope of the levee. The field tests show a negligible beneficial effect on the steady state phreatic level by an impermeable plate. In case the seal is applied on a levee without damage to the outer slope, the time to reach steady state increased by 12%, compared with the reference case. For a levee with a damaged slope and more potential infiltration, an impermeable seal increased the time to reach steady state conditions by 20%.

The time-delay effect of a seal on the phreatic surface for three-dimensional, heterogeneous field trials and two-dimensional, homogeneous laboratory tests were consistent. A seal, which can adjust itself to the outer slope, i.e., a flexible layer that folds over surface irregularities on the levee slope leads to an increase of the time to reach the steady state conditions in the levee volume directly underneath the seal. Idealized numerical conditions show that a seal can increase the time required to reach steady state conditions by a factor of 2.5, when covering half of the outer slope.

To properly model the influence of a seal on the spatiotemporal development of the phreatic line, an interface layer was introduced, consisting of a certain width and hydraulic conductivity. The width of the interface layer in the model is the maximum observed distance between the seal and the surface. The hydraulic conductivity of the interface layer is a calibration parameter, which represents the percentage of slope covered by the seal. Numerical model runs of the laboratory case show that the presented interface layer can be used to match the experiments quite accurately.

The delays found in reaching steady state conditions can contribute to postponing or preventing levee failure, triggered by either slope instabilities or internal erosion. For that reason, sealing of the outer slope of a levee is only recommended as a preventive measure, which should be applied before the phreatic surface of the levee reaches the steady state conditions. For practical reasons, the seal should be placed before the water

level rises when installing it from the land. However, when using waterborne emergency measures, one could extend the timeframe for placement. Future research should improve the predictability of the sealing effect, allowing practitioners to use simple calculations to estimate the extra time acquired and the quantity of seal required to achieve this effect. Also, the results of this study can be used to develop and improve emergency procedures for flood fighting using measures for sealing (parts of) flood defenses.



# 3

## REDUCING WATER FLOW THROUGH A LEVEE BREACH USING A PONTOON

*Once more unto the breach, dear friends, once more*

William Shakespeare

---

This chapter has been submitted as: D. Janssen, B. Hofland, A.J.M. Schmets, E. Dado, S.N. Jonkman. Reducing water flow through a levee breach using a pontoon.



### 3.1. INTRODUCTION

For flood management in the Netherlands, a small risk of levee failure is considered as acceptable. This accepted risk level is based on levee failure mechanisms and is determined by probabilistic methods. Currently, these design probabilities are based on the assessment of individual, societal and economic risks (Slootjes and Most, 2016). The accepted flood risk is very small, as the consequences of a levee failure are severe: people may lose their lives, and properties can be significantly damaged (Jonkman, 2007). Therefore, emergency response strategies are intended to be applied locally and temporarily to increase the residual strength of a levee in case of exceedance of its design loads.

A levee can fail in several ways (Schierreck, 1998), as a consequence of either of two fundamental mechanisms: failure by water flowing over a levee or by water flowing through a levee. In addition, both pathways to failure may enhance each other. An example of both failure pathways together contributing to a real levee failure is the case in Breitenhagen, Germany (Kool et al., 2019). Here, saturation of the levee mass led to a local crest height reduction resulting in overflow over that levee section; which initiated the breaching process. The breaching process itself can be considered to have various stages (Visser, 1998). In the first stages, water flows through the initial breach, while the inner slope slowly evolves towards the outer slope and the surface area of the breach remains the same. Then, at the final stages of the breaching process, the width and depth of the breach increase significantly. The breaching process of homogeneous sand levees mainly consisting of gradual erosion of the soil (Visser, 1998). The governing process in clay (Zhu, 2006) and heterogeneous levees (D'Eliso, 2007) is head-cut erosion. An emergency response intervention to prevent or postpone breaching, is ideally applied in the early stage of the breach growth process. This is because the breach width, depth, as well as water flow velocities, are small during the initial stages of the breaching process, thereby increasing the probability of a successful outcome.

Historical attempts to stop the breaching process in the early stages mainly involved the application of vessels and sandbags. The success of these attempts was mainly due to adequate and timely actions of the people in the area, combined with the phase within the breaching process that the intervention had been initiated (Rijkswaterstaat, 1961). Unsuccessful attempts are primarily characterized by high flow velocities through the breach, resulting in unstable conditions for the application of emergency measures (Henning and Jüpner, 2015; Seed et al., 2008). There are more known cases of unsuccessful than successful interventions in the (initial) breaching process.

In general, an emergency response intervention can be successful and feasible if the time required until placement is shorter than the time available (Janssen et al., 2021). The available time is the time window until intervention becomes obsolete. After application of an emergency response measure, the breaching process can either be stopped, postponed or, in the most unfavorable case, be accelerated. The most important parameter that prevents or postpones the breaching process by an emergency response intervention is the breach discharge. The success of an emergency response measure depends on the extent that the total discharge and especially water flow velocity through the breach is reduced. A reduction of flow velocity decreases the drag forces on soil particles and consequently reduces the erosion rate of the soil (Shields, 1936). Reduced

erosion rates will increase the time for a breach to ‘grow to failure’. Altogether, this leads to a time benefit, compared with the undisturbed discharge case.

In the present study, we consider an emergency response method that further builds on the use of vessels. Its specific design is referred to as BresDefender from here on. The BresDefender is a floating pontoon normally used by the military to construct temporary bridges, see figure 3.1 (Janssen et al., 2021). By proper adjustments, these pontoons can be positioned on the outer slope of a levee, locally reinforcing a weakened levee section. This paper outlines the effectiveness of the BresDefender methodology in terms of discharge reduction through a levee breach. The discharge reduction has been studied experimentally in field conditions through tests at various length scales. Medium-scale tests were conducted in the outdoor testing area of Flood Proof Holland in Delft, the Netherlands, and full-scale tests were done at the Hedwige-Prosperpolder LivingLab (abbreviated as Hedwigepolder). At Flood Proof Holland, the BresDefender was mimicked by a stiff plate attached to the outer slope of a levee. In the Hedwigepolder, full-scale experiments were conducted using an actual real BresDefender.

In this research, first the effect of placement of the BresDefender on the breach discharge is evaluated experimentally in Flood Proof Holland and the Hedwigepolder. As breach closure by the BresDefender will never be complete due to seepage under the BresDefender, the effectiveness of the method is determined by measuring the leakage discharge. The experimental data can be interpreted by means of an empirical model that predicts the leakage of water along the BresDefender for given characteristics of the closure intervention and the surface properties of the levee. Finally, this leads to advice on the application limits of the BresDefender in terms of time benefit and application limits.

This remainder of this paper is organized as follows. Section 3.2 presents the experimental setups of the experiments in Flood Proof Holland and the Hedwigepolder. Section 3.3 shows the experimental output from both experiments and section 3.4 introduces the empirical flow model. Finally, the performance of the BresDefender, in terms of time benefit and application limits, is discussed in section 3.5.

## 3.2. METHODS

The effect of an emergency measure on discharge through a levee breach was tested at two different experimental facilities: Flood Proof Holland, and in the Hedwigepolder. Flood Proof Holland is an experimental facility where temporary flood defenses can be tested at an intermediate scale on a 1.6 m high levee. The Hedwigepolder was part of prototype environment, in which emergency response methods could be tested at full scale. The aim of the experiments was to determine the overall performance of the BresDefender in terms of the reduction in the leakage discharge. The acquired data may be used to estimate the changes in breach times with and without a BresDefender. Figure 3.1 shows images of the test setups in Flood Proof Holland and the Hedwigepolder, respectively. Characteristic dimensions of the two test setups are listed in table 3.1.



Figure 3.1: (left) physical model of the BresDefender in Flood Proof Holland and (right) the actual BresDefender in the Hedwigepolder.

Table 3.1: Characteristic test dimensions for Flood Proof Holland and Hedwigepolder

Structure		Flood Proof Holland	Hedwigepolder
		Plywood plate	Military pontoon (with tarpaulin)
Maximum pressure head retained	$h$ [m]	0.5	0.58
Maximum breach width	$B_{up}$ [m]	1.25	3.0
Width of structure	$W_{plate}$ [m]	4.0	6.7
			8.1 up
Length of structure	$L_{plate}$ [m]	3.0	6.1 down

### 3.2.1. GEOMETRICAL PARAMETERS

A sketch of the test-setup is shown in figure 3.2. The BresDefender is schematized as an object or plate that is positioned on the outer slope of the levee in the plane  $efgh$ . The BresDefender is located in front of a locally weakened levee section, represented by a reduction in the crest height with trapezoidal cross section. The plane  $abcd$  is the surface area of the breach, in the direction of the outer slope of the levee.

Three coordinate systems are defined in figure 3.2: an  $xyz$ -system, where  $z$  equals zero at the crest of the levee, an  $(xyz)'$ -system, where  $z'$  equals zero at the median plane through the outer slope of the levee and an  $(xyz)''$ -system, where  $z''$  equals zero at the bottom of the plate. The  $(xyz)''$  system defines the orientation of the plate, assuming that the plate is stiff and its orientation depends on the three elevated contact points with the levee surface, which support the plate.

Figure 3.3 shows a front view of the levee, i.e., a projection of the experimental setup in the  $y$ -direction. Here,  $A_{plate}$  represents the projected area of the plate below, and  $A_{rest}$  the projected area above the seaward water level. The sum of  $A_{plate}$  and  $A_{rest}$  represents the projected area of plane  $efgh$  in figure 3.2.  $A_{breach}$  is the surface area of the plate, below the outer water level, which is not in contact with the outer slope, while  $A_{b,rest}$  is the unsupported area above the average water level. Plane  $abcd$  (figure 3.2) is the sum of  $A_{breach}$  and  $A_{b,rest}$ .

The (artificial) breach has a trapezoidal cross section, with widths  $B_{down}$  at the bottom of the breach and  $B_{up}$  at the top, respectively (figure 3.3). The slopes of the breach have an angle  $\phi$  relative to the  $x$ -direction.  $B'$  is the average width of the breach below

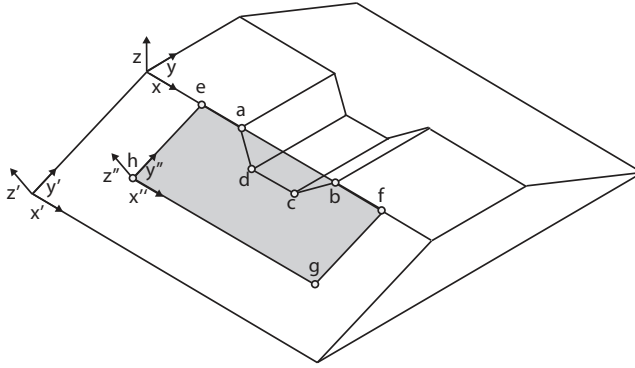


Figure 3.2: 3D sketch of the experimental set-up

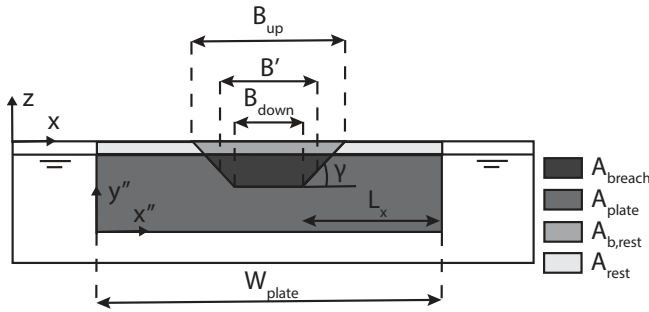


Figure 3.3: Front view levee and water level outside the levee

the water level, (equation 3.1).  $L_x$  is the shortest horizontal distance from the side of the plate to the horizontal part of the breach.  $W_{plate}$  is the width of the plate.

$$B' = B_{down} + \frac{h}{\tan \gamma} \qquad L_x = \frac{W_{plate}}{2} - \frac{B_{down}}{2} \qquad (3.1)$$

The definition of the geometrical parameters at a cross section through the levee at the center of reduced crest height are shown in figure 3.4. Here, the reduction in crest height is given by  $h_{br}$ , while  $h$  is the vertical distance from the bottom of the breach to the outer water level, which equals the pressure head.  $h_{br}'$  and  $h'$  are projections of vertical distances  $h_{br}$  and  $h$  in the direction of the outer slope. The angle of the slope is indicated by  $\varphi$ .  $L_{plate}$  is the length of the plate in contact with the subsoil in the direction  $y''$ .  $L_y$  is the distance from the lowest part of the plate to the lowest part of the breach. The relation between these parameters is given by equation equation 3.2.

$$h'_{br} = \frac{h_{br}}{\sin \varphi} \qquad h' = \frac{h}{\sin \varphi} \qquad L_y = L_{plate} - h'_{br} \qquad (3.2)$$

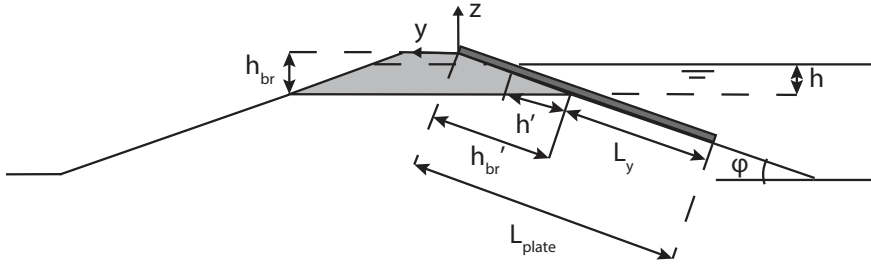


Figure 3.4: Geometric parameters defined at the cross section of the levee through the middle of its lowered crest

### 3.2.2. INTERMEDIATE SCALE EXPERIMENTS: FLOOD PROOF HOLLAND

An initial set of experiments to measure leakage around a stiff plate covering an artificial breach were conducted at the experimental facility at Flood Proof Holland. The aim of these experiments was twofold. First, it allowed for the iterative design of an experiment at intermediate scale in preparation of the large-scale experiments at Hedwigepolder. Secondly, this experimental facility allowed for control and assessment of the influence of environmental parameters that will not be easily accessible during full-scale experiments.

The test setup was located in a basin which was divided by a levee. The experiments were performed at a section of the levee, with a 1:2.9 outer slope, a crest width of 1.1 m and a height of 1.6 m, see figure 3.5. The levee was completely covered by grass on a 0.3 m thick layer of clay at the outer slope and 0.5 m thick at the inner slope, while the core of the levee consisted of sand. The water level within the basin could be adjusted using pumps with a maximum capacity of 80 l/s. The experiments were performed at two different locations of this levee. At each test location, trapezoidal breaches were created. Breach depths,  $h_{br}$ , varied from 0.3 to 0.5 m, while the lower widths,  $B_{down}$ , varied from 0.7 to 1 m and the upper widths ( $B_{up}$ ) varied from 0.84 to 1.25 m.

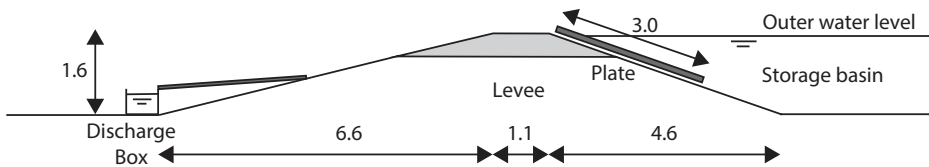


Figure 3.5: Overview of intermediate scale experimental setup at Flood Proof Holland, dimensions are in meters

The BresDefender, used to close the breach, was modelled as an impermeable plate of shuttering plywood, with  $L_{plate}$  of 3 m,  $W_{plate}$  of 4 m, and a thickness of 0.018 m, see figure 3.5. The plate was positioned before water entered the basin, i.e., the dynamic process of positioning the BresDefender under high water conditions was not tested in

this experiment. To overcome the buoyancy forces of the water, and to determine the effect of mass on leakage discharge, the plate was subjected to the weight of either 50, 100 or 150 sandbags (figure 3.1). These sandbags had an average weight of 17 kg with a standard deviation of 0.7 kg, leading to a surcharge of 695, 1390 and 2085 N/m<sup>2</sup>. To prevent the sandbags from sliding and to equally distribute the surplus load, four rows of partition plates were applied. These partition plates increase the stiffness of the plywood plate in horizontal direction,  $x$ , allowing for less deflection of the plywood plate in horizontal direction, compared to the vertical direction,  $y$ . In the middle of the plate, a rectangular structure was mounted, with a surface area of 0.5 times 0.5 m and a height of 0.5 m. This cubicle was intended to contain a PIV to measure local flow velocities underneath the plate. However, these PIV measurements were unsuccessful.

Each experiment started by allowing water to flow into the storage basin, increasing the outer water level from the toe up to the crest of the levee. As soon as the water level reached the lowest part of the breach, leakage water started to flow through the breach. The leakage discharge was directed via a flume into a discharge measuring box (figure 3.5). The box had a height of 52 cm, a cross sectional surface area of 0.5 m times 0.99 m at its bottom, and 0.61 times 1.10 m at its rim. As soon as the box was filled with water, pumps were switched on to empty the box, to allow a new measurement. The time in-between reaching the maximum water level in the basin and the end of an experiment was at least 3 hours. During these experiments the water level in the basin was kept at a constant level, by manually refilling the basin before each new test.

The filling rate of the tray was monitored using a *Temptonics G-Series GH* rod position sensor, operated at a frequency of 1 Hz. The outer water level was measured using a CTD-diver, which recorded the water pressure every 30 seconds.

The data acquired with the rod position sensor provided the water level in the box as a voltage over time. This voltage was then converted into the water level in the box using an appropriate calibration factor. The filling rate of the box was calculated by how long it took to fill the box between two specific water levels. Finally, from this the leakage discharge could be obtained by multiplying the characteristic surface area of the box by the water level difference per second.

### 3.2.3. FULL SCALE EXPERIMENTS: HEDWIGEPOLDER

In the Hedwigepolder, experiments were conducted in an enclosed basin of 150 x 50 m, in which the water level could be regulated by valves and two pumps, with capacities of 3.0 and 5.0 m<sup>3</sup>/s respectively. The basin was enclosed by a levee with a crest height of 5 m and a 1:3 outer slope, see figure 3.1 and figure 3.6. The levee consisted of a sandy core, covered by a 0.5 m thick clay layer. The outer slope at the test side was covered by grass divots, which were retrieved from a Westerschelde sea levee. The quality of the grass cover could be classified as bad. Irregularities of the grass cover have been estimated using a 1 m long beam and a ruler. The maximum distance measured from beam to grass was 20 cm, while the median distance was estimated to be 10 cm. At the test location, a trapezoidal breach was excavated. The dimensions of this artificial breach were  $h_{br} = 1$  m,  $B_{down} = 1$  m and  $B_{up} = 3$  m, see figure 3.3 and figure 3.4. The slope of the trapezoidal breach, i.e., the angle  $\gamma$ , was set at 45 degrees. After excavation, the breach was sealed with a watertight plastic layer, covered by an impermeable impermeable geotextile, to

avoid erosion of the breach. A movable weir (figure 3.7), which allowed to generate a pressure head difference before the start of the experiment was constructed in the middle of the breach. Opening the weir would allow the water to flow from the storage basin through the breach.

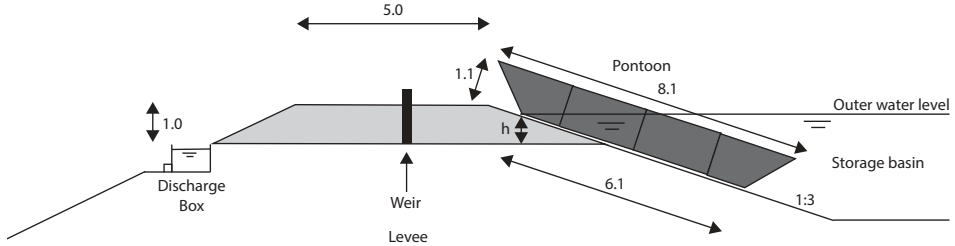


Figure 3.6: Cross section of full-scale experimental setup at the Hedwigepolder, dimensions are in meters



Figure 3.7: (left) Weir to regulate water through breach, (right) BresDefender with white tarpaulin

The breach was closed with the BresDefender prototype, a military floating pontoon with a top length of 8.1 m and a thickness of 1.1 m. The pontoon's surface located at the outer slope of the levee was  $L_{plate}$  6.1 m long and  $W_{plate}$  of 6.7 m wide. The mass of an empty pontoon is 5,450 kg. In the first experiment, the stiff pontoon was placed directly on top of the levee surface, while in a second experiment, a flexible reinforced PVC tarpaulin was attached to the bottom of the pontoon (figure 3.7). This tarpaulin served as a flexible material interface between the stiff pontoon and the outer slope's surface. Application of the tarpaulin was intended to establish improved contact between the stiff pontoon and the irregular outer slope of the levee by shaping itself to these irregularities.

To position the pontoon at the right spot, the water level was first increased to 0.1 m below crest, while the weir was closed. Then the pontoon was moved to the center of the breach, with the center of the pontoon aligned with the center of the breach. At this location the pontoon was docked using anchors. Then the empty ballast tanks of the pontoon were filled with water by using hoses, until the water level inside the pontoon equaled the water level in the basin. Finally, the water level in the basin was decreased to, 0.2 m above the bottom of the breach ( $h$ ). This procedure was applied to test the effectiveness of the pontoon at multiple water levels, to make sure the horizontal part covered the wet surface area of the breach, at various water levels. The water level in the pontoon was able to adjust itself to the new conditions, through pre-prepared holes in the pontoon. These holes were located on top and at the sides of the pontoon enabling

it to be sunk in front of the breach.

With the pontoon anchored, starting with a water level  $h$  of 0.2 m, the weir was opened, and water started to flow through the breach caused by the pressure head. This leaked water was collected in a discharge box at the end of the breach, neglecting the first gulp of storage water between the weir and the pontoon. The pallet box had a cross section of 1.1 times 0.9 m and a height of 0.55 m. After reaching the maximum capacity of the box, a valve was opened to release the water and to start a new measurement. The filling rate of the pallet box and the outer water level were measured using a Tasseron pressure sensor (6 m range), operated at a measurement frequency of 1 Hz. Three sensors were used for the determination of the outer water level and three for determining the fill rate of the box.

During the first test, without the tarpaulin, a maximum water level of 0.13 m in the breach was applied. For the second test series, water levels,  $h$ , of 0.2, 0.4, 0.54 and 0.58 m were applied. The measurements started with the lowest water level  $h$ , and the water level was increased after one hour of measuring the leakage discharge. The leakage discharge through the breach, was obtained by a similar approach as presented in paragraph 3.2.2, using the dimensions of the discharge box as applied in the polder.

Next to the experiments presented in the previous paragraph, two experiments were conducted with partly sunk pontoons. During these experiments, first the tarpaulin-covered pontoon was anchored to the breach, and was not entirely filled with water. Figure 3.8 shows the draught of the pontoon for two filling scenarios: a case where no ballast water was added to the pontoon and a case where the pontoon was filled to such a level that the rear part of the pontoon just stayed above water. The effective length of the tarpaulin, sealing the outer slope of the levee is not exactly known. For determining of  $A_{plate}$ ,  $L_{plate}$  of 0.5 m is assumed for the no water case and 1 m for the just floating case. Since the pontoon is pushed on the levee using a boat, the pontoon is slightly tilted, even for the no water case.

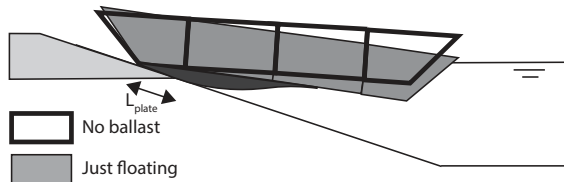


Figure 3.8: Scenarios for a partly sunk tarpaulin-covered pontoon with tarpaulin (dark grey)

### 3.3. EXPERIMENTAL RESULTS

#### 3.3.1. EXPERIMENTAL RESULTS: INTERMEDIATE SCALE

In table 3.2 and 3.3 the results of the leakage discharge experiments in Flood Proof Holland are listed. The table shows the mean leakage discharge for the experiments at the two different sections of the Flood Proof Holland levee. Each experiment was executed for a range of top loads and for various breach dimensions. Experiments at location 1



with  $h = 0.3$  m were conducted by hand, using a ruler and a stopwatch to measure the filling rate of the discharge box. The results of the experiments at location 2 with  $h = 0.3$  m are based on only one measurement, since the capacity of the pump was insufficient, and the discharge box could only be filled once. Thus, for the data of this measurement, a standard deviation could not be determined. The other experiments were based on at least 8 independent measurements.

Table 3.2: Leakage discharge through plate-covered artificial breaches at Flood Proof Holland location 1

Dimensions breach [m]			Location		
$h$	$B_{Up}$	$B_{Down}$	1		
			Number of sandbags		
			50	100	150
Discharge $\pm$ standard deviation [l/s]					
0.3	0.84	0.7	0.45 $\pm$ 0.09	0.38 $\pm$ 0.07	
0.4	0.84	0.69			
0.4	1.25	1.0			
0.5	1.25	1.0	0.82 $\pm$ 0.05	0.69 $\pm$ 0.05	0.83 $\pm$ 0.06

Table 3.3: Leakage discharge through plate-covered artificial breaches at Flood Proof Holland location 2

Dimensions breach [m]			Location			
$h$	$B_{Up}$	$B_{Down}$	2			
			Number of sandbags			
			50	100	150	
Discharge $\pm$ standard deviation [l/s]						
0.3	0.84	0.7	1.48		1.49	1.33
0.4	0.84	0.69	2.16 $\pm$ 0.11	1.98 $\pm$ 0.03	2.30 $\pm$ 0.46	
0.4	1.25	1.0	2.42 $\pm$ 0.07		2.14 $\pm$ 0.02	
0.5	1.25	1.0	2.94 $\pm$ 0.13	2.89 $\pm$ 0.07	2.92 $\pm$ 0.18	

Closer inspection of the results in table 3.2 and 3.3 shows that the leakage discharges at location 1 are approximately 3 to 3.5 times smaller than the leakage discharge at location 2. Furthermore, the top load applied to the plate does not seemingly influence the total leakage discharge underneath the plate.

The data in table 3.2 have been obtained by averaging all of the independent discharge measurements conducted for the specific conditions, over a certain timespan. After removing the outliers, the mean leakage discharge with its corresponding standard deviation could be determined. Due to the high discharge rates at location 2, water was continuously pumped out of the box, for that reason, a discharge of 1.76 l/s, has to be added to the measured discharge, which represents the discharge of the pump. The correction for the continuous pumping has already been applied in the data as presented in table 3.2.

The water level in the basin is obtained from the output of the CTD sensors, corrected for the distance from sensor to bottom of the breach. The difference of the water level is

caused by both leakage and refilling the basin at several times. The variation of the water level in the breach is of the order of 5%, which relates well with the observed spread in discharge values (2.4%).

**3.3.2. EXPERIMENTAL RESULTS: FULL SCALE EXPERIMENTS**

The results for the leakage discharge experiments at full scale as conducted in the Hedwigepolder are presented. The measured discharge through the breach without a tarpaulin between the pontoon and outer levee slope, was found to be 21.5 l/s for a water level ( $h$ ) of 13.4 cm above the breach level. Measurements at higher water levels were not possible for the case without the tarpaulin, since the leakage discharge became too high for the measurement setup; the valve could not drain the incoming discharge anymore.

Table 3.4 shows the measured leakage discharges through the breach for the case with a tarpaulin attached to the bottom of the pontoon, averaged for the different water levels. Figure 3.9 shows the measured time history of both, the leakage discharge through the breach and the water level ( $h$ ) in the breach. The figure shows a reduction in leakage discharge over time, which may indicate that the tarpaulin keeps adjusting itself over time, reducing the spaces between slope and tarpaulin. The opposite effect is observed for  $h = 0.22$  m, this may be due to the initial unclogging of the channels underneath the tarpaulin. The flow removes all obstacles in the channels, to generate a continuous flow path.

Table 3.4: Leakage discharge through artificial breaches with docked tarpaulin-covered pontoon at Hedwigepolder

Dimensions breach [m]			$h$ [m]			
$h_{br}$	$B_{up}$	$B_{down}$	0.22	0.4	0.54	0.58
			$A_{breach}$ [m <sup>2</sup> ]			
			0.90	1.72	2.34	2.51
			Average discharge [l/s]			
1	3	1	1.90	2.11	2.85	2.85

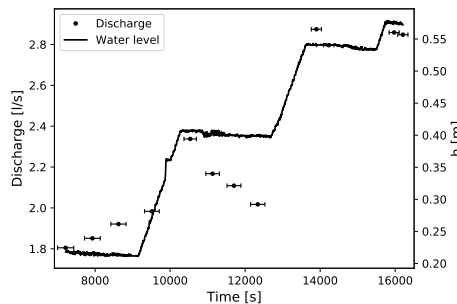


Figure 3.9: Measured time history data of discharges and water level ( $h$ ) in breach for a tarpaulin-covered pontoon at Hedwigepolder

The measured discharges for the case of the partly sunk pontoon are shown in table

3.5. The measured discharge for the partly sunk pontoon is 33% greater than the discharge measured for the completely sunk pontoon (with tarpaulin). The discharge for the not ballasted pontoon, is 121% greater than the case of the completely sunk pontoon.

Table 3.5: Measured discharges partly sunk pontoon case

Case	Dimensions breach [m]				$h$ [m]
	$L_y$	$h_{br}$	$B_{up}$	$B_{down}$	0.4
					$A_{breach}$ [m <sup>2</sup> ]
					1.72
					Discharge [l/s]
No ballast	0.5	1	3	1	2.82
Just floating	1	1	3	1	4.62

### 3.4. ANALYSIS OF RESULTS: THE LEAKAGE MODEL

Now that the experimental results have been presented, these results should be evaluated in the context of the application of the plate or pontoon to stabilize weakened sections of levees during high water crises. Therefore a physics-based leakage model is introduced to determine the relative importance of the parameters that steer the desired discharge reduction effect. This defines the boundary conditions and user scenarios where stiff plates or pontoons qualify as an effective emergency response measure. However, it should be emphasized that because of large spatial variations of levee surface topology and other underlying assumptions, the model with its input remains rather uncertain. The model is mainly developed to establish useful relations between the parameters that cause the leakage water. For development of the model the results of the Flood Proof Holland experiments are leading since more detailed information on the outer slope irregularities is available.

#### 3.4.1. LEVEE SURFACE ANALYSIS

The precise topology of the grass surface at the outer slope of the Flood Proof Holland levee was measured using a LiDAR setup, a *LeicaP40* LiDAR system operated at a resolution of 0.8 mm at 10 m distance. This surface topology data is then used to determine the distance between the bottom of the plate and the grass layer. As the outer slope of the levee is not perfectly flat, this distance varies over the surface area on which the plate is resting. Considering that the plate is stiff, it is in contact with the surface at the three highest points of that surface. After determination of these highest points at the surface area of interest, the LiDAR retrieved topological dataset was transformed to a new coordinate system. This new coordinate system was defined by the plane through the three highest points. Subsequently, the plane through these points was defined as  $z''$  is zero, and the outer slope topology data were expressed relative to this plane. Figure 3.10 shows the distance from the bottom of the plate to the levee surface, for both test locations in Flood Proof Holland. The coordinate systems used are introduced in figure 3.2, where  $abcd$  indicates the dimensions for the largest breach as applied in the Flood

Proof Holland experiments.

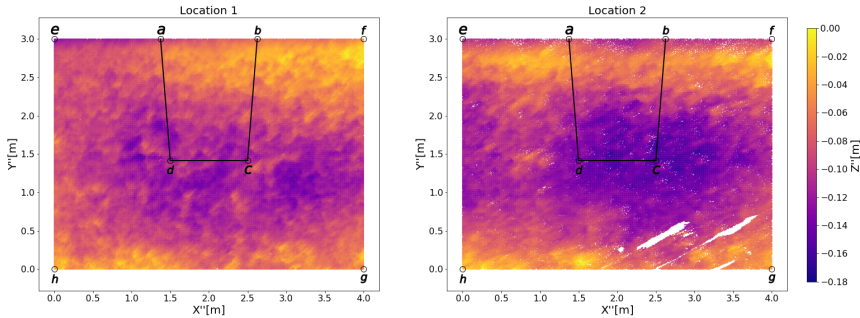


Figure 3.10: LiDAR height map for location 1 and 2, also showing the outline of maximum breach dimensions

The measured irregularities of the outer levee slope underneath the plate applied in Flood Proof Holland are analyzed to obtain an estimate of the dimensions of the spatial area through which leakage discharge will develop. Therefore, the point cloud, as shown in figure 3.10, is divided in a square grid with cells of 0.01 m by 0.01 m. The average height value of each grid cell is determined, reducing high frequency scatter caused by the grass, meanwhile catching the overall spatial variations of the outer slope as good as possible.

The plate as applied in Flood Proof Holland was able to adjust itself to the outer slope surface, as can be observed in figure 3.11, which shows a curved levee profile in  $y''$  direction, after removal of the plate at the end of a test cycle. This curved shape is less prominent in  $x''$  direction, caused by the reinforcement of the plate, as shown in figure 3.1. This visual observed curve levee slope can be observed in the LiDAR data in figure 3.10.



Figure 3.11: Location 2, after removal plate, red lines indicate curved shape of the subsoil

Water is entering the breach from three different directions: through area  $x_1$  and  $x_2$  in  $x''$ - direction and through area  $y_1$  in  $y''$ - direction, see figure 3.12. The characteristic levee profile for each area is equal to the average value of the grid cells over a length of 0.5 m in flow direction. The levee profile is averaged over a width of 0.5 m, to reduce

scatter as much as possible. This analysis results in the average levee profiles for area  $x_1$ ,  $x_2$  and  $y_1$ , for both experimental location 1 and 2 (figure 3.13 and 3.14), in Flood Proof Holland.

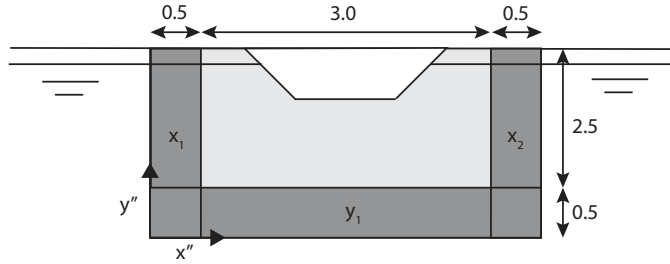


Figure 3.12: Definition of areas for determining average levee profile for Flood Proof Holland

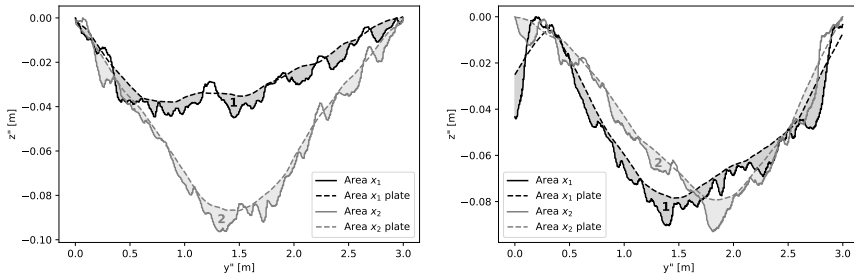


Figure 3.13: (left) Average levee profile at location 1 and, (right) 2 for the areas  $x_1$  and  $x_2$ , the colored areas indicate the channels, with a random channel indicated by the numbers 1 and 2

The flexibility of the plate is schematized by a low-pass filter with a cut-off length scale of 2 m for section  $y_1$  and 0.5 m for sections  $x_1$  and  $x_2$ . To reduce the number of peaks crossing the plate, a translation is applied, equal to the mean distance from plate to the peaks which are located above the plate. The dashed lines in figure 3.13 and 3.14 represent the deformed plate, which is located on top of the outer levee slope. Triangular shaped channels can be recognized in the colored surface area between plate (dashed line) and outer slope (solid line). These channels are considered to establish the discharge leakage pathways, as indicated by the solid areas.

A channel is defined as an area between two plate-profile crossings (colored areas in figure 3.13 and 3.14). The channel heights and channel widths can be determined for each representative profile, for which the numerical values are presented in table 3.6. Is The channel height is obtained as the average distance from plate to the outer levee slope. The average channel width is equal to the sum of channel widths divided by the number of channels.

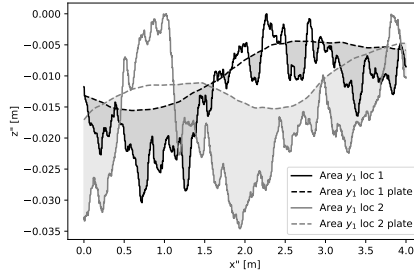
Figure 3.14: Average profile location 1 and 2 for area  $y_1$ 

Table 3.6: Averaged irregularity parameters (geometry of triangular channels) of outer slope in Flood Proof Holland

	$h_{ch}$ [mm]	$W_{ch}$ [mm]
Location 1, area $x_1$	5.8	400
Location 1, area $x_2$	6.2	400
Location 1, area $y_1$	6.8	390
Location 2, area $x_1$	8.7	620
Location 2, area $x_2$	7.5	340
Location 2, area $y_1$	12.5	790

### 3.4.2. PHYSICAL PARAMETERS TO CHARACTERIZE LEAKAGE

Now, the physical parameters which determine the leakage discharge underneath the plate are combined to a model. Then this model is calibrated using the experimental data from the experiments in Flood Proof Holland.

The total leakage discharge flowing underneath the plate is equal to the sum of the discharge flowing in vertical ( $Q_{x1}$ ,  $Q_{x2}$ ) and horizontal ( $Q_{y1}$ ) direction, (equation 3.3). Here the subscripts  $x_1$ ,  $x_2$  and  $y_1$  correspond to the inflow areas, as presented in figure 3.12.

$$Q_{leakage} = Q_{x1} + Q_{x2} + Q_{y1} \quad (3.3)$$

Leakage water is assumed to flow through the triangular shaped channels with characteristic channel height ( $h_{ch}$ ) and width ( $W_{ch}$ ), as described in the previous paragraph (figure 3.12). The channels are schematized as straight lines, taking the shortest path from the point of entry, at the edge of the plate, to the point of exit, where the channel reaches the breach. The flow lengths are  $L_x$  (equation 3.1) in horizontal and  $L_y$  (equation 3.2) in vertical direction (figure 3.15). The number of channels,  $N_n$  is defined as the inflow area of the channels, divided by the average width of a channel,  $W_{ch}$  (equation 3.4). The  $N_n$  parameter for the Flood Proof Holland case ranges from 0.75 to 2.56 for the different breach dimensions and inflow directions. For the channels in  $x_1$  and  $x_2$  direction, the inflow area is set to half times the projected pressure head, which is the average pressure between the top and at the bottom of the breach. For channel  $y_1$ , the inflow area is equal to the lower width of the breach,  $B_{down}$ . Diagonal channels are not taken

account within the model, since the contribution of these channels is considerably less, since the diagonal flows experience more friction as the flow paths are longer.

$$N_{x1/x2} = \frac{0.5h'}{W_{ch,x1/x2}} \quad N_{y1} = \frac{B_{down}}{W_{ch,y1}} \quad (3.4)$$

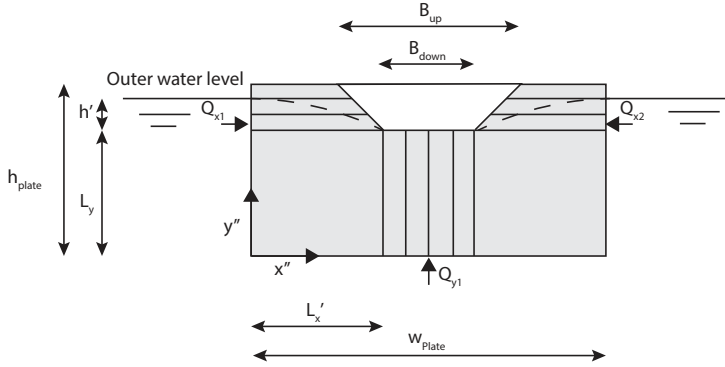


Figure 3.15: Parameters describing the flow channels within the leakage model

The discharge  $Q_n$  in a given direction, is equal to the surface area,  $A_n$ , of all the channels in the flow direction times the flow velocity  $u_n$  in these channels, (equation 3.5). Subscript  $n$  relates to the corresponding flow directions, perpendicular to  $x_1$ ,  $x_2$  or  $y_1$ . The surface area of the channels is defined as the surface area of a single channel, with the shape of a triangle with height  $h_{ch}$  and base  $W_{ch}$ , times the total number of channels in the flow direction (equation 3.6).

$$Q_n = A_n + u_n \quad (3.5)$$

$$A_n = \frac{1}{2} N_n h_{ch,n} W_{ch,n} \quad (3.6)$$

The velocity in a single channel is determined using Bernoulli's approximation, applying the Darcy- Weisbach equation to account for friction (Weisbach, 1845)(equation 3.7), in which  $D_{ch}$  is the hydraulic radius of the channel, which is the surface area of the channel divided by its wetted perimeter.

$$u_n = \sqrt{\frac{2gh}{1 + f \frac{L_n}{D_{ch}}}} \quad (3.7)$$

The friction factor,  $f$ , is approximated by implicitly solving the friction definition of Colebrook and White (Colebrook, 1939), (equation 3.8). Assuming a turbulent flow regime within the channels, in which  $Re$  is the Reynolds number. The roughness parameter  $\epsilon$  is determined using the method proposed by Pegram (Pegram and Pennington,

1996). This was achieved by applying a low-pass filter with a length-scale of 0.01 m to the average profiles  $x_1$ ,  $x_2$  and  $y_1$  for both locations. The average, absolute distance between the filtered to real data was then used to obtain an estimate the roughness parameter  $\epsilon$  at 0.15 mm.

$$\frac{1}{\sqrt{f}} = -2\log_{10}\left(\frac{\epsilon}{3.7D_{ch}} + \frac{2.51}{Re\sqrt{f}}\right) \quad (3.8)$$

Finally, a non-dimensional parameter is required to calibrate the model, which has to be multiplied by the estimated leakage discharge, while using the above model, equation (3.9). The fit parameter  $\beta$  is calibrated to a value of 0.2 for the Flood Proof Holland measurements, which results in the smallest root mean squared error, of 0.3 l/s. The  $\beta$  value is required to cover simplifications in the such as the stiffness of the grass, and the simplification of the surface area of the flow.

$$Q_{leakage} = \beta \sum Q_n \quad (3.9)$$

In figure 3.16 the measured leakage discharges are compared to the leakage discharges as calculated with the leakage model, using the calibrated value of the fit parameter. The performance of the model performs better for the cases on location 2, which results in the highest discharges, compared with the cases on location 1. This may indicate that the channel parameters for location 2 are better defined.

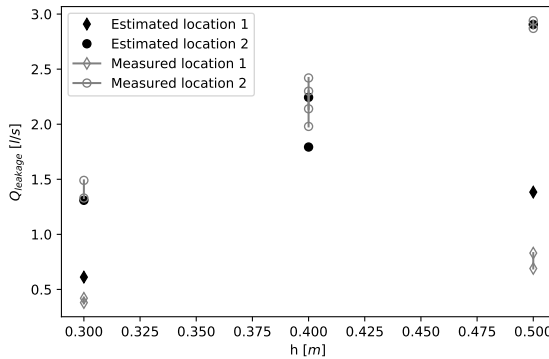


Figure 3.16: Estimated and measured leakage discharge as a function of hydraulic head ( $h$ ) for the Flood Proof Holland case

The leakage model provides a way to estimate the leakage discharge underneath the BresDefender. However, the data that enter this model rely heavily on the outer slope topology as determined by LiDAR. In practical cases, such data is usually not available. Combining equation 3.3 to equation 3.7 leads to the a simplified  $Q_{leakage}$ , equation 3.10. This equation assumes equal irregularities of the outer levee slope, over the entire contact area,  $A_{plate}$ . This definition still requires the determination for the average channel height,  $h_{ch}$ .



$$Q_{leakage} = \frac{1}{2} \beta (B_{down} + h') h_{ch} \sqrt{\frac{2gh}{1 + f \frac{L_{ch}}{D_{ch}}}} \quad (3.10)$$

### 3.4.3. DISCHARGE REDUCTION

The discharge through a breach, without the implementation of an emergency response measure in the form of a plate can be determined using the hydrodynamic part of the BRES model of Visser, 1998. This has been applied to determine the discharge ( $Q_0$ ) through a breach in its initial stages (equation 3.11). Thus,  $Q_0$  represents the undisturbed discharge through a trapezoidal breach, i.e., the discharge in case no plate or other emergency response intervention has been placed at the breach location. This equation assumes conservation of energy and mass at critical flow conditions ( $Fr = 1$ ). The discharge coefficient  $m$  is set to 1.

$$Q_0 = m \left(\frac{2}{3} h\right)^{\frac{3}{2}} \sqrt{g} B' \quad (3.11)$$

The leakage discharge, summarizes the expected leakage discharge when the plate is present, as described in the previous sections (equation 3.10). Now, the ratio of the leakage discharge to the undisturbed discharge can be determined. This comes down to dividing equation 3.10 by equation 3.11, resulting in equation 3.12. This ratio represents the discharge reduction as achieved by a specific intervention measure. Hence, this reduction factor ratio estimates the effectiveness of the intervention. The characteristic breach width  $B'$  is in the same order of magnitude as  $(B_{down} + h')$ , this reduces to 1.

$$\frac{Q_{leakage}}{Q_0} = 1.3 \frac{h_{ch}}{h} \left(1 + f \frac{L_{ch}}{D_{ch}}\right)^{-\frac{1}{2}} \quad (3.12)$$

The reduction factor depends on the channel height,  $h_{ch}$ , which can take on any value between 0 and  $h$ . If  $h_{ch}$  is equal to  $h$ , there is still a reduction to be expected, caused by the friction term. For a smaller channel height, caused by a better connection of the measure to the levee surface, the performance of the measure increases. In case of an increased potential head difference,  $h$ , the reduction parameter decreases, since this value raised to power 3/2 in equation 3.11. The friction term in equation 3.12, the part within the square root, includes the dimensions of the plate. It expresses the fact that more energy is dissipated in the channels underneath the plate, when the size of the plate increase. Hence, larger plates, with all other parameters being equal, will lead to smaller leak discharges, as might be expected.

The undisturbed discharge ( $Q_0$ ) has been determined for each breach configuration as tested in Flood Proof Holland and the Hedwigepolder. The undisturbed discharges are divided by the measured leakage discharges which are listed in table ??, 3.4 and 3.5. For the Flood Proof Holland experiments, it was found that the top load on the plate had no significant effect on the leakage discharge into the breach. Therefore, all measured discharges for the same location and same breach dimensions have been averaged. Figure 3.17 shows all discharge reduction factors for the experiments that were earlier presented. The horizontal axis indicates the leakage channel height ( $h_{ch}$ ) divided by the

water level  $h$ . For the Flood Proof Holland cases,  $h_{ch}$  is set to the mean value of the channel heights presented in table 3.6. For the Hedwigepolder, an average  $h_{ch}$  of 0.1 m is applied, as roughly measured in the polder.

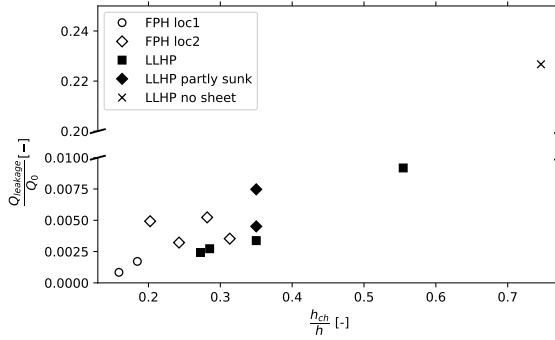


Figure 3.17: The undisturbed discharge reduction as obtained for the experiments in this work

The average reduction factor as plotted in figure 3.17, excluding the measurement without the tarpaulin, is 0.003. This indicates that the leakage discharge is 0.3% of the discharge without application of the BresDefender emergency response strategy. Both the stiff plate in Flood Proof Holland and the pontoon with tarpaulin in the Hedwigepolder show a very significant reduction in measured leakage discharge. The discharge reduction of the pontoon without tarpaulin is less, 23% of the undisturbed breach flow. Moreover, smaller channels lead to a larger reduction of discharge. Decreasing the water level difference  $h$ , leads to a reduction in effectiveness of the measure.

## 3.5. DISCUSSION

### 3.5.1. SOIL EROSION

An emergency response intervention is considered successful if the time to levee failure increases, compared to the situation without a measure. In the ideal case, no erosion occurs and the sediment in the breach is within the *no motion* regime for the load exerted by the leakage flow on the grain particles. This regime can be found by applying the Shields, 1936 criterion. If the actual Shields parameter ( $\theta$ ) is smaller than a critical value ( $\theta_{cr}$ ), no movement of the sediment is to be expected. For the analysis of the initiation of erosion, it is assumed the sandy core of the levee is not covered by a cohesive top layer. The presence of such layer would reduce the erosion process considerably. A sample of the core material of the Hedwigepolder levee was collected and analyzed. It was found that the core sand had a median size  $d_{50}$  of 0.144 mm, and a  $d_{90}$  of 1.481 mm. The Shields parameter ( $\theta$ ) of the flow-sand system can be estimated by a method proposed by equation 3.13 (van Rijn, 1993), using the experimental sieve parameters  $d_{50}$  and  $d_{90}$ .

$$\begin{aligned}\theta &= \frac{\tau_b}{(\rho_s - \rho_w) g d_{50}} \\ \tau_b &= \frac{\rho_w g u^2}{C^2} \\ C &= 5.75 g^{\frac{1}{2}} \log\left(\frac{12 d_c}{\alpha d_{90}}\right)\end{aligned}\quad (3.13)$$

Here,  $\rho_w$  is the density of the water,  $\rho_s$  the density of the sand,  $\tau_b$  the shear stress exerted by the water flow with velocity  $u$  on an average sand particle with diameter  $d_{50}$ .  $C$  is the Chézy coefficient,  $d_c$  is the critical flow depth in the breach (equation 3.15) and  $\alpha$  is a coefficient that accounts for the coarseness of the sand, usually set to 3. Then, the critical Shields parameter,  $\theta_{cr}$ , can be determined by equation 3.14 (Soulsby, 1998).

$$\begin{aligned}\theta_{cr} &= \frac{0.3}{1 + 1.2 D_*} + 0.055(1 - e^{-0.02 D_*}) \\ D_* &= d_{50} \frac{(s - 1) g^{\frac{1}{3}}}{\nu^2}\end{aligned}\quad (3.14)$$

In which  $D_*$  is the dimensionless sediment grain size,  $\nu$  is the kinematic viscosity of the fluid and  $s$  is the relative density ( $\rho_s / \rho_w$ ). In summary, this critical Shields parameter defines the onset of erosion of the breach, i.e., if  $\theta > \theta_{cr}$  erosion effects are expected to occur.

Following the experimental results presented earlier, the estimated discharge in the breach while applying an emergency measure is set to 1 percent of the discharge in case of undisturbed breach flow (3.17), all of the measured discharge reductions were below this value (except for the case in the Hedwigepolder without tarpaulin). From this, the average flow velocity in the breach can be estimated applying a critical flow depth,  $d_c$ , which holds for the flow velocity on the crest-to-inner-levee slope transition (equation 3.15).

$$u = \frac{Q}{d_c B'} \quad d_c = \sqrt[3]{\frac{Q^2}{g B'^2}} \quad (3.15)$$

Using the method presented above, the Shields parameter is determined for a hydraulic head of 0.5 m. The critical Shields parameter for the specific soil is 0.06. The calculated Shields parameter for the Hedwigepolder breach without an emergency measure is 4.86, which indicate movement of soil in the breach. However, the Shields parameter obtained for the case of applying an emergency response measure is found to be 0.75, which is one order of magnitude lower compared to the free discharge case. Thus, when an emergency response measure is placed properly, erosion rates of the soil in the breach decreases, and time to failure of the levee increases.

The breach model of (Visser, 1998), describes five different stages in breach flow. In breach stage II, the inner slope of the levee shifts towards the outer slope of the levee,

caused by erosion. During this stage, the dimension of the breach and the flow velocities are limited. Within this analysis it is assumed that the BresDefender cannot be applied anymore, if breach formation stage II is exceeded. The expected duration of breach stage II is shown in equation 3.16. The geometrical parameters used in this equation are the ones that were found from the Hedwige polder experiments (figure 3.6). The definitions of  $W_1$  and  $l_a$  are to be found in appendix A. The parameter  $S_s$ , the suspended load transport capacity, requires the selection of a proper sediment transport formula. The recommended erosion formula for the first breach stages of the Visser-model, is the equation of Bangold-Visser (Visser, 1988). However, experimentally obtained flow velocities for the case with emergency measure are outside the application limits. For this reason, the Engelund-Hansen (Engelund and Hansen, 1967) approach is adopted. Although this approach may overestimate the erosion rates, it can still be used for comparison of the separate case.  $B_w$  is the top width of the water in the breach and  $\psi$  is the inclination angle of the inner levee slope after stage I, which is set to an estimated value of  $33^\circ$ , the average angle of response of sand.

$$\Delta t_{II} = \frac{B_{up}}{B_w} \frac{W_1(1-p)l_a \sin \psi}{S_s} \quad (3.16)$$

The results computed from equation 3.16 to determine the time of breach stage II, for a head difference of 0.5 m, are found to be 9.3 min for the undisturbed case and 1698 min for the case with an emergency measure. The pressure head difference is incorporated in the  $W_1$  term of the equation. The time for the breach to develop is more than 100 times larger while applying an emergency response measure, assuming a leakage discharge of 0.01 times the undisturbed discharge. This holds for the full range of pressure heads considered. This extra time would allow for additional measures to be taken to completely stop development of the breaching process. Furthermore, the calculated breach formation time extended to an expected value of the order of 30 hours, which may be longer than the flood event. It should be noted that this approach is rather conservative, since it assumes erosion of sand, while in reality, a levee has a clay layer on top, which may prevent or slow down further erosion of the subsoil.

### 3.5.2. STABILITY OF A SINGLE PONTOON ELEMENT DOCKED AT A LEVEE

For the two-dimensional case, as schematized in figure 3.18, two potential failure mechanisms regarding the stability of a single pontoon element will be considered. The first stability failure mechanism of a docked pontoon element is the rotation around point A and subsequent downward sliding of the pontoon. The weight of the pontoon is the sum of its own weight,  $F_p$ , and the load of the ballast water,  $F_w$ . The water level within the pontoon is considered equal to the outer water level, which can be acquired by opening valves in the separate sections. The pontoon consists of four separate sections, indicated by roman numbers I to IV in figure 3.18. A steeper slope of the levee leads to more water storage in the sections, as plotted in figure 3.19. Analytic expressions of the fill percentages of the individual pontoon sections, for several levee angles  $\varphi$ , are to be found in appendix II.

The water pressures on the pontoon are  $p_1$  and  $p_2$ , caused by a hydrostatic pressure distribution with water depth,  $h_1$  and  $h_2$ . The water pressure at the point where water

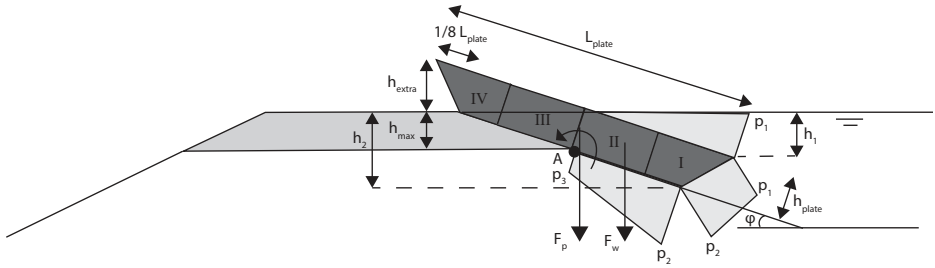


Figure 3.18: Stability schematization of a floating pontoon (BresDefender) docked at the outer slope of a levee

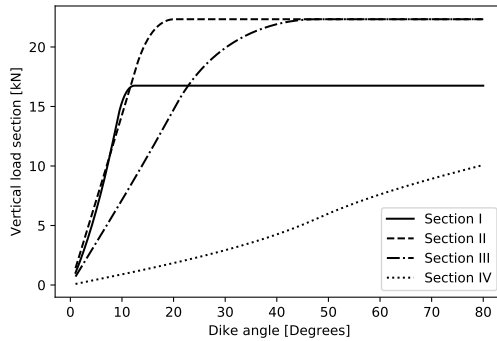


Figure 3.19: Contribution to the vertical load from the various sections of the pontoon, as function of the levee slope angle  $\varphi$

enters the breach, caused by water flowing underneath the pontoon, is  $p_3$ . The minimum value of  $p_3$  equals 0, for the case where friction of the flow between plate and grass dissipates the entire pressure head. The maximum value of  $p_3$  is the hydrostatic pressure one would expect if the water level in the breach equals the outer water level. Equation 3.17 shows the definition of the different pressures.

$$p_1 = \rho_w g h_1 \quad p_2 = \rho_w g h_2 \quad 0 \leq p_3 \leq \rho_w g h_{max} \quad (3.17)$$

The maximum water retaining height,  $h_{max}$ , describes the ultimate state for which the BresDefender can be applied. Water level  $h_{extra}$  is the minimum required space that is required for the freeboard of the pontoon, caused by the geometry of the pontoon. A freeboard lower than the minimum required vertical freeboard, as introduced in equation 3.18, will lead to more leakage water, caused by the diagonal part of the pontoon.

$$h_{extra} = \frac{1}{8} L_{plate} \sin \varphi + h_{plate} \cos \varphi \quad (3.18)$$

The maximum water retaining height,  $h_{max}$ , before the pontoon starts to rotate around point A, is determined using the momentum equation. The pontoon starts to rotate if the

driving moment has become larger than the resisting moment. Application of the momentum equation for angles ranging from 5 to 45 degrees leads to figure 3.20, in which  $p_3 = 0$  represents the most favorable situation, and  $p_3 = \rho_w g h_{max}$  the least favorable situation. The effective breach depth becomes larger for a steeper levee angle, since the horizontal arm towards the rotation point becomes smaller for larger levee angles.

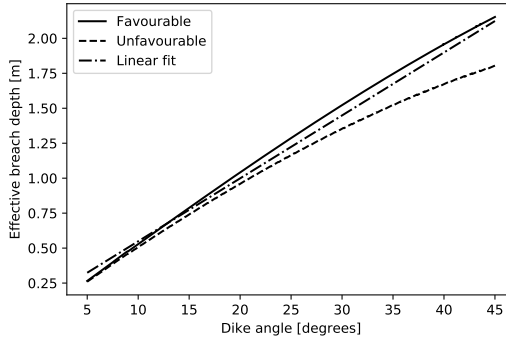


Figure 3.20: Maximum retaining height pontoon

Equation 3.19 shows a linear approximation of the maximum retainable breach depth, in which  $\varphi$  is the angle of the levee slope in degrees. This approximation applies for levee angles between  $5^\circ$  and  $45^\circ$ , and is presented as linear fit in figure 3.20. The equation is linearized by taking the mean of the favorable and unfavorable values of the effective breach depth for  $\varphi = 26.6^\circ$  and  $18.4^\circ$ , these angles correspond to levee slopes of 1:2 and 1:3, which are the most common levee slopes in practice.

$$h_{max} = 0.045\varphi + 0.099 \quad (3.19)$$

The second stability failure mechanism of the docked pontoon element is sliding. This mechanism describes the event of the pontoon sliding downwards caused by gravity. The factor of safety (FOS) for sliding is determined using equation 3.20. The positive loads are facing in positive  $F'_x$  and negative  $F'_z$  direction (figure 3.18). The static friction factor  $\mu_s$  is estimated to be 0.64, based on experiments using woven polypropylene plastic bags on a grass surface (Klipalo et al., 2022). This polypropylene plastic bags are assumed to have similar friction parameters as the tarpaulin. For the stability analysis,  $h_{max}$  is set to zero, leading to the most unfavorable load condition. Figure 3.21 shows the factor of safety for sliding at different levee angles. If the factor of safety becomes less than 1, anchorage is required to ensure the stability of the pontoon. This occurs if the levee angle becomes larger than  $32.6^\circ$ , which is steeper than levee slopes encountered in practice.

$$FOS = \frac{F'_{x,pos} + \mu_s F'_{z,pos}}{F'_{x,neg} + \mu_s F'_{z,neg}} \quad (3.20)$$

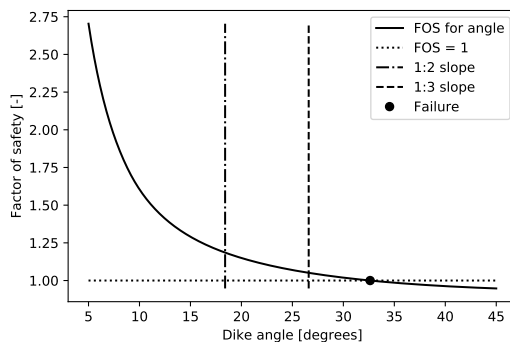


Figure 3.21: Factor of safety against sliding of the pontoon, instability occurs if levee angle becomes larger than  $32.6^\circ$

### 3.5.3. PONTOON PLACEMENT UNDER DYNAMIC CONDITIONS

In case of a real emergency, the pontoon, as tested in the Hedwigepolder, will be positioned while water is already flowing through a breach. These discharges may be even higher when enclosing more developed breaches (Sattar et al., 2008). One dynamic test with the pontoon, thus with water already flowing through the breach, was conducted in the Hedwigepolder. The pontoon was placed 2 meters from the breach, anchored to the levee, and then the weir was opened. Water started to flow around the pontoon, and the pontoon was pushed towards the breach location, which reduced the flow area of the water. This reduction caused a temporary increase of water flow velocities. The placement of the pontoon under dynamic conditions is shown in the sequence of photos in figure 3.22. The increased water flow velocity is clearly visible from the middle picture in figure 3.22. The presented scenario resulted in the no ballast case, as shown table 3.5. Further research should investigate local flow velocities during the closure process, and its local effect on erosion. The erosion of the soil during the dynamic placement procedure might cause large leakage channels, and can lead to extra leakage discharge in static conditions.



Figure 3.22: Dynamic placement of the BresDefender at Hedwigepolder. From left to right: pontoon at the breach before opening the hatch, pontoon during impact levee and pontoon after adjustment of the tarpaulin

### 3.6. CONCLUSIONS

In this research, the effectiveness of the BresDefender as an emergency response measure that intends to prevent or postpone a levee breach in its early phases, is presented. The focus is on the effectiveness of the emergency measure on the total leakage discharge for the case of early breach conditions. Intermediate scale experiments in Flood Proof Holland and real scale experiments in the Hedwigepolder were conducted to quantify the discharge flowing through a breach after applying the emergency measure. An empirical model has been developed to estimate the leakage discharge around the intervention. This empirical model provides a means to estimate the effectiveness of this method, given a range of environmental conditions.

Application of a flexible material at the bottom of the pontoon, able to adjust itself to irregularities at the levee slope, significantly decreases the leakage discharge through the breach, and hence increases the effectiveness of the BresDefender. The measured leakage discharge in a breach protected by the BresDefender was found to be only 0.3% compared to the undisturbed discharge, i.e., without deployment of the BresDefender. Hence, deployment of a system consisting of a stiff, sinkable frame, covered with a flexible material, reduces the erosion rates of a breach significantly. In this case one might speak of an emergency repair method.

It is demonstrated that the application of a stiff structure leads to significant reduction of flows through a breach. This leakage discharge is caused by the roughness of the grass and surface irregularities of the levee slope. Notwithstanding the effective reduction of breach discharges, leakage flow velocities are still expected to cause some erosion of the breach. Hence, application of this breach closure method always prevents or at least, extends the time to failure of the levee due to erosion mediated breach growth. Thus, it has been demonstrated that the time to failure is significantly increased by application of this measure. Breaching of a levee may even be completely avoided, depending on the flood wave.

The reported performance of the BresDefender was found for pressure head differences between 0.22 to 0.58 meters. An empirical based model has been proposed to estimate the leakage discharge and potential applicability of the pontoon for breach dimensions that were not tested. Although the BresDefender needs some further development, it is demonstrated to be a potential solution to stop or postpone the breaching process of a levee and protect the hinterland against flooding.





# 4

## OPERATIONAL RELIABILITY OF EMERGENCY MEASURES, A CASE STUDY FOR THE BRESDEFENDER

*Drove my Chevy to the levee  
but the levee was dry*

Don Mclean

---

This chapter has been submitted as: D. Janssen, S.N. Jonkman, A.J.M. Schmetts, B. Hofland and E. Dado. Operational reliability of emergency measures, a case study for the Bresdefender

## 4.1. INTRODUCTION

Levee systems play a critical role in safeguarding both lives and infrastructure from the devastating impacts of flooding. While these systems accept a small risk of flooding, the potential consequences in terms of loss of life and damage of an actual flood are severe (Jonkman, 2007). Additionally, the anticipated increase in loads on the levee system, driven by climate change (Kundzewicz et al., 2013), calls for measures to enhance its resilience. One way to address these challenges is the implementation of emergency response measures for floods. This study exclusively focuses on the application of emergency response measures. These measures are intended to mitigate unforeseen circumstances, and for which the required quantity and location of application are not known beforehand (Delfland, 2011; Knotter and Krikke, 2021).

Successful application of emergency measures relies on several critical aspects: detection of the weak spot that has to be reinforced, timely deployment at the required location, safe conditions to properly place the emergency measure safeguarding people positioning the measure and sufficient structural resistance (Lendering, 2018). Both the time required to implement the emergency measure as well as the time available to failure of a levee are subject to uncertainty.

In this study, we develop a probabilistic model that aims to identify the likelihood of an effective application of emergency measures. Here, successful application of the emergency measure means that the failure process is interrupted and the water retaining function of the levee is maintained. The results obtained from this study will contribute to a more informed decision-making processes and better preparation, ultimately improving the probability of successful application of emergency measures.

Then the probabilistic model is implemented in a case study featuring the emergency response measure BresDefender. The BresDefender is a military pontoon, normally applied to construct temporary floating bridges (figure 4.1). In this context, the BresDefender is used to stop the breaching process in its early phases by locally reinforcing a weakened levee section (Janssen et al., 2021). Application of the BresDefender prevent or delay a levee breach caused by overflow. The system can also contribute to reduce the risk of slope instability, as it influences the phreatic line inside the levee. An advantage of the BresDefender is its ability to be transported and applied from the water, eliminating the requirement for heavy equipment on the levee.



Figure 4.1: BresDefender prototype as applied during large scale experiments in the Hedwige-Prosperpolder (March, 2022)

In this paper, first a comprehensive theoretical framework is presented, providing an overview of the steps in the proposed probabilistic model (section 4.2). This is followed by detailing of the estimates of the time available (until breaching) in section 4.3 and the time required to implement measures in emergency response situations in section 4.4. These times, with their corresponding uncertainty interval are input to the overall model as presented in section 4.2. To estimate the uncertainty in the time required, an expert judgment analysis amongst Dutch water managers has been conducted following the classical model of Cooke, 1991. Subsequently, an expert judgment analysis, with the input of Dutch water experts, is conducted and presented in section 4.4.2, offering insights into the time requirements. Hereafter the probabilistic model is used for two different case studies - one describing a levee in the Rhine basin and one in the Meuse (section 4.5).

## 4.2. GENERAL MODEL FRAMEWORK

The leading parameters for the application of an emergency measure are time ( $t$ ) and damage, resulting from a characteristic elevation level ( $h$ ) (Janssen et al., 2021). These levels are separated into the water level in the river, ( $h_{river}(t)$ ) with the maximum water level  $h_{max}$ , and the water retaining height of the levee, ( $h_{levee}$ ). These parameters are plotted on the axes in figure 4.2. The time is separated into a time required to apply an emergency measure, ( $t_{req}$ ) and the time available before failure of the levee, ( $t_{avail}$ ).

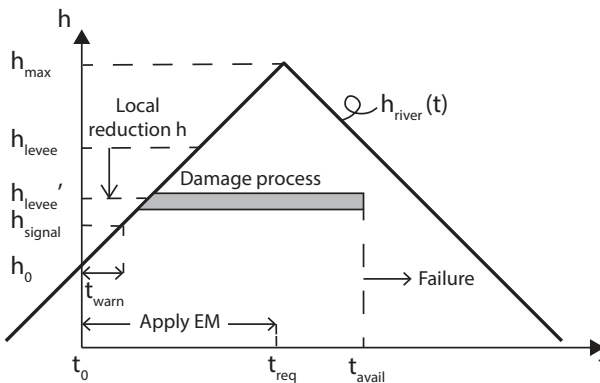


Figure 4.2: Flood water wave with time required and time available, for scenario with local reduction crest level. The thick solid line symbolizes an arbitrary high water wave

The emergency response process starts if the water authorities issue a state of emergency, at time ( $t_0$ ), with corresponding river water level  $h_0$ . This state of emergency is issued if the water level in the river is predicted to exceed a certain agreed threshold level ( $h_{signal}$ ) within a certain amount of time. The time available between issuing a state of emergency and exceeding the water level threshold is equal to  $t_{warn}$ . This warning time depends on the predictive accuracy of water level forecast systems installed by the local water authority (MinIenM, 2022).

In case the water level in the river exceeds the maximum retaining height of the levee,

( $h_{levee}$ ), the damage process starts. The time available,  $t_{avail}$ , is the time from issuing a state of emergency until the damages to a specific levee section are not repairable by the considered emergency measure. This is the case when the dimensions of the damage to the levee (the breach dimensions) are larger than the physical application limits of the emergency measure itself, or if the emergency measure cannot be placed without the risk of serious harm to the people involved in construction of the measure. The installation of the emergency measure is too late if the required time is larger than the available time (equation 4.1).

$$t_{req} > t_{avail} \quad (4.1)$$

No overflow occurs if the maximum water level in the river,  $h_{max}$ , is smaller than the levee height,  $h_{levee}$ . The levee failure starts when the loads on the levee has become larger than its resistance. The failure process can consist of several internal and external processes, which may enhance each other, ultimately leading to failure of the levee (Van et al., 2022). In the model that is presented here, a failure process is a crest height reduction caused by (successive) slope instabilities. This failure process reduces the crest height from  $h_{levee}$  to  $h'_{levee}$ , figure 4.3. This failure mechanism may be triggered by accumulation of pore water in the levee over time (Schierreck, 1998). It is important to note that a single, more shallow failure plane may not cause an immediate reduction in crest height, as a slope instability may not extend all the way to the crest, see figure 4.3 (Remmerswaal et al., 2021; Van Der Krogt et al., 2019).

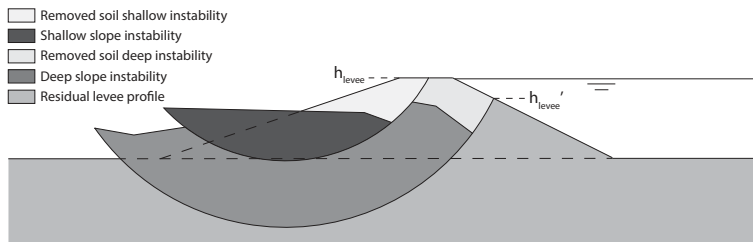


Figure 4.3: Definition of slope instability, where a shallow instability did not lead to a reduction of the crest height while a deep instability did, these circles could either occur sequentially or independently

Application of an emergency measure during a flood wave can have several effects on the failure process (figure 4.4). Application of an emergency measure will increase the water retaining level with an extra height,  $h_{EM}$ . Then either of two scenarios may occur. In scenario 1, the maximum water level in the river ( $h_{max}$ ) will be lower than the height of the levee with the emergency measure. In this scenario the damage process is successfully arrested. In scenario 2, the combined levee and emergency measure height are lower than the maximum water level in the river, hence the damage process will continue (equation 4.2), however it may develop at a slower pace.

$$\begin{aligned} 1) & h_{levee} + h_{EM} > h_{max,1} \\ 2) & h_{levee} + h_{EM} < h_{max,2} \end{aligned} \quad (4.2)$$

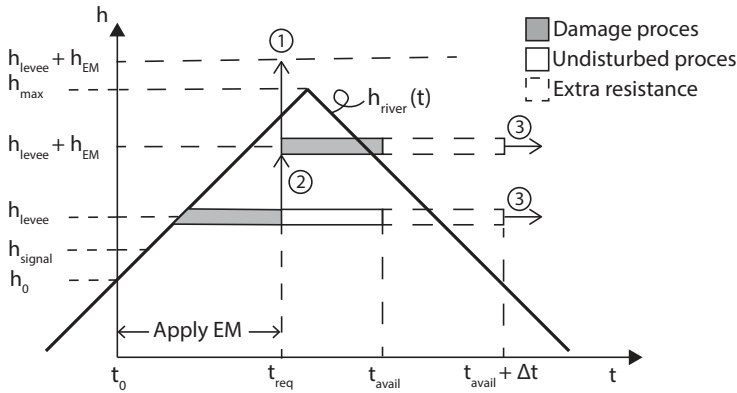


Figure 4.4: Three possible scenarios for the application of an emergency measure (EM) within a flood water wave. The thick solid line symbolizes an arbitrary high water wave

Next to increasing the levee height, placement of an emergency measure may also extend the time available until failure ( $\Delta t$ ), either by reducing the head of the flow, or by increasing the erosion resistance of the levee and its soil (scenario 3). Application of the emergency measure is assumed to be successful if the water level in the river decreases below the (temporarily increased) levee height, before the levee had reached complete failure.

The BresDefender case study only considers scenario 1 and 2, omitting scenario 3 to simplify the analysis. In practice, the BresDefender may enhance damage resistance as well (scenario 3) as real scale experiments with the BresDefender prototype showed a significant reduction in water flowing through the breach (chapter 3). It was found that reduction in flow rate through the breach decreases the erosion rate of soil and herewith increases the breaching time.

## 4.3. DAMAGE PROCESS: AVAILABLE TIME

### 4.3.1. GENERAL

Now, the time available until levee failure,  $t_{avail}$  in figure 4.3 and 4.4, will be elaborated. In further developing the model, two failure processes are to be considered, one for failure caused by overflow (figure 4.5) and one for failure by slope instability (figure 4.6). In the overflow failure process (figure 4.5), the water level of the river initially rises, eventually leading to overflow of the levee. From this moment onwards, observable damage is assumed within the model. This continuous overflow will cause damage to the inner slope, exposing the sand core of the levee to the water flow. Then the breaching process starts, followed by failure of the levee when the erosion has reached the outer crest line.

The failure path for slope instabilities starts with the occurrence of a single deformation in the levee cross section. After this moment, the damage can be visibly observed. This deformation process is continuous, ultimately leading to a crest height reduction. After that, water will rise until the water level in the river becomes higher than the re-

duced crest level. Lastly, the breaching process starts as soon as water starts to flow over the levee, ending up at failure of the levee (figure 4.6). Each of these sequential steps within both failure processes will be elaborated in more detail below.

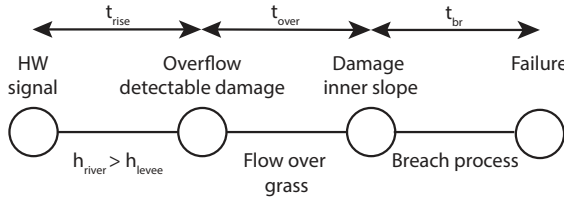


Figure 4.5: Sequence of failure process events caused by flow over grass inner slope in which circles represent space-time events. HW signal corresponds to  $t_0$ . Symbols are introduced in coming paragraphs

4

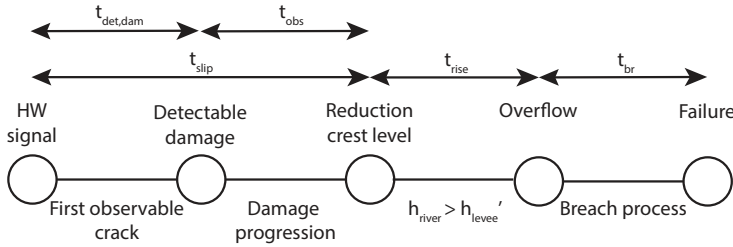


Figure 4.6: Sequence of failure process events caused by slope instabilities in which circles represent space-time events. HW signal corresponds to  $t_0$ . Symbols are introduced in coming paragraphs

### 4.3.2. OVERFLOW

The time of overflow ( $t_{over}$ ) is defined as the interval between the moment of initial overflow of the levee and the time of occurrence of damage to the protective grass layer. Once damage has occurred in the grass layer, a new phase set in, the actual breaching process. The overflowing water exerts a shear stress on the protective grass layer. The resistance of the grass against this shear is quantified as the overflow velocity sustained over a specific duration (Hewlett et al., 1987), depending on the quality of the grass. This quality is categorised as good, normal or poor. The interdependence between the mentioned parameters is illustrated in figure 4.7.

The velocity on the outer levee slope can be determined using the Manning equation (equation 4.3). Here,  $N$  is the Manning coefficient, set to 0.03 (Hewlett et al., 1987);  $R$  is the hydraulic radius of the flow, configured for a flow width of 1 m;  $S$  denotes the slope of the energy line, adjusted to a slope of 1:3, equal to the slope on which the BresDefender has been tested. Pressure head is equal to the difference between the maximum water level in the river and the levee height.

$$v = \frac{1}{N} R^{\frac{2}{3}} s^{\frac{1}{2}} \tag{4.3}$$

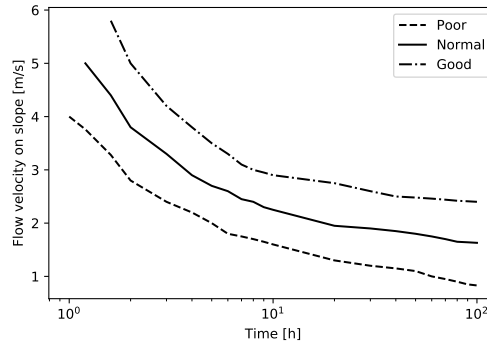


Figure 4.7: Time to failure of protective grass layer of a certain quality as a function of maximum flow velocity on the inner slope of the levee (Hewlett et al., 1987)

Based on the expected velocity (equation 4.3), the time to failure of poor and good quality grass cover can be obtained from figure 4.7. The time-to-failure of the poor and good quality protective grass layer, given the determined flow velocity, will serve as lower and upper bound in the probabilistic model. In the simulation, time to overflow ( $t_{over}$ ) is randomly selected within the bounds, based on a uniform distribution. In situations where the velocity falls outside the available data range, the time-to-failure is set to the smallest or largest values within the available dataset.

### 4.3.3. SLOPE INSTABILITY

The model integrates the probability of the occurrence of slope instability corresponding to a specific river water level, utilizing a site-specific fragility curve, as available from a Dutch database (Kolen et al., 2021), and elaborated on in the section case studies. The time until reduction of the crest height ( $t_{slip}$ ) is approximated and linked to the flood water wave, as illustrated in figure 4.8. The asymmetric normalized distribution of the time required for the first failure is centered around the peak of the flood water wave ( $t_{max}$ ). A standard deviation for both the left and the right side of the peak is equal to 1/3 of the time differential between  $t_{signal}$  and  $t_{max}$ . These boundaries are selected, acknowledging a small probability of slope instabilities at  $t_{signal}$  in site-specific fragility curves. For the Dutch case, this signal water level threshold is exceeded 1/50 years (MinlenM, 2022).

A levee starts to show visible damage, before a total crest height reduction, in the form of cracks and soil deformation. The time of observable damage,  $t_{obs}$ , is the time interval between the moment of first visible damage and total crest height reduction. The time of observable damage is estimated as a value between 0 and 18 hours in a uniform distribution. Here the lower limit of  $t_{obs}$  is 0 hours is known to be a conservative assumption. The upper limit is determined using data of real levee failure occurrences at Breitenhagen (Kool et al., 2019) and Fishbeck (Henning and Jüpner, 2015). Here detectable damage was observed 12 and 17 hours respectively before levee failure. The time to detectable damage,  $t_{det,dam}$ , is the time between the high water signal and the first observable damage, and is defined in equation 4.4.



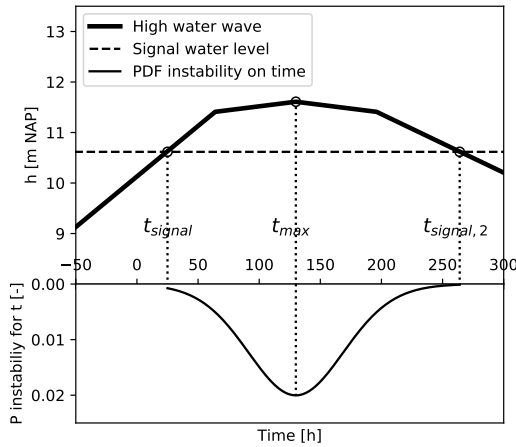


Figure 4.8: Probability of occurrence first slope instability, coupled to a typical flood water wave for Rhine river (flood water wave based on Chbab, 2016)

$$t_{det,dam} = t_{slip} - t_{obs} \tag{4.4}$$

The crest height reduction of the levee is randomly assigned as a value ranging from 0.5 to 2 m, after the occurrence of a slip failure. This is based on reported slip failures, which showed a crest height reduction of 1 to 2 m, as indicated by Hart et al., 2016. Recent levee failure cases at Fishbeck (Henning and Jüpner, 2015), showed a crest height reduction of 0.5 meters and, while a reduction of 1 meter was observed at Breitenhagen, shortly after overflow (Brauneck et al., 2016).

#### 4.3.4. BREACH FORMATION TIME

The breach formation time,  $t_{br}$ , starts either after the damage to the protective grass layer (for overflow) or the reduction in crest level (instability). The total breach formation time is the time required for the breach to develop itself beyond feasible repair. Within the model it is assumed that a levee becomes irreparable once the breach formation advances beyond stage II as defined by Visser, 1998. At this stage, the inner slope extends to the outer slope of the levee. After completion of stage II, breach width starts to increase over time (figure 4.9, right panel).

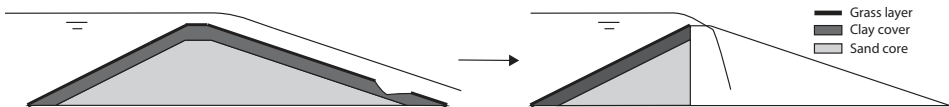


Figure 4.9: (Left) Cross section at location of breach at start breach formation process and (right) breach dimensions on the end of stage II, inspired by Visser, 1998

This breach formation rate has been found to depend on the water level in the breach,

the composition of the levee and the failure mechanism (Janssen et al., 2021). The  $t_{br}$  is randomly selected from a normal distribution with a mean of 15 minutes with a standard deviation of 5 minutes. These values have also been derived from the real levee failure case Breitenhagen (Brauneck et al., 2016) and the large scale breaching experiment at the Zwin (Visser et al., 1996). These values are valid for erosion of the sand core of the levee. The effect of rising water levels within the breach during the breach process is not taken into account within the model.

## 4.4. PREPARATION OF EMERGENCY MEASURES: REQUIRED TIME

### 4.4.1. GENERAL FRAMEWORK

As the times involved with the two selected failure scenarios have been addressed, now the emergency response intervention has to be bought in. The application of the emergency measure, *Apply EM*, which requires a time interval of  $t_{req}$ , to install, as presented in the theoretical framework in figure 4.2. Two different flow charts are possible to estimate the total time required: a series model (appendix B) and a parallel model (figure 4.11). In the series scheme, all steps in the water crisis event path are modelled consecutively. Whereas in the parallel scheme, the preparation of the emergency measure and the levee inspection process are decoupled, i.e. they are assumed to occur simultaneously in time. The levee inspection process for the Dutch case involves visual inspections for deformations on the levee surface conducted by (trained) personnel. The schematization of both models is derived from emergency guidelines and discussions with experts in flood emergency management in the Netherlands (Knotter and Krikke, 2021; MinIenM, 2022). The description and schematisation of the series model is to be found in appendix I. The parallel model will now be elaborated further. This model will provide predictions of lower failure probabilities, and is most in line with current practice.

The decoupling of the preparation of the emergency measure and the levee watch, results in three different sub-paths for the parallel scheme (figure 4.11). Sub-path I represents the preparation of the levee watch. It starts after a high water signal and ends after detection of damage at the levee (circles). Sub-path II represents the preparation of the emergency measure. It starts following the decision to prepare the measures and ends if material and personal are ready at a storage point (squares). Sub-path III describes the transportation and placement of the emergency measure (triangles). This path starts after completion of both sub-paths I and II. At the end of sub-path III the emergency measure has been successfully installed. The total time,  $t_{req}$ , is then given by (equation 4.5). The times  $t_1$  to  $t_6$  are the times taken for each branch in the process figure 4.11. This is further elaborated in the next section.

$$\begin{aligned}
 t_{req,par} &= \max(t_I, t_{II}) + t_{III} \\
 t_I &= \max(t_1 + t_2, t_{det,dam}) + t_{insp} + t_3 \\
 t_{II} &= t_4 + t_6 \\
 t_{III} &= t_5 + t_{place}
 \end{aligned}
 \tag{4.5}$$

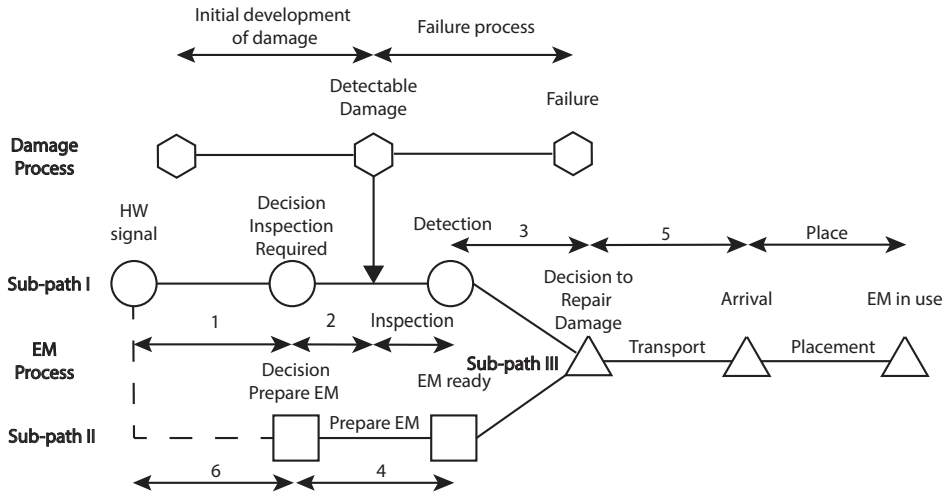


Figure 4.10: Time required to apply emergency measure, parallel, numbers indicate question in expert judgement (table 4.1)

#### 4.4.2. ESTIMATION OF TIME REQUIRED: EXPERT JUDGEMENT ANALYSIS

It is challenging to obtain proper estimates for the various process steps for rare and diverse emergency events. In order to obtain as realistic values as possible experts were interviewed in a systematic manner. In both the series (figure B.1) and parallel (figure 4.11) flow diagrams, the steps 1 to 6 have been labelled. These numbers correspond to a question, as posed in a structured expert judgement analysis, utilising the classical model developed by Cooke, 1991. The questions, directed at the experts, serve as input for the model, and are detailed in appendix B. A total of 22 experts participated in the questionnaire, with the majority being members of the Dutch CTW (Crisis Expertise Team Flood Defences). CTW members work within organisations as Rijkswaterstaat, Water Boards, Deltares and Defence. These experts are deployable during a high-water crisis in the Netherlands. Mostly by offering expert advice to local water authorities, based on their specialized knowledge. The remaining participants have experience with Dutch water safety systems over an extended period of time. The questionnaire was completed on April 19, 2023.

During a 30-minute session, the experts were initially briefed on fundamental statistics and the purpose of the expert judgement session. Subsequently, each expert received a paper questionnaire, consisting of 10 calibration questions and 20 questions of interest for estimating the desired parameters. For each question, the experts were requested to provide their estimated 5, 50 and 95 percent quantile answers. The calibration questions were presented on a screen, with supporting background information and visuals. The questions of interest did not contain any extra information. The experts were not allowed to discuss the answers during the session. A complete list of the questions and the anonymised attendees of the questionnaire is to be found in the appendix B.

The expert data has been analysed with the ANDURYL software package (Rongen et al., 2020), which allows to analyse several expert judgement decision makers within a user interface. The output of three decision makers are analysed. First, the equal decision maker, in which all of the experts responses are weighted equally. Second, the global decision maker, where the weight of the different experts is based on its expert performance. Third, the global optimised, where the most competent experts (which answered the calibration questions best) are selected. The elicitation results of the analysis are presented in appendix B.

#### EXPERT OUTPUT QUESTIONS OF INTEREST WITHIN THE MODEL

The results of the expert judgement analysis, determined though the application of the global decision maker, are displayed in table 4.1. Additional results and an explanation for choosing this specific decision maker can be found in Appendix II. For each question, a cumulative density function (CDF) can be generated, suitable for employment in the critical time model. Among the inquiries, distinct time frames are addressed. First, those concerning preparation and decision-making related to the levee watch (questions 1, 2 and 3). Second, those addressing the decision to prepare emergency measures (question 4 and 6). Third, those projecting transport velocities during a high water crisis (question 5a and 5b).

Table 4.1: Model parameters as obtained from expert judgement session

Question	Topic	Sub-path	Unit	5%	50%	95%
1	Decision: levee watch	I	h	0.3	1.4	7.3
2	levee watch preparation	I	h	0.6	3.3	11.8
3	Decision: repair required	I	h	0.0	0.5	3.2
4	Preparation emergency measure	II	h	0.5	5.4	12.0
5a	Velocity road transport	III	km/h	17.9	56.2	78.0
5b	Velocity water transport	III	km/h	2.2	5.8	29.3
6	Decision: to apply EM	II	h	0.2	7.8	23.8

#### 4.4.3. INSPECTION

The time required to detect a weak spot after the occurrence,  $t_{insp}$ , depends on the speed of inspection of the levee watch and the probability of detecting the damage by the levee watch. A study aimed at measuring the successfulness of the levee inspection during summer inspection gave an average detection probability of  $p_{detection} = 0.7$  per inspection round, for section damages (Klerk et al., 2021). External conditions such as availability of daylight, weather conditions, levee accessibility and experience of the levee watch may influence the detection probability (Bakkenist et al., 2012; CIRIA, 2013), but are further neglected here.

During levee surveillance, a designated section of the levee is monitored by trained personnel named , the levee watch. The levee watch inspects the section, with a certain length,  $l_{section}$ , and the inspection is conducted with a certain velocity,  $v_{insp}$  (figure 4.11). The average  $l_{section}$  is set to 10 km (Knotter and Krikke, 2021). The parameter  $v_{insp}$  is configured to 3 km/h, representing the average walking speed of an adult. The levee

watch keeps inspecting the same levee section, for a number of rounds,  $n_{rounds}$ , until the damage has been spotted, which is affected the probability of detection,  $p_{detection}$ . Within the model, the damage will be located randomly on the levee section, with a distance  $l_{damage}$  from the inspector. The total inspection time is the number of rounds times the length of the section, plus the distance to the damage, multiplied by the inspection speed (4.6). Inspection values applied within the model are summarized in table 4.2. The model only includes the occurrence of a single damage per section.

$$t_{insp} = v_{insp}(n_{rounds}l_{section} + l_{damage}) \tag{4.6}$$

$$n_{round} = \text{rounds before detection damage, with probability of succes } p_{detection} \tag{4.7}$$

Table 4.2: Input parameters detection

Aspect	Value	Ref
$p_{detection}$	0.7	Klerk et al., 2021
$l_{section}$	10 km	Knotter and Krikke, 2021
$v_{insp}$	3 km/h	Expert practice

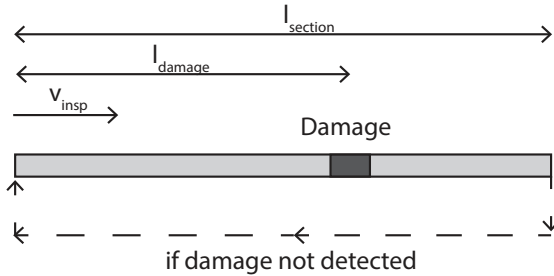


Figure 4.11: Inspection model, with arbitrary damage on levee section

#### 4.4.4. TRANSPORT

The time of transport,  $t_{trans}$ , depends on the distance over road ( $l_{land}$ ) and water ( $l_{water}$ ) from the storage to the affected levee section, alongside their respective transportation velocities (equation 4.8). The standard distances applied in the model are set to a transportation distance of 20 km over land over land ( $l_{land}$ ) and 1 km over water ( $l_{water}$ ) unless stated otherwise. The velocity over land ( $v_{land}$ ) and water ( $v_{water}$ ) are randomly selected from the expert judgement results for question 5a and 5b (table 4.1). If the model is being applied for land-based emergency measures, the water distance can be disregarded.

$$t_{trans} = t_5 = v_{land}l_{land} + v_{water}l_{water} \tag{4.8}$$

#### 4.4.5. PLACEMENT

In the current model, only the placement of the BresDefender emergency measure is considered. Large scale experiments in the living lab Hedwige-Prosperpolder have been executed to evaluate the placement procedure, see chapter 3. Detailed information on the placement procedure and the conducted experiments can be found in Velde, 2022. The mean time required to install the BresDefender after arrival was found to be 46 minutes with a standard deviation of 10 minutes (table 4.3). The placement time,  $t_{place}$ , is a randomly selected value originating from a normal distribution defined by the previous parameters. It should be noted that the time applied in the model is rather conservative; a potential reduction in placement time of at least 15 minutes is expected to be possible through improvements to the prototype pontoon and enhanced of personnel training (Velde, 2022).

In the current placement procedure, the BresDefender can effectively raise the crest height of a levee by 0.3 m. The performance of the BresDefender, when the water level surpasses this threshold remains uncertain. It is anticipated that the pontoon would remain operational, however, more leakage water is expected to flow through the breach, entering from the sides of the BresDefender. In the model, application of the BresDefender increases the levee height by 0.3 meters ( $h_{em}$ , table 4.3). In the model, it is assumed that the BresDefender consistently raises the levee height by 0.3 m, disregarding the impact of the specific timing requirement for placement within the flood wave. If the river water level surpasses this value, failure occurs. Further improvements to the placement procedure may enlarge the application range and performance, as the maximal water level the BresDefender can stop is determined at 1 m (chapter 3.5.2).

Table 4.3: Placement performances prototype BresDefender emergency measure

Aspect	Value
mean placement	46 min
std placement	10 min
$h_{em}$	0.3 m

## 4.5. CASE STUDIES

Two case study areas are selected to investigate the contribution of several parameters to the probability of success of emergency measures. One case is in the Rhine and the other in the Meuse river basin. These cases represent two different load conditions within the Dutch flood protection system, with a larger warning time for the flood waves in the Rhine compared to the Meuse (table 4.4). The Rhine case is located at levee ring 43 at the Waal river branch (table 4.4). The Meuse case is located in the Southern part of the Limburg province, near Meers..

The model employs a Monte Carlo analysis, incorporating 10,000 unique values for each individual probability distribution mentioned in the previous chapter. The total times required and available are determined for each unique combination of samples, assessing whether the measure is implemented on time. The structural requirements of the emergency measure are incorporated by adding the additional height to the (re-

duced) levee height. If the river water level surpasses the total (reinforced) height, assuming the measure was implemented in time, structural failure of the measure will occur within the model.

Table 4.4: Input parameters for case studies (MinlenM, 2022), levee height determined extracted from elevation map, received on June 30th, 2023 (AHN, 2023)

	Rhine basin	Meuse basin
River	Waal	Meuse
levee ring and section	43 – 5	87 – 1
Levee reference	DT120.D	0.77
Nearby village	Ochten	Meers
Return period code red (year)	50	50
Warning time (h)	24	12
h levee (m above NAP datum)	12.8	37.7
Main failure process	Instability before overflow	Overflow

### 4.5.1. WARNING TIMES

The warning times, which serve as input for the model, are based on the Dutch national procedure for floods (MinlenM, 2022). Within this guideline, a return period for a code red in the Rhine river is assumed to be 50 years, while the code red return period for the Meuse is 25 to 50 years. If a code red is issued, national safety may be at stake. A code red starts 12 to 48 hours before the water level is expected to exceed the signal water level for the Rhine river, and 12 hours for the Meuse river (table 4.4).

A standard flood wave shape over time for both the Rhine and Meuse case is implemented in the model, following the findings of Chbab, 2016. The water levels, corresponding to the selected return period are determined with Hydra-NL as described by Kolen et al., 2021. The fragility curves providing the probability of a slope instability given a certain water level have been determined with data from OKADER (Kolen et al., 2021). The flood waves for different return periods are plotted in figure 4.12.

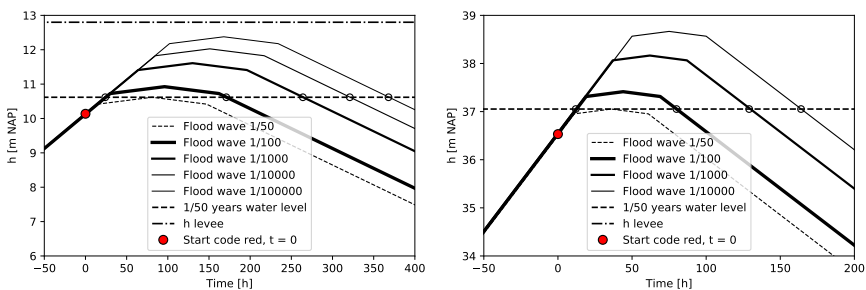


Figure 4.12: Flood water waves for Rhine (left) and Meuse case (right)

### 4.5.2. RHINE CASE

A conditional and a probabilistic subcase have been implemented for the Rhine river basin case. In the conditional subcase, the model is run given the occurrence of a slope instability (thus the probability of a slope instability is set to 1). In the probabilistic subcase, the fragility curve for slope instabilities determine the probability of this instability. The results of a conditional run for the Rhine case are summarized in table 4.5, 4.6, 4.7 and 4.8, assuming a slope instability leads to a reduction of crest height of 1 to 2 meters. The transportation distance is 20 km over land and 1 km over water. The return period of the high-water wave is 1000 year. In total 10,000 independent samples are used for the determination of the distributions of the time required and available.

The output in table 4.6 indicates that the time required to prepare the levee inspection and the emergency measure is one order of magnitude smaller than the time required for damage to occur. This indicates that the preparation of the levee watch and the emergency measures is not likely to be a critical step in the process if its preparation begins promptly after the issuing of a code red.

Comparing the failure paths in series (appendix B) and parallel (figure 4.11), a median difference of 6 hours in deployment time after issuing code red is observed (table 4.5), stemming from the time required to prepare the emergency measure after detection of damage (table 4.6), in the series assumption. Table 4.8 displays the time available before levee failure. The time to overflow refers to the duration between the start of code red and the initiation of overflow over the crest of the levee.

When comparing the median time available until levee failure with the median time required for the series and parallel process, it becomes apparent that the series approach exceeds the available time, while the parallel approach requires approximately the same amount of time as it takes to reach overflow. The conditional probability of being too late ( $t_{req} > t_{avail}$ ) for the serial assumption is 58% while this percentage for the parallel assumption it is 32%. For the remainder of the analysis, only the parallel model will be considered, as it presents the lowest probability of exceeding the time limit.

Table 4.5: Outcomes for the time required for model runs for the series and parallel schematization, too late is defined as:  $t_{req} > t_{avail}$

	Series	Parallel
Median [h]	134.5	128.5
Standard deviation [h]	40.6	39.6
Probability of being too late [-]	0.58	0.32

Table 4.6: Model results, for the Rhine test case for 1/1000 per year conditions, time required in hours, DW = levee watch, EM = Emergency measure

	Period until damage		
	Prepare DW	Prepare EM	Time to damage
Median [h]	5.2	13.9	120.6
Standard deviation [h]	18.5	26.5	39.4



Table 4.7: Model results, for the Rhine test case for 1/1000 per year conditions, time required in hours, DW = levee watch, EM = Emergency measure

	Period after damage			
	Detect damage	Decision EM	Trans	Place
Median [h]	2.4	0.5	0.5	0.8
Standard deviation [h]	2.8	3.1	0.8	0.2
Fraction of total duration after damage [-]	0.5	0.15	0.16	0.18

Table 4.8: Model results for time available for the Rhine test case

	Time to overflow	Breach time
Median [h]	126.8	0.3
Standard deviation [h]	34.3	0.1

4

Four different steps in the process are important to consider after the occurrence of damage to the levee: detection of damage, the decision to apply the emergency measure, transportation of the measure and the placement of the measure. Detection of damage has the largest expected duration in the post-damage stage (table 4.7) followed up by placement of the emergency measure. Reducing the time required for these four steps, will decrease the likelihood of being too late and increases the overall performance of the emergency measure (see discussion). The ‘fraction of total duration’ value in table 4.7 is the median value of a step in the period after damage, divided by the total median duration of period after damage.

Figure 4.13 gives the modelled conditional probability of success, when slope instability occurs, for various return periods of flood waves for the Rhine case. The emergency measure is expected to have a high likelihood of success for events with return periods around 100 years. Notably, the success of the emergency measure decreases as the return period becomes smaller. The primary factor contributing to this effect is the increase in the disparity between the river water level and the height of the levee if the return period becomes smaller. The right graph in figure 4.13 shows the distribution of outcomes, given levee failure. Both figures show a reduction in the effectiveness of the emergency measure for smaller return periods. The proportion of cases where the emergency measure arrives too late remains relatively constant for the different return periods.

Another observation from figure 4.13 is the reduction in success for smaller return periods while the probability of being in time without success increases, this may indicate the lack of retaining height of the emergency measure for smaller return periods. Figure 4.14 shows a run of the model with a variable extra height ( $h_{em}$ ) of the applied emergency measure for a return period of 1/1000 years for the conditional case. This highlights that increasing the height to 0.8 m leads to a significant increase in the likelihood of success. The current BresDefender prototype is able to increase the levee height with 0.3 m above still water level. Considering stability requirements, a maximum retaining height in the order of 1 m (chapter 3.5.2) is to be found for the emergency measure, thus 0.8 m is in reach.

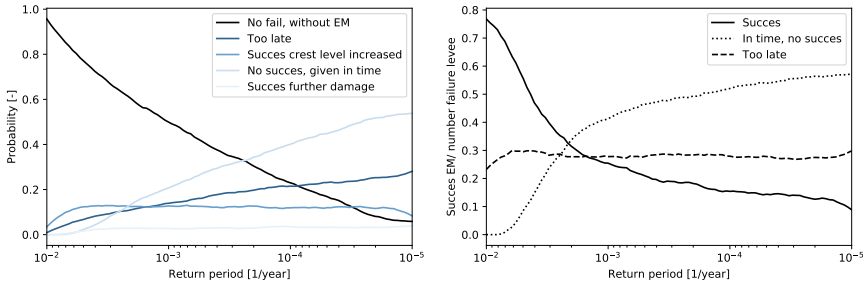


Figure 4.13: (Left) Conditional probability of successful mitigation by emergency measure Rhine case, given slope instability (right) relative success rate of emergency measures, where the relative value is the variable divided by number of levee failures. The base case can be extracted from the right figure.

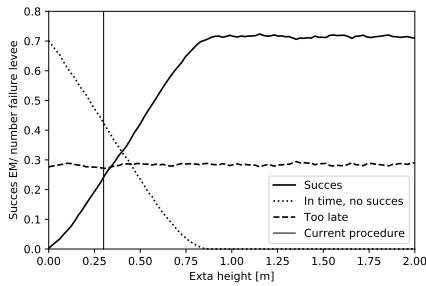


Figure 4.14: Effect retaining height measure ( $h_{em}$ ) on success rate, Rhine river, return period 1/1000 years.

When considering the complete probabilistic scenario for the Rhine river case, which incorporates the probability of slope instability coupled with the maximum water level in the river based on site-specific fragility curves, it is observed that the probability of success is rather low (figure 4.15). This is primarily due to the large share of no failure cases in for the lower return periods. The relative success of the emergency measure is similar to the conditional case.

### 4.5.3. RIVER MEUSE CASE

MModel runs were performed for the probabilistic scenario for the Meuse case, which represents a levee prone to overflow (figure 4.16). This case represents the probabilistic case, where the probability of a slope failure is determined by a fragility curve, given the water level in the river. The results for a run for a 500 year return period flood wave are given in table 4.9, with the probability of a slope instability incorporated as a fragility curve (probabilistic case). The estimated probability of being too late for the Meuse case is equal to 1, with the assumption that one starts to prepare the emergency measure after the start of overflow.

The time available until levee failure due to overflow is limited by the 0.3-meter height difference between the levee and the river water level in this specific case. The time to install the emergency measure at the right location is too long for all cases, if one starts

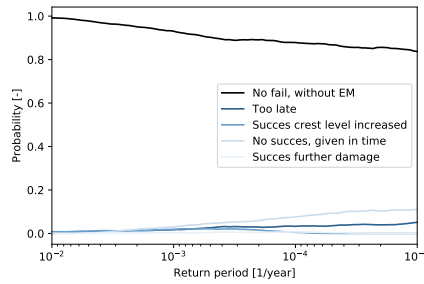


Figure 4.15: Results full probabilistic run Rhine case

4

the logistical emergency measure process after the start of overflow.

Table 4.9: Outcomes run model for series and parallel run data for period after damage is equal to data in table 4.7

	Time available			Time required	
	Time to overflow	Resistance overflow	Breach time	Series	Parallel
Median [h]	29	1.2	0.3	38.9	32.9
Standard deviation [h]	0.2	0	0.1	17.1	25.6
Probability of being too late [-]				1	1

### 4.6. DISCUSSION

The probabilistic model as described in the previous section, includes several assumptions. The first assumption is the overall performance of the prototype BresDefender. During large-scale experiments involving the BresDefender (Maat et al., 2023; Schmets et al., 2024), leakage water seeping through the pores at the soil-structure interface has been noted. However, the observed amount of leakage water is not expected to lead to severe damage progression. Furthermore, in the model, a water level exceeding the increased crest level is incorporated as failure, however, in reality the emergency measure reduces the flow potential, and herewith increases the time to failure. This will improve the overall performance of the levee. The exact effect on the breaching time needs further research.

A second assumption is neglecting spatial variations in levee properties: the resistance of the grass varies spatially in crest direction; the presence of e.g. animal burrows may decrease the resistance of a levee locally (Koelewijn et al., 2022). This effect is not taken into account within the model. These irregularities of the levee cross section does explain the relatively large standard deviation in the occurrence of damage.

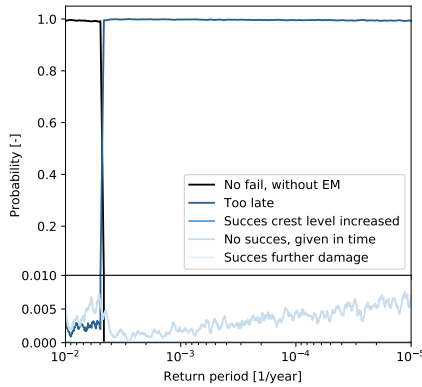


Figure 4.16: Probabilistic probability of failure for case Meuse

#### 4.6.1. PROACTIVE APPLYING EMERGENCY MEASURES

The essential parameter contributing to the failure of emergency measures is being too late, i.e. the damage of the levee already progressed beyond a repairable level before preparation of the emergency measure. This preparation include the steps of detection of damage, the decision to repair the damage, the transport of emergency measures to the weak spot, and proper placement.

Possible improvements in the application of an emergency measure after the detection of damage include better detection of the damage, in particular by sensors in the levee (Schenato, 2017), or monitoring by drones (Shoemaker et al., 2019) or satellites (Özer et al., 2018). Transportation and placement of the emergency response measure BresDefender, can be improved by faster transportation, for example airborne. Creating a denser network of more storage places will also reduce the transportation time to the site. Another possibility is to decrease the placement times by improving the current BresDefender prototype. This includes both training of personnel and structural improvements to the physical system.

The impact of reducing the duration of these steps on the probability of being too late is depicted in figure 4.17 (return period 1000 years, standard Rhine parameters and return period 500 years, standard Meuse parameters). For the Rhine case, the probability of being too late reduces almost linearly for increased reduction factor, ultimately approaching zero for a hundred percent reduction factor. For the Meuse case, a reduction in the probability of being too late is only achieved when reducing the time required by more than 90 percent. This reduction in being too late can only be achieved by proactively sending the emergency measure to a spot on the levee, where future damage is to be expected. The median time required after damage is 3.2 hours, without the reduction factor.

#### 4.6.2. IMPLICIT ASSUMPTIONS WITHIN THE MODEL

Within the presented model, it is implicitly assumed that the high water prediction models lead to perfect predictions of the flood water wave. Next to that, it is assumed that the

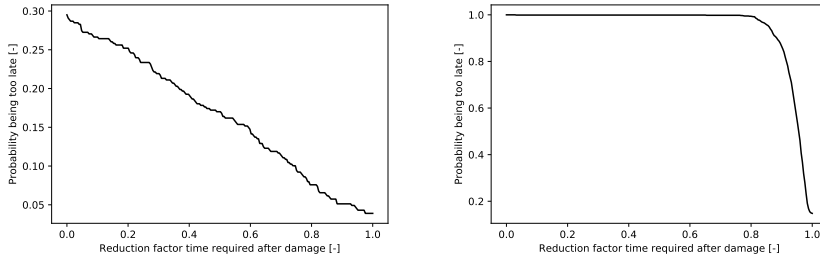


Figure 4.17: Reduction probability too late by reducing time required after occurrence of damage (left) for the standard Rhine river basin case and (right) for the standard Meuse river case

## 4

levee managers do not make wrong decisions within the crisis process. Incorporating these aspects with corresponding uncertainties into the model, may decrease the overall performance of the emergency measure.

#### 4.7. CONCLUSIONS

A model to estimate the overall performance of emergency measures and specifically the BresDefender, to locally increase the residual strength of a levee in case of a high water crisis has been developed. Model runs have been performed for two cases within the Dutch water system, one at the Rhine river basin and one at the Meuse river basin. An expert judgment assessment study has been conducted to estimate the time required to deploy an emergency measure at a weakened levee section.

The probability of successful application of an emergency measure is mainly depending on the amount of time required from the occurrence of damage until installment of the emergency measure. In this timeframe, the detection of damage, the decision to repair that damage, the transport of the emergency measure to the weakened spot, and the placement of the emergency measure are included. According to the model, there will be sufficient time to prepare both people and materials before the occurrence of damage if the authorities embed these steps in the flood safety system. This conclusion results from a comparison of both a series and parallel logistical approach.

For the case study for the Rhine river, assuming a slope instability, the conditional expected probability of being too late is 30% for all considered return periods. Reducing the time required after occurrence of damage (mainly by decreasing the time required to detect a damage) by 50% may decrease the failure rate to 17%. The unconditional success rate of the BresDefender is 1.5%, this percentage is relatively low, caused by the high share of no levee failure.

The primary finding of the Meuse case study is that, following an overflow event, there is a limited window of opportunity, often just a few hours, to implement emergency measures. This results in a relatively low probability of success for the application of the BresDefender. An important finding is the need of acting proactively if extreme water levels are expected, this is expected to increase the successfulness of emergency measures. One recommendation is to couple the preparation of an emergency measure

to a high water alarm, this reduces the time required to bring an emergency measure to a weak spot, after the occurrence of damage. A second recommendation is proactively bringing an emergency measure towards a specific levee section, before the detection of damage. This requires substantial knowledge of the levee system and its potential weak spots as well as earlier detection.

The time required for detection of damage is the most critical step within the model. Innovative measures for levee inspection could increase the inspection speed and here-with the reduce the time required to detect a damage after its occurrence. Possible improvements could be the monitoring of damages with satellites or sensors.

More research on the BresDefender emergency measure is advised. Further research should test methods to increase its retaining height. An optimized installation procedure could increase the achieved retaining height of the BresDefender to its the full potential of 1 m. This will increase the range of return periods in which the emergency measure can be applied. Furthermore, optimization of the placement procedure is recommended, to decrease the operation time, as measured during pilot test of the BresDefender.

Overall, emergency measures are expected to be a valuable asset to locally increase the residual strength of a levee in case of expected levee failure. The overall success rate of emergency measures is expected to decrease for events with smaller return periods. Embedding emergency measures within high-water emergency procedures will reduce the uncertainty in the estimated required time of application together with a reduction in the probability of being too late.



# 5

## CONCLUSIONS AND RECOMMENDATIONS

*Quick as flash he saw his duty.  
Throwing away his flowers, the boy clambered up the heights until he reached the hole.  
His chubby little finger was thrust in, almost before he knew it.  
The flowing was stopped! 'Ah!' he thought, with a chuckle of boyish delight,  
'the angry waters must stay back now!  
Haarlem shall not be drowned while I am here!'*

Hans Brinker or the Silver Skates  
by Mary Mapes Dodge, 1865

### 5.1. CONCLUSIONS

The research in this thesis aims to identify and quantify the key parameters for the successful application of emergency response measures. Both the effectiveness and reliability of these measures are derived from case studies related to the BresDefender. This section summarizes the main conclusions derived from the research findings in the previous chapters and addresses the primary research questions.

#### EFFECT OF EMERGENCY MEASURE ON THE PHREATIC SURFACE

Applying an emergency measure as an impervious seal to intervene in the development of the phreatic surface through a levee is only beneficial if the measure is installed long before reaching a steady-state phreatic level. Physical experiments on both laboratory and intermediate scales showed an increase in time to a steady state phreatic surface of up to 50% when applying an emergency measure, when starting from unsaturated conditions. The steady state phreatic level has been found to remain roughly the same



for the cases with and without a seal. Compared to physical experiments, numerical model runs demonstrated a more significant influence of an emergency measure, in the form of an impermeable seal, on the spatiotemporal development of the phreatic surface level through a levee. This difference could be attributed to the theoretical model's perfect soil-structure interface, which is challenging, and probably impossible, to achieve in practice.

In experiments with more realistic, heterogeneous levee layouts, the influence of an impermeable seal on the phreatic surface level was measured. The effect of a seal on the phreatic surface level appeared to be more prominent in the case with damage on the outer slope than in the case without damage. However, both the damaged and undamaged cases exhibited the same steady-state conditions as found in the experiments conducted without the impermeable seal. The time required to reach steady-state conditions in the damaged case was found to increase by 50% compared to the case without a seal. Thus, timely application of an impermeable seal in the early stages of a flood wave to reduce water inflow in a levee, can be successful. This is particularly the case for damaged levees, in accordance with emergency response guidelines.

5

#### EFFECT OF EMERGENCY MEASURES IN MITIGATING LEVEE BREACH FORMATION

Large-scale experiments demonstrated that using the BresDefender as a stiff structure along with a flexible tarpaulin can reduce the discharge flowing through an initial breach by over 99% compared to situations without applying a measure. The emergency measure is expected to allow a certain amount of leakage water through the breach, which is sufficient to remove soil particles, according to the Shields criterion. However, it is clear that the expected time to levee failure with an emergency measure is significantly longer than the anticipated breach time without a measure. The expected time to levee failure without the BresDefender is determined to be in the order of 30 minutes, whereas the total time with the BresDefender is anticipated to exceed 24 hours. This time gain potentially surpasses the duration of the flood wave in the river, or allows to install additional measures to close the remaining smaller gaps. This indicates that a successfully installed emergency measure is able to stop the breaching process in its early phases.

The success of the BresDefender pontoon was primarily achieved by application of a flexible tarpaulin that could adapt to the irregularities of outer slope of the levee. A physics-based model has demonstrated that the effectiveness of the emergency measure is related to the average distance between the levee surface and the structure, and the pressure head difference between both sides of the breach. Based on stability assumptions, the current BresDefender prototype is able to withstand a one meter difference in water levels inside and outside of the breach.

#### RELIABILITY OF SUCCESSFUL APPLICATION OF EMERGENCY MEASURES

The successful application of an emergency measure requires a well timed course of actions within the emergency response process. A probabilistic model has been developed, considering the BresDefender, which was then applied to high-water scenarios within the Rhine and the Meuse river basins. Essentially, the model estimates the time it would take to install the BresDefender. The model starts with details of a high-water scenario, details of the specific levee system and it assumes a dominant failure path. Then process parameters are introduced. These process parameters, together with probabilistic

estimates of the time to failure, lead to probability of timely successful placement of the emergency measure. Here it is assumed that on time placement of the seal, will 100% guarantee the water retaining function of the protected levee stretch. The model indicates that the probability of too late application of an emergency intervention for a levee breach in the Rhine River basin, suffering from a slope instability during a flood wave, is only 30%. In contrast, the same probability of being too late for the Meuse River basin scenario is found to be approximately 100%. The different results for the Rhine and Meuse scenarios originates from the main failure path for both scenarios. During high-water events, levees along the Rhine are expected to fail through slope instability, whereas levees at the Meuse river will most likely fail by water overflow. The latter failure mechanism will lead to a shorter time-to-failure, and hence an increased probability of being too late for placing emergency measures.

The most critical event in the time-line of the application of an emergency measure is the detection of visible damage to the levee. The model indicates that preparing emergency measures and levee monitoring are not expected to be key parameter in the entire process, at least if authorities start preparations directly after receiving a flood warning signal, before the occurrence of damage. The critical time consuming activity between the occurrence of damage and the installation of the emergency measure at the correct spot can be attributed to damage detection. With the current model input, this activity happen to take 50% of the total time required after the occurrence of damage, of which the median is 4.2 hours. Next to the damage detection activity the shares of the other activities are emergency measure installation (18%), transportation (16%), and the time to decide weather to repair a damaged section (15%). For the Rhine case, reducing the time required to install an emergency measure after occurrence of damage, resulted in a proportional reduction in the probability of being too late.

The conclusions drawn from the various research chapters allows to address the primary question of this research:

*What are the key factors and critical parameters that allow for the effective application of early-stage emergency measures, specifically the BresDefender, preventing or postponing the development of levee breaches?*

The critical factor for the successful application of an emergency measure is time, both in the logistical process before and the damage progression after placement of the intervention, as depicted in figure 1.3. Shortening the time to identify the location of a (potential) levee breach, will increase the success of emergency measure application considerably. This allows flood managers to proactively prepare and apply emergency measures to strengthen weakened levee sections before they fail. Another time-related aspect concerns the duration of the failure process. This research indicates that the successful application of emergency measures can extend the duration of the levee failure process, even beyond the duration of the flood. This effect is achieved either by increasing the breaching time of a levee, or slowing down the development of the phreatic surface level in a levee. The importance of both effects have been demonstrated for model and real sized interventions.

The second most important parameter for success is structural resistance, which

comprises two components: the resistance to loads on the levee, and the resistance to loads of the emergency measure. The resistance of the levee affects the likelihood and location of failure, and the resistance of the emergency measure particularly steers the maximum water-retaining height. The BresDefender can enhance the resistance of a levee by locally increasing the retaining height, either by extending the time to reach steady-state phreatic conditions in a levee, or by increasing the time to failure caused by water flowing over a levee. This research showed that the BresDefender can offer a maximum water-retaining height of one meter, based on stability considerations, while the maximum achieved retaining height during experiments was 0.3 meter above outer water level during placement.

The third parameter for the successful implementation of emergency measures is the ability to adapt to the irregularities and asperities at the levee's surface. Through this adaptability the intervention acts as a seal. Physical experiments have shown that attaching a flexible tarpaulin to a non-floating stiff structure can effectively reduce water flux through a levee. The better the emergency measure seals the openings between the structure and the levee, the more effectively its performance will be.

When taking all of the above-mentioned parameters into account, it is expected that the BresDefender emergency measure can increase the local resistance of a levee to avoid its failure.

## 5.2. RECOMMENDATIONS

The following recommendations are formulated with a focus on advancing the professionalization of emergency response, enhancing the effectiveness of emergency measures and improving the BresDefender prototype. These recommendations are divided into recommendations for further research and practical recommendations directed to the flood risk professional.

### 5.2.1. RECOMMENDATIONS FOR FURTHER RESEARCH

#### DYNAMIC TESTS BRESDEFENDER PROTOTYPE

During the reported research, experiments were conducted with a prototype BresDefender emergency response measure. The experiments assumed a perfect placement of the measure in front of a reduced crest, without considering the dynamical process which occur when sailing the pontoon in front of an initial breach. These dynamic conditions are caused by water flowing through this breach. Physical experiments are recommended to optimize the placement procedure for the BresDefender, while safeguarding the people installing the structure, and increase the success rate of the intervention measure. Experiments on both laboratory and full-scale are recommended for this optimization step. By laboratory-scale experiments, the most efficient placement procedure can be determined, along with the design of a measurement plan for the full-scale experiments. In the laboratory, the BresDefender prototype could be represented by a 3D-printed model. In the full-scale experiments, the actual BresDefender pontoon must be deployed in front of a breach that is capable of eroding. The safety of the personnel placing the pontoon should be the first priority during these experiments.

### DEFINE MAXIMUM RETAINING HEIGHT OF THE BRESDEFENDER

During the experiments described in this thesis, the water level difference was never raised until the BresDefender system failed itself. Future research should aim to determine the maximum water retaining height of the BresDefender. This information could then be incorporated into probabilistic models to improve the prediction of the success range of the emergency measure. It would also lead to improved guidelines for its use.

### EFFECT OF REDUCED DISCHARGE ON EROSION RATES

In this research, the effectiveness of the BresDefender prototype has been assessed for an initial breach with fixed dimensions, which was covered with a geo-textile. To gain a deeper understanding of the breach development under reduced flow velocities, it is recommended to remove the protective geo-textile in the breach and establish more realistic real-world conditions. Measuring the erosion rates of the unprotected soil would then allow for an improved prediction of the time to failure.

### THREE DIMENSIONAL INFLUENCE OF THE EMERGENCY MEASURE ON THE PHREATIC SURFACE LEVEL

The impact of an impermeable structure on the spatio-temporal distribution of the phreatic surface level was only assessed for one specific structure size. The effect of the variation of the dimension of the seal on the phreatic surface level, in all three dimensions, was not taken into account within this research. Enlarging the area of the seal cover could result in an increase in the affected area where the phreatic surface level is influenced by the seal. It is recommended to first explore this effect with three dimensional numerical models, followed up by the experiments on a real levee.

### IMPROVE MODELING TO PREDICT SUCCESS RATE OF THE EMERGENCY MEASURE

The probabilistic model used to predict the probability of success for an emergency measure includes several assumptions and simplifications. Therefore, further research could improve this prediction model. The accuracy of the time-to-failure, i.e. crest height reduction, can be improved by introducing additional experimentally obtained data. Furthermore, the spatial variability of levee resistance could be incorporated in the model. This relates to the heterogeneity of the soil and the possible presence of animal burrows in the levee.

Improving the accuracy of estimating the probability of being too late can be achieved by including more failure mechanisms in the flow chart. The model presented in this thesis assumes a perfectly accurate flood wave prediction, perfect decision-maker choices, favorable conditions for levee inspections and a single potential breach location. Enhancing these aspects of the model would provide a more comprehensive understanding of the possible deployment and optimization of the emergency process.

## 5.2.2. RECOMMENDATIONS FOR PRACTICE

### OPTIMIZE THE BRESDEFENDER PROTOTYPE

Improvement of the placement procedure for the BresDefender prototype is recommended. Aspects that should be improved in the current prototype are i) automatic filling of the hollow parts of the pontoon without the use of pumps, ii) removing the requirement for

anchoring the pontoon during application and iii) improved methods of connecting the flexible tarpaulin to the pontoon. Overall, reducing the installation time of the BresDefender, reduces the probability of being too late.

The above-mentioned improvements only consider the military BresDefender pontoon prototype. One advantage of the current pontoon is the presence of a stiff structure with a certain rigidity, which is readily available. Developing an alternative solution that combines a stiff structure and a tarpaulin could also be effective in preventing breach formation. The structural resistance of the tarpaulin against water pressure differences should not be overlooked in this design to prevent tearing of the seal. The tarpaulin is the most crucial aspect for the proper functioning of the emergency measure, at least when it remain attached at the desired site during the flooding phase.

#### EMBED THE BRESDEFENDER IN EMERGENCY PROTOCOLS

To make the BresDefender emergency response measure a successful addition to the emergency response toolbox, it should be incorporated into the existing emergency response catalogs, specifically as part of the third layer of safety in the Dutch context. This necessitates an agreement and coordinated efforts between those responsible for levee maintenance and those overseeing the emergency response process.

The embedding of emergency measures such as the BresDefender into emergency protocols involves the requirement of prepositioning of the measures at strategic locations. Selecting these locations efficiently, covering all vulnerable areas of the country, will reduce the transportation distance and herewith time required for deployment.

#### PREDICT THE LOCATION OF DAMAGE

Decreasing the time to detect damage on a levee section increases the success rate of an emergency measure. Current protocols mainly prescribe the involvement of (trained) personnel to detect the damage. Increasing the speed of detection of changes in the levee that might be precursors of damage can be achieved by e.g. sensors (Schenato, 2017), drones (Shoemaker et al., 2019) or satellites (Özer et al., 2018).

#### TRAIN PERSONNEL

A factor for successful placement of emergency measures is the level of skill of the people placing it. Large scale experiments showed a reduction in installation time after subsequent deployment of the emergency measure (Velde, 2022). Especially since operating the BresDefender emergency measure is relatively complex, skill and training of personnel is required to successfully place the measure during a flood crisis, to increase the probability of success rate and decrease the installation time of the measure.

#### MAINTAIN THE LEVEES

This research showed that the slope-surface interface is an important parameter for reducing leakage water flowing around the emergency measure. This can be achieved by using a flexible tarpaulin in the emergency measure itself or by reducing the irregularities on the levee. Proper levee slope maintenance should make the surface more regular and will enhance both emergency measure effectiveness and resistance against damage itself.

# BIBLIOGRAPHY

- AHN. (2023). Actueel hoogtebestand nederland. <https://www.ahn.nl/>
- Albers, T. (2014). *Emergency closure of dike breaches - the effect and applicability of emergency measures* [Thesis].
- Bakkenist, S., van Dam, O., van der Nat, A., Thijs, F., & de Vries, W. (2012). *Principles of professional inspection - organizational part* (Report No. ISBN: 978.90.5773.565.3). [STOWA.nl](http://STOWA.nl)
- Beber, R., Tarantino, A., & Becker, P. (2023). Climate change adaptation of elbe river flood embankments via suction-based design. *International Journal of Geomechanics*, 23(3). <https://doi.org/10.1061/ijgnai.Gmeng-7693>
- Bently. (2021). *Plaxis le groundwater: 1d/2d/3d saturated / unsaturated finite element groundwater modeling* (Report). [Help%20button%20Plaxis](http://Help%20button%20Plaxis)
- Berg, F. v. d., & Koelewijn, A. R. (2023). *Graverij door dieren, verschillende praktijkcases, inspectietechnieken en uitsplitsing invloed op overstromingskans* (Report No. 11209262-001-ZWS-0001). Deltares. [Deltares](http://Deltares)
- Bosoni, M., Tempels, B., & Hartmann, T. (2021). Understanding integration within the dutch multi-layer safety approach to flood risk management. *International Journal of River Basin Management*, 21(1), 81–87. <https://doi.org/10.1080/15715124.2021.1915321>
- Brauneck, J., Jüpner, R., Pohl, R., & Friedrich, F. (2016). Auswertung des deichbruchs breitenhagen (juni 2013) anhand von uas-basierten videoaufnahmen. *Gewässerentwicklung und Hochwasserrisikomanagement-Synergien, Konflikte und Lösungen aus EU-WRRL und EU-HWRM-RL*, (57), 119–128.
- Chaudhry, M. H., Elkholy, M., & Riahi-Nezhad, C. (2010). *Investigations on levee breach closure procedures* (Report).
- Chbab, H. (2016). *Waterstandsverlopen rijntakken en maas wettelijk toetsinstrumentarium wti-2017* (Report). [Deltares](http://Deltares)
- CIRIA. (2013). *The international levee handbook* (Report). [ciria.org](http://ciria.org)
- Colebrook, C. F. (1939). Turbulent flow in pipes, with particular reference to the transition region between the smooth and rough pipe laws. *Journal of the Institution of Civil Engineers*, 11(4), 133–156. <https://doi.org/10.1680/ijoti.1939.13150>
- Cooke, R. (1991). *Experts in uncertainty: Opinion and subjective probability in science*. Oxford University Press, USA.
- Darmstadt, R. (2006). Instruktion zur deichverteidigung. *Regierungspräsidium Darmstadt, Darmstadt*.
- Delfland. (2011). *Calamiteitenbestrijdingsplan regionale en overige waterkeringen* (Report). [Wiki%20noodmaatregelen](http://Wiki%20noodmaatregelen)
- D'Eliso, C. (2007). *Breaching of sea dikes initiated by wave overtopping* [Thesis].

- Elsing, K. (2018). *Bresdefender: Een geïmproviseerde beschermingsmaatregel bij mogelijke dijkdoorbraken - bresdefender: An improvised emergency response strategy for potential dike failures* [Bachelor's Thesis].
- Engelund, F., & Hansen, E. (1967). *A monograph on sediment transport in alluvial streams* (Report). <http://resolver.tudelft.nl/uuid:81101b08-04b5-4082-9121-861949c336c9>
- Foster, U. (2011). Kpp meerlaagsveiligheid: Emergency response - inventarisatie van wereldwijd beschikbare snelle reparatietechnieken en/of noodmaatregelen bij dijk-bressen.
- Fredlund, D. G., & Xing, A. (1994). Equations for the soil-water characteristic curve. *Canadian Geotechnical Journal*, 31(4), 521–532. <https://doi.org/10.1139/t94-061>
- Henning, B., & Jüpner, R. (2015). Deichbruch fischbeck — zwei jahre danach. *Wasser und Abfall*, 17(11), 15–19. <https://doi.org/10.1007/s35152-015-0576-6>
- Hewlett, H., Boorman, L. A., & Bramley, L. (1987). *Design of reinforced grass waterways*. Construction Industry Research; Information Association.
- Hofmann, M., Grimmer, M., & Steuernagel, J. (2006). Instruktion zur deichverteidigung. *Regierungspräsidium Darmstadt, Darmstadt*.
- Hommel, D. (2022). *Bresdefender: The effect of an emergency measure on the phreatic surface of a dike in space and time* [Thesis].
- Janssen, D. (2023). Dataset: Bresdefender, an experimental study on an emergency response measure for levee breaches. <https://doi.org/10.4121/152663fc-0e02-46bf-a0c7-2ebb7b509f68>
- Janssen, D., Schmetts, A., Hofland, B., Dado, E., & Jonkman, S. (2021). BresDefender: A potential emergency measure to prevent or postpone a dike breach. *FLOODrisk 2020 - 4th European Conference on Flood RiskManagement*. <https://doi.org/10.3311/floodrisk2020.19.3>
- Jonkman, S. N. (2007). *Loss of life estimation in flood risk assessment; theory and applications* [Thesis].
- Joore, I. (2004). *Noodsluiting van een dijkdoorbraak bij hoogwater* [Thesis].
- Klerk, W. J., Kanning, W., Kok, M., Bronsveld, J., & Wolfert, A. R. M. (2021). Accuracy of visual inspection of flood defences. *Structure and Infrastructure Engineering*, 1–15. <https://doi.org/10.1080/15732479.2021.2001543>
- Klipalo, E., Besharat, M., & Kuriqi, A. (2022). Full-scale interface friction testing of geotextile-based flood defence structures. *Buildings*, 12(7). <https://doi.org/10.3390/buildings12070990>
- Knotter, H., & Krikke, A. (2021). *Crisisbestrijdingsplan van waterschap rivierenland, hoogwater* (Report). [Wiki%20Noodmaatregelen](https://www.waterschap-rivierenland.nl/wiki/Noodmaatregelen)
- Koelewijn, A. R., Rikkert, S. J. H., Peeters, P., Depreiter, D., van Damme, M., & Zomer, W. (2022). Overflow tests on grass-covered embankments at the living lab hedwige-prosperpolder: An overview. *Water*, 14(18). <https://doi.org/10.3390/w14182859>
- Kolen, B., Caspers, J., & Pol, J. (2021). *Actualisatie okader, voor toepassing bij de irm-mer* (Report). [Rijkswaterstaat](https://www.rijkswaterstaat.nl)
- Kool, J. J., Kanning, W., Heyer, T., Jommi, C., & Jonkman, S. N. (2019). Forensic analysis of levee failures: The breitenhagen case. *International Journal of Geoengineering Case Histories* 5.2 (2019): 70-92.

- Koopman, R. (2022). Landmacht docu: Terugblik inzet landmacht militairen hoogwater limburg 2021. [www.youtube.com](http://www.youtube.com)
- Kundzewicz, Z. W., Kanae, S., Seneviratne, S. I., Handmer, J., Nicholls, N., Peduzzi, P., Mechler, R., Bouwer, L. M., Arnell, N., Mach, K., Muir-Wood, R., Brakenridge, G. R., Kron, W., Benito, G., Honda, Y., Takahashi, K., & Sherstyukov, B. (2013). Flood risk and climate change: Global and regional perspectives. *Hydrological Sciences Journal*, 59(1), 1–28. <https://doi.org/10.1080/02626667.2013.857411>
- Lendering, K. (2018). *Advancing methods for evaluating flood risk reduction measures* [Thesis]. <https://doi.org/https://doi.org/10.4233/uuid:5d45d298-9c1d-4454-9206-495faf4109fe>
- Maat, W., Balemans, M., Schmits, A. J. M., & Janssen, D. (2023). *Pilot breach defender (bresdefender) (d.2.1.1)* (Report). [www.polder2cs.eu](http://www.polder2cs.eu)
- Marijnissen, R., Kok, M., Kroeze, C., & van Loon-Steensma, J. (2019). Re-evaluating safety risks of multifunctional dikes with a probabilistic risk framework. *Natural Hazards and Earth System Sciences*, 19(4), 737–756. <https://doi.org/10.5194/nhess-19-737-2019>
- Massolle, C., Lankenau, L., & Koppe, B. (2018). Emergency flood control: Practice-oriented test series for the use of sandbag replacement systems. *Geosciences*, 8(12). <https://doi.org/10.3390/geosciences8120482>
- MinDef. (2020). *Defensievisie 2035: Een nieuw profiel voor defensie* (Report). [www.defensie.nl](http://www.defensie.nl)
- MinIenM. (2009). *Nationaal waterplan 2009-2015* (Report). [www.helpdeskwater.nl](http://www.helpdeskwater.nl)
- MinIenM. (2022). *Landelijk draaiboek hoogwater en overstromingsdreiging* (Report). [Rijkswaterstaat](http://Rijkswaterstaat)
- Nat, v. d. A. (2012). *Hoogwaterklapper noodmaatregelen* (Report).
- Norfolk, C. C. (2020). *Investigation into the flooding in wainfleet in june 2019* (Report).
- Özer, I. E., van Leijen, F. J., Jonkman, S. N., & Hanssen, R. F. (2018). Applicability of satellite radar imaging to monitor the conditions of levees. *Journal of Flood Risk Management*, 12(S2). <https://doi.org/10.1111/jfr3.12509>
- Pappenberger, F., Cloke, H. L., Parker, D. J., Wetterhall, F., Richardson, D. S., & Thielen, J. (2015). The monetary benefit of early flood warnings in europe. *Environmental Science and Policy*, 51, 278–291. <https://doi.org/10.1016/j.envsci.2015.04.016>
- Peeters, P., Zhao, G., De Vos, L., & Visser, P. (2015). Large-scale dike breaching experiments at lillo in belgium.
- Pegram, G., & Pennington, M. (1996). *A method for estimating the hydraulic roughness of unlined bored tunnels*. Water Research Commission. <https://books.google.nl/books?id=fPRSGQAACAAJ>
- Pinkard, F., Pratt, T., Ward, D., Holmes, T., Kelley, J., Lee, L. T., Sills, G., Smith, E., Taylor, P. A., & Torres, N. (2007). *Flood-fighting structures demonstration and evaluation program: Laboratory and field testing in vicksburg, mississippi* (Report).
- Pol, J. C., Kindermann, P., van der Krogt, M. G., van Bergeijk, V. M., Remmerswaal, G., Kanning, W., Jonkman, S. N., & Kok, M. (2023). The effect of interactions between failure mechanisms on the reliability of flood defenses. *Reliability Engineering and System Safety*, 231. <https://doi.org/10.1016/j.res.2022.108987>



- Rahimi, A., Rahardjo, H., & Leong, E.-C. (2015). Effects of soil–water characteristic curve and relative permeability equations on estimation of unsaturated permeability function. *Soils and Foundations*, 55(6), 1400–1411.
- Reijnen, D., Eimers, D., Scholts, N., & Brouwer, C. (2018). *Catalogus nationale operaties* (Report). Defensiestaf, directie operaties, J34 nationale operaties.
- Remmerswaal, G., Vardon, P. J., & Hicks, M. A. (2021). Evaluating residual dyke resistance using the random material point method. *Computers and Geotechnics*, 133. <https://doi.org/10.1016/j.compgeo.2021.104034>
- Resio, D. T., Boc, S. J., Ward, D., Kleinman, A., Fowler, J., Welsh, B., Matalik, M., Goodwin, P., & TN, O. R. N. L. (2011). *Us army engineer research and development center: Rapid repair of levee breaches*. US Army Engineer Research; Development Center.
- Rijkswaterstaat. (1961). *Verslag over de stormvloed van 1953* (Report).
- Rijkswaterstaat. (2019). *Schematiseringshandleiding microstabiliteit* (Report). Rijkswaterstaat. [www.helpdeskwater.nl](http://www.helpdeskwater.nl)
- Rijkswaterstaat. (2023). Rijkswaterstaat waterinfo extra. <https://waterinfo.rws.nl/>
- Rongen, G., Hart, C. M. P. ', Leontaris, G., & Morales-Nápoles, O. (2020). Update (1.2) to anduril and anduryl: Performance improvements and a graphical user interface. *SoftwareX*, 12. <https://doi.org/10.1016/j.softx.2020.100497>
- Rongen, G., Strijker, B., Pol, J., Kok, M., Kolen, B., Rikkert, S., Schlumberger, J., van Haren, M., & Wüthrich, D. (2021). Hoogwater 2021: Feiten en duiding.
- Sattar, A. M., Kasseem, A. A., & Chaudhry, M. H. (2008). Case study: 17th street canal breach closure procedures. *Journal of Hydraulic Engineering*, 134(11), 1547–1558. [https://doi.org/10.1061/\(asce\)0733-9429\(2008\)134:11\(1547\)](https://doi.org/10.1061/(asce)0733-9429(2008)134:11(1547))
- Schenato, L. (2017). A review of distributed fibre optic sensors for geo-hydrological applications. *Applied Sciences*, 7(9). <https://doi.org/10.3390/app7090896>
- Schiereck, G. (1998). Grondslagen voor waterkeren. report, rijkswaterstaat, 1998b. [TU%20Delft%20repository](https://www.tu-delft.nl/repositories/20)
- Schindler, U. (1980). Ein schnellverfahren zur messung der wasserleitfähigkeit im teilgesättigten boden an stechzylinderproben. *Archiv für Acker- und Pflanzenbau und Bodenkunde*, 4 (1): 1-7.
- Schmets, A. J. M., Janssen, D., Krabbenborg, D., Leertouwer, S. T., & Dado, E. (2024, May). Novel emergency response interventions for flood resilience. In G. Frerks, R. Geertsma, J. Klomp, & T. Middendorp (Eds.), *Climate security and the military - concepts, strategies and partnerships* (pp. 231–252). Leiden University Press.
- Schmidt, K. (2014). *Einsatztaktik für die feuerwehr hinweise zum einatz von sandsäcken bei hochwasser* (Report). [www.wikinoodmaatregelen.nl](http://www.wikinoodmaatregelen.nl)
- Seed, R. B., Bea, R. G., Abdelmalak, R. I., Athanasopoulos, A. G., Boutwell Jr, G. P., Bray, J. D., Briaud, J.-L., Cheung, C., Cobos-Roa, D., & Cohen-Waeber, J. (2006). Investigation of the performance of the new orleans flood protection system in hurricane katrina on august 29, 2005: Volume 2. *Independent Levee Investigation Team: Final Report*, 2.
- Seed, R. B., Bea, R. G., Athanasopoulos-Zekkos, A., Boutwell, G. P., Bray, J. D., Cheung, C., Cobos-Roa, D., Harder, L. F., Moss, R. E. S., Pestana, J. M., Riemer, M. F., Rogers, J. D., Storesund, R., Vera-Grunauer, X., & Wartman, J. (2008). New orleans and

- hurricane katrina. iii: The 17th street drainage canal. *Journal of Geotechnical and Geoenvironmental Engineering*, 134(5), 740–761. [https://doi.org/10.1061/\(asce\)1090-0241\(2008\)134:5\(740\)](https://doi.org/10.1061/(asce)1090-0241(2008)134:5(740))
- Sellmeijer, C. (2019). *Nederlandse defensie doctrine* (Report).
- Sene, K. (2008). *Flood warning, forecasting and emergency response*. Springer Science; Business Media.
- Shields, A. (1936). *Anwendung der aehnlichkeitsmechanik und der turbulenzforschung auf die geschiebewegung* [Thesis].
- Shoemaker, T. A., McGuire, M. P., & Roussel, G. (2019). Remote sensing approach to upstream slope inspection. *Journal of Geotechnical and Geoenvironmental Engineering*, 145(11). [https://doi.org/10.1061/\(asce\)gt.1943-5606.0002159](https://doi.org/10.1061/(asce)gt.1943-5606.0002159)
- Slotjes, N., & Most, H. v. d. (2016). *Achtergronden bij de normering van de primaire waterkeringen in nederland* (Report). Ministerie van Infrastructuur en Milieu, DG Ruimte en Water, Directie Algemeen Waterbeleid en Veiligheid.
- Soulsby, R. (1998). *Dynamics of marine sands*. ICE virtuellibrary. <https://doi.org/10.1680/doms.25844>
- TAW. (1995). Druk op de dijken 1995: De toestand van de rivierdijken tijdens het hoogwater van januari-februari 1995. *TAW publicatie*.
- t Hart, R., De Bruijn, H., & De Vries, G. (2016). *Fenomenologische beschrijving faalmechanismen wti* (Report). Technical report, Technical report. [Deltares](https://www.deltares.nl)
- Vahedifard, F., Jasim, F. H., Tracy, F. T., Abdollahi, M., Alborzi, A., & AghaKouchak, A. (2020). Levee fragility behavior under projected future flooding in a warming climate. *Journal of Geotechnical and Geoenvironmental Engineering*, 146(12), 04020139.
- Van, M., Rosenbrand, E., Tourment, R., Smith, P., & Zwanenburg, C. (2022). Failure paths for levees. *International Society of Soil mechanics and Geotechnical Engineering (ISSMGE), Technical Committee TC201 'Geotechnical aspects of dikes and levees'*.
- Van Der Krogt, M. G., Schweckendiek, T., & Kok, M. (2019). Do all dike instabilities cause flooding. *Proceedings of the 13th International Conference on Applications of Statistics and Probability in Civil Engineering, ICASP*. <https://doi.org/https://doi.org/10.22725/ICASP13.461>
- Van Emelen, S., Soares-Frazão, S., Riahi-Nezhad, C. K., Hanif Chaudhry, M., Imran, J., & Zech, Y. (2012). Simulations of the new orleans 17th street canal breach flood. *Journal of Hydraulic Research*, 50(1), 70–81. <https://doi.org/10.1080/00221686.2011.642578>
- van Rijn, L. C. (1993). *Principles of sediment transport in rivers, estuaries and coastal seas*. Aqua Publications. <https://books.google.nl/books?id=gGIYAQAAlAAJ>
- Velde, R. v. d. (2022). *Optimalisatie plaatsingsmethode bresdefender* [Bachelor's Thesis].
- Visser, P. J. (1988). A model for breach growth in a dike-burst. *Coastal Engineering Proceedings*, 1(21). <https://doi.org/10.9753/icce.v21.140>
- Visser, P. J. (1998). *Breach growth in sand-dikes* [Thesis].
- Visser, P. J., Smit, M., & Snip, D. (1996). Zwin'94 experiment: Meetopstelling en overzicht van alle meetresultaten. *TAW-C 4-1996*.
- Waal, H. d. (2018). *Basisrapport wbi 2017, v1.2* (Report). [www.helpdeskwater.nl](http://www.helpdeskwater.nl)

- Weisbach, J. L. (1845). *Lehrbuch der ingenieur-und maschinen-mechanik: Theoretische mechanik* (Vol. 1). Druck und Verlag von Friedrich Vieweg und Sohn.
- Zhu, Y. (2006). *Breach growth in clay-dikes* [Thesis].
- Žilys, V., Jakštienė, N., Jasiulionis, M., & Ulevičius, A. (2009). Morphological alteration of land reclamation canals by beavers (castor fiber) in lithuania. *Estonian Journal of Ecology*, 58(2). <https://doi.org/10.3176/eco.2009.2.06>

# A

## ADDITIONAL INFORMATION CHAPTER 3

### A.1. DETERMINATION BREACH TIME

To determine the time which it takes to complete breach stage II, for a homogeneous sand dike. equations A.1, A.2, A.3 and A.4 apply, as defined by Visser, 1998. Parameters which are already introduced in the main text, are to be found in the notations section.

### A.2. GEOMETRICAL PARAMETERS IN STABILITY MODEL

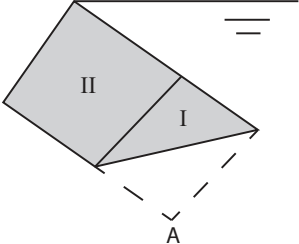
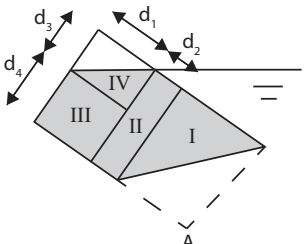
$$\Delta t_{II} = \frac{B_{up}}{B_w} \frac{W_1(1-p)l_a \sin \psi}{S_s} \quad (\text{A.1})$$

$$W_1 = W_d + h \left( \frac{1}{\tan \alpha} + \frac{1}{\tan \psi} \right) \quad (\text{A.2})$$

$$l_a = \xi \frac{B_w}{B_{up}} \frac{ud}{w_s \cos \psi} \quad (\text{A.3})$$

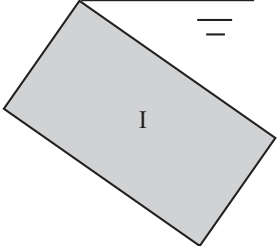
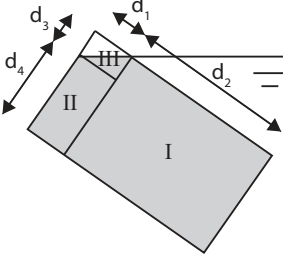
$$ud = \frac{2\sqrt{gh}h}{3} \quad (\text{A.4})$$

A

Section 1	I - Completely filled	II - Partly filled water level > 0.5 section
Scheme		
Distances		$d_1 = L_{sec} - L_{pont}$ $d_2 = \frac{1}{2}L_{sec} - d_1$ $d_3 = h_{pont} - d_4$ $d_4 = d_1 \tan \varphi$
Volume	$I = \frac{1}{4}L_{sec}h_{pont}$ $II = \frac{1}{2}L_{sec}h_{pont}$	$I = \frac{1}{4}L_{sec}h_{pont}$ $II = d_2 h_{pont}$ $III = d_1 d_3$ $IV = \frac{1}{2}d_1 d_4$
Arm cog to $A_x$	$a_{xI} = \frac{2}{3}h_{pont}$ $a_{xII} = \frac{1}{2}h_{pont}$ $a_x = \frac{\sum_{n=I}^{II} a_{xn}n}{\sum_{n=I}^{II} n}$	$a_{xI} = \frac{2}{3}h_{pont}$ $a_{xII} = \frac{1}{2}h_{pont}$ $a_{xIII} = \frac{1}{2}d_3$ $a_{xIV} = \frac{1}{3}d_4 + d_3$ $a_x = \frac{\sum_{n=I}^{IV} a_{xn}n}{\sum_{n=I}^{IV} n}$
Arm cog to $A_y$	$a_{yI} = \frac{1}{3}L_{sec}$ $a_{yII} = \frac{3}{4}L_{sec}$ $a_y = \frac{\sum_{n=I}^{II} a_{yn}n}{\sum_{n=I}^{II} n}$	$a_{yI} = \frac{1}{3}L_{sec}$ $a_{yII} = \frac{1}{2}d_2 + \frac{1}{2}L_{sec}$ $a_{yIII} = \frac{1}{2}d_1 + d_2 + \frac{1}{2}L_{sec}$ $a_{yIV} = \frac{1}{3}d_1 + d_2 + \frac{1}{2}L_{sec}$ $a_y = \frac{\sum_{n=I}^{IV} a_{yn}n}{\sum_{n=I}^{IV} n}$

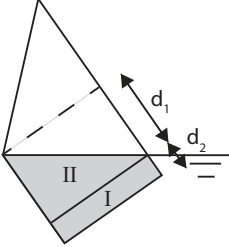
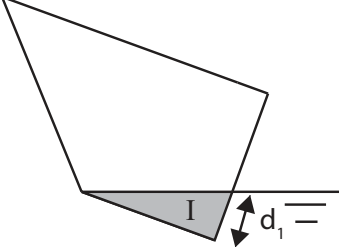
Section I	III – Partly filled water level < 0.5 section	IV – Partly filled water level < h pontoon
Scheme		
Distances	$d_1 = \frac{1}{2} L_{sec}$ $d_2 = \frac{1}{2} L_{sec} - d_3$ $d_3 = L_{pont}$ $d_4 = d_1 \tan \varphi$ $d_5 = h_{pont} - d_4 - d_6$ $d_6 = d_2 \tan \varphi$ $d_7 = d_1 \tan \varphi_{pont} - d_6$ $d_8 = h_{pont} - d_6 - d_7$	$d_1 = (d_4 + d_5) \cos \varphi_{pont}$ $d_2 = \tan\left(\frac{1}{2}\pi - \varphi_{pont}\right) d_1$ $d_3 = (d_4 + d_5) \sin \varphi_{pont}$ $d_4 = (L_{pont2} - L_{sec} + d_6) \tan \varphi - d_5$ $d_5 = (L_{pont2} - L_{sec}) \tan \varphi$ $d_6 = \frac{1}{2} L_{sec}$
Volume	$I = \frac{1}{2} d_3 (d_6 + d_7)$ $II = \frac{1}{2} d_2 d_8$ $III = d_2 d_7$ $IV = \frac{1}{2} d_2 d_6$ $V = d_1 d_5$ $VI = \frac{1}{2} d_1 d_4$	$I = \frac{1}{2} d_1 d_2$ $II = \frac{1}{2} d_1 d_3$ $III = \frac{1}{2} d_4 d_6$ $IV = d_5 d_6$

Section 1	III – Partly filled water level < 0.5 section	IV – Partly filled water level < h pontoon
Arm cog to $A_x$	$a_{xI} = \frac{2}{3}(d_6 + d_7) + d_8$ $a_{xII} = \frac{2}{3}d_8$ $a_{xIII} = \frac{1}{2}d_7 + d_8$ $a_{xIV} = \frac{1}{3}d_6 + d_7 + d_8$ $a_{xV} = \frac{1}{2}d_5$ $a_{xVI} = \frac{1}{3}d_4 + d_5$ $a_x = \frac{\sum_{n=I}^{VI} a_{xn}n}{\sum_{n=I}^{VI} n}$	$a_{xI} = \left(\frac{1}{3}d_1 + \frac{1}{3}d_2 + d_3\right) \sin \varphi_{pont}$ $a_{xII} = \left(\frac{1}{3}d_1 + d_3\right) \sin \varphi_{pont}$ $a_{xIII} = \frac{1}{3}d_4 + d_5$ $a_{xIV} = \frac{1}{2}d_5$ $a_x = \frac{\sum_{n=I}^{IV} a_{xn}n}{\sum_{n=I}^{IV} n}$
Arm cog to $A_y$	$a_{yI} = \frac{2}{3}d_3$ $a_{yII} = \frac{2}{3}d_2 + d_3$ $a_{yIII} = \frac{1}{2}d_2 + d_3$ $a_{yIV} = \frac{1}{3}d_2 + d_3$ $a_{yV} = \frac{1}{2}d_1 + d_2 + d_3$ $a_{yVI} = \frac{1}{3}d_1 + d_2 + d_3$ $a_y = \frac{\sum_{n=I}^{VI} a_{yn}n}{\sum_{n=I}^{VI} n}$	$a_{yI} = \frac{\frac{1}{3}d_1}{\sin \varphi_{pont}} + \frac{h_{pont} - a_{xI}}{\tan \varphi_{pont}}$ $a_{yII} = \left(\frac{1}{3}d_1 + D_{pont} - \frac{2}{3}d_3\right) \cos \varphi_{pont}$ $a_{yIII} = \frac{1}{3}d_6 + \frac{1}{2}L_{sec}$ $a_{yIV} = \frac{1}{2}d_6 + \frac{1}{2}L_{sec}$ $a_y = \frac{\sum_{n=I}^{IV} a_{yn}n}{\sum_{n=I}^{IV} n}$

Section 2 and 3	I – Completely filled	II – Water level > Pontoon up
Scheme		
Distance		$d_1 = \#_{sec} L_{sec} - L_{pont}$ $d_2 = L_{sec} - d_1$ $d_3 = d_1 \tan \varphi$ $d_4 = h_{pont} - d_3$
Volume	$I = L_{sec} h_{pont}$	$I = d_2 h_{pont}$ $II = d_1 d_4$ $III = \frac{1}{2} d_1 d_3$
Arm cog to $A_x$	$a_x = \frac{1}{2} h_{pont}$	$a_{xI} = \frac{1}{2} h_{pont}$ $a_{xII} = \frac{1}{2} d_4$ $a_{xIII} = \frac{1}{3} d_3 + d_4$ $a_x = \frac{\sum_{n=I}^{III} a_{xn} n}{\sum_{n=I}^{III} n}$
Arm cog to $A_y$	$a_y = \frac{1}{2} L_{sec}$	$a_{yI} = \frac{1}{2} d_2$ $a_{yII} = \frac{1}{2} d_1 + d_2$ $a_{yIII} = \frac{1}{3} d_1 + d_2$ $a_y = \frac{\sum_{n=I}^{III} a_{yn} n}{\sum_{n=I}^{III} n}$



Section 2 and 3	III – Water level < Pontoon up
Scheme	
Distance	$d_1 = \tan(\varphi)(L_{pont2} - (\#_{sec} + 1)L_{sec} - d_2)$ $d_2 = \tan(\varphi)(L_{pont2} - \#_{sec}L_{sec})$
Volume	$I = L_{sec}d_2$ $II = \frac{1}{2}L_{sec}d_1$
Arm cog to $A_x$	$a_{xI} = \frac{1}{2}d_2$ $a_{xII} = \frac{1}{3}d_1 + d_2$ $a_x = \frac{\sum_{n=I}^{II} a_{xn}n}{\sum_{n=I}^{II} n}$
Arm cog to $A_y$	$a_{yI} = \frac{1}{2}L_{sec}$ $a_{yII} = \frac{1}{3}L_{sec}$ $a_y = \frac{\sum_{n=I}^{II} a_{yn}n}{\sum_{n=I}^{II} n}$

Section 4	I – Water level > Pontoon up	II – Water level < Pontoon up
Scheme		
Distance	$d_1 = \frac{h_{pont}}{\tan \varphi}$ $d_2 = \frac{1}{2} L_{sec} - d_1$	$d_1 = \frac{1}{2} \tan(\varphi) L_{sec}$
Volume	$I = d_2 h_{pont}$ $II = \frac{1}{2} d_1 h_{pont}$	$I = \frac{1}{4} d_1 L_{sec}$
Arm cog to $A_x$	$a_{xI} = \frac{1}{2} h_{pont}$ $a_{xII} = \frac{1}{2} h_{pont}$ $a_x = \frac{\sum_{n=I}^{II} a_{xn} n}{\sum_{n=I}^{II} n}$	$a_x = \frac{1}{3} d_1$
Arm cog to $A_y$	$a_{yI} = \frac{1}{2} d_2$ $a_{yII} = \frac{1}{3} d_1 + d_2$ $a_y = \frac{\sum_{n=I}^{II} a_{yn} n}{\sum_{n=I}^{II} n}$	$a_y = \frac{1}{6} L_{sec}$



# B

## ADDITIONAL INFORMATION

### CHAPTER 4

#### B.1. SERIES MODEL

In this appendix, the series model is elaborated on. Within the series model it is assumed that emergency response measures are only prepared after detection of a damage to the levee. This sequence begins with a high water signal, after which a decision is made to intensify the levee watch on the levee. Levee inspectors start to inspect the levee until a damage is detected. After detection of the damage, a decision has to be made on the required emergency measure. This decision results in preparation of the emergency measure in terms of material and personnel. Then, the measure is transported from storage to the damaged levee section. At last, the emergency measure is placed, ready to fulfil its purpose. The total time required ( $t_{req,ser}$ ) is the sum of all the steps in the scheme ( $t_{path}$ ) (equation B.1). The numbers  $t_1$  to  $t_5$  are defined in figure B.1.

$$t_{req,ser} = \max(t_1 + t_2 \cdot t_{det,dam}) + t_{insp} + t_3 + t_4 + t_5 + t_{place} \quad (B.1)$$

#### B.2. EXPERT JUDGMENT

This appendix shows the results of the expert judgement session, as conducted on the 30th of April 2023. The calibration questions asked to the experts are shown in table B.1, while the questions of interest are shown in table B.2. The participants of the expert judgement session are not made available here, for privacy reasons. The attendees are arranged in alphabetical order, with randomly assigned expert IDs as employed within the analysis. The overall performance of the experts is shown in table B.3. The calibration scores of 18 out of the 22 experts is smaller than  $1 \cdot 10^{-2}$ . This is a rather low score for most of the experts, where scores close to or higher than one are to be expected. This suggests a potential misalignment between the calibration questions and the expertise of the experts. The calibration questions encompassed estimations of discharges and

B

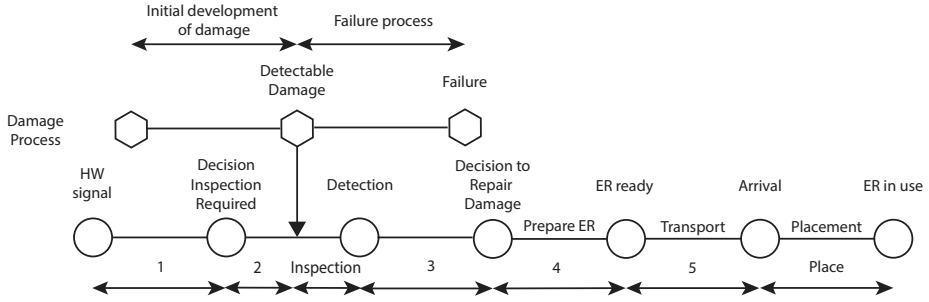


Figure B.1: Time required to apply emergency measure, steps in series, numbers indicate question in expert judgement (B.2)

velocities of river flows, which differs from the unit of time requested in the questions of interest. A comparison between the mean values of the questions of interest for the equal decision maker (all experts are weighted equally) and the global decision maker (the weight of the experts is based on the performance of the calibration questions) reveals that the weighted mean values for the equal and global decision maker are in the same order of magnitude. However, the uncertainty intervals are broader for the equal decision maker. Consequently, it can be inferred that all experts are converging towards the values postulated by the best experts. Given this observation, the global decision maker is applied, to include the best experts, but do not exclude the experts who perform bad in the calibration questions.

Table B.1: Calibration questions expert judgment session

#	Question	Realization	
1	Arrival military in Sittard during floodings in Limburg, 2021 (Koopman, 2022; Rongen et al., 2021)	6.5	h
2	Placement sandbags at dike which suffered macro instability at Fishbeck 2014 (Henning and Jüpner, 2015)	6	h
3	Failure dike after detection first damage, Fishbeck 2014 (Henning and Jüpner, 2015)	17	h
4	Time first water till failure in experiments Lillo 2015 (Peeters et al., 2015)	30	min
5	Expected return period of a code red at Lobith (MinIenM, 2009)	50	year
6	Discharge of Rhine at Lotith on the 26th of April 2023 at noon (question was asked the 19th of April around noon) (Rijkswaterstaat, 2023)	2202	m <sup>3</sup> /s
7	Width of the breach which was enclosed, using the vessel "de twee gebroeders" during the Dutch Watersnoodramp in 1953 (Rijkswaterstaat, 1961)	6.5	m
8	Initial discharge through breach initiated with explosives during experiments in Marnewaard, 2023 (own dataset)	1.46	m <sup>3</sup> /s
9	Placing 1 row of sandbags over a length of 100 meters (Nat, 2012)	8	min
10	Evacuation of 237 people out of hospital Venlo, during the Limburg flood in 2021 (Rongen et al., 2021)	10	h

Table B.2: Questions of interest expert judgment session

#	Question
11 (1)	How much time do you think is needed between receiving a high-water alarm, code red, and the decision to intensify dike surveillance?
12	What is your estimate of this time for a code orange?
13	What is your estimate of this time for a code yellow?
14 (2)	How much time do you expect it will take for the dike watch to become operational on location after the decision to 'intensify the dike watch' has been made?
15 (6)	How much time do you think is needed between receiving a high-water alarm code red and the decision to prepare emergency measures?
16	What is your estimate of this time for a code orange?
17	What is your estimate of this time for a code yellow?
18 (4)	How much time after giving the signal to prepare emergency measures do you expect the emergency measures to be ready for transport, when using civilian resources (both personnel and equipment), in general?
19	Using sandbags?
20	Using Bigbags?
21	How much time after giving the signal to prepare emergency measures do you expect the emergency measures to be ready for transport, when using military resources (both personnel and equipment), in general?
22	Using the BresDefender?
23	Using explosives?
24 (5a)	What do you estimate the average speed is for transporting emergency measures by road to the required location during a high-water crisis?
25 (5b)	By transport over water?
26 (3)	How much time do you expect is needed between the discovery of a significant dike damage and the decision to repair the damage, under code red?
27	What is your estimate of this time for a code orange?
28	How much time do you think can be gained through informal channels before the high-water alarm is officially given, during a high-water event from the Rhine river (3+ days before the peak, with accurate prediction)?
29	How much time do you think can be gained through informal channels before the high-water alarm is officially given, during a high-water event from the Meuse river (1 day before the peak, with accurate prediction)?
30	How much time do you expect to start transporting materials to the location after detecting actual damage at a recognized weak spot in the dike?

Table B.3: Calibration, information and weight scores experts

ID	Cali	Info real	Info tot	Weight (Global)	Weight (Global opt)
Exp A	$1.7 \cdot 10^{-4}$	3.706	2.629	$7.12 \cdot 10^{-4}$	0
Exp B	0.037	3.691	3.564	0.151	0.184
Exp C	$7.4 \cdot 10^{-4}$	4.044	4.090	$3.32 \cdot 10^{-3}$	0
Exp D	0.121	3.786	3.339	0.509	0.616
Exp E	$3.7 \cdot 10^{-6}$	4.506	3.876	$1.87 \cdot 10^{-5}$	0
Exp F	$2.2 \cdot 10^{-4}$	3.515	3.253	$8.41 \cdot 10^{-4}$	0
Exp G	$4.7 \cdot 10^{-4}$	4.287	4.156	$2.25 \cdot 10^{-3}$	0
Exp H	0.037	4.092	3.301	0.168	0.200
Exp I	0.020	4.112	3.256	0.090	0
Exp J	$3.1 \cdot 10^{-3}$	3.199	3.140	0.011	0
Exp K	$1.1 \cdot 10^{-3}$	3.818	3.928	$4.66 \cdot 10^{-3}$	0
Exp L	$4.0 \cdot 10^{-5}$	3.666	3.599	$1.63 \cdot 10^{-4}$	0
Exp M	$3.2 \cdot 10^{-5}$	3.010	2.236	$1.08 \cdot 10^{-4}$	0
Exp N	$1.7 \cdot 10^{-3}$	2.323	1.924	$4.31 \cdot 10^{-3}$	0
Exp O	$1.7 \cdot 10^{-4}$	4.210	3.797	$8.09 \cdot 10^{-4}$	0
Exp P	$2.0 \cdot 10^{-5}$	3.926	3.639	$8.89 \cdot 10^{-5}$	0
Exp Q	$4.7 \cdot 10^{-4}$	3.605	3.445	$1.89 \cdot 10^{-3}$	0
Exp R	$1.7 \cdot 10^{-4}$	3.703	3.287	$7.12 \cdot 10^{-4}$	0
Exp S	$1.7 \cdot 10^{-4}$	3.143	3.247	$6.04 \cdot 10^{-4}$	0
Exp T	$4.9 \cdot 10^{-3}$	4.285	3.841	0.023	0
Exp U	$2.8 \cdot 10^{-9}$	3.633	2.879	$1.13 \cdot 10^{-8}$	0
Exp V	$8.3 \cdot 10^{-3}$	2.992	2.481	0.028	0
Global	0.640	2.506	2.111		
Global opt	0.754	4.008	3.619		
Equal	0.190	1.950	1.707		





# CURRICULUM VITÆ

## Danny JANSSEN

31-07-1994 Born in Delft, the Netherlands.

### EDUCATION

2016–2018 MSc. Civil Engineering (specialization Coastal Engineering)  
Delft University of Technology

2015–2016 Bridging program for access MSc. program  
Delft University of Technology

2011–2015 Civil engineering  
Rotterdam University of Applied Sciences

### EXPERIENCE

2019 – present PhD researcher  
Delft University of Technology  
Netherlands Defence Academy

2018 Graduation internship MSc.  
BAM Infraconsult

2015 Graduation internship  
Royal HaskoningDHV



# LIST OF PUBLICATIONS

## JOURNAL CONTRIBUTIONS

1. **Janssen, D.**, Hommes, D.P., Schmets, A.J.M., Hofland, B., Zwanenburg, C., Dado, E. and Jonkman, S.N. *Experimental study of water infiltration into a partially sealed levee*, (submitted, under review).
2. **Janssen, D.**, Hofland, B., Schmets, A.J.M., Dado, E. and Jonkman, S.N. *Reducing water flow through a levee breach using a pontoon*, (submitted, under review).
3. **Janssen, D.**, Jonkman, S.N., Schmets, A.J.M., Hofland, B. and Dado, E. *Operational reliability of emergency measures, a case study for the Bresdefender*, (submitted, under review).

## CONFERENCE CONTRIBUTIONS

**Janssen, D.**, Schmets, A.J.M., Hofland, B., Dado, E. and Jonkman, S.N. (2021). *BresDefender: A potential emergency measure to prevent or postpone a dike breach..* In FLOOD-risk 2020 - 4th European Conference on Flood Risk Management

## OTHER

Schmets, A.J.M., **Janssen, D.**, Krabbenborg, D., Leertouwer, S.T., and Dado, E. (2024). *Novel emergency response interventions for flood resilience*. In G. Frerks, R. Geertsma, J. Klomp, and T. Middendorp (Eds.), *Climate security and the military - concepts, strategies and partnerships* (pp. 231–252). Leiden University Press.